The Hysucat Development

By

Dr. K.G.W. Hoppe

Internal Report 1989
Lecturer Research Activities
Mechanical Engineering Department
University of Stellenbosch, RSA
The Hysucat Development Project

By

K.G. Hoppe *), Dr. – Ing. (Germany), Pr.-Ing,. SAIMENA

Resumé :

The abbreviation Hysucat stands for Hydrofoil Supported Catamaran and describes a new High Speed Small Craft, a seagoing planing catamaran with a hydrofoil arrangement between the two demi-hulls which carries a part of the craft's weight at speed.

The efficient load carrying capacity of the hydrofoil in combination with the high stability and pleasant sea-keeping of the planing catamaran resulted in a most economical craft with unparalleled sea -keeping.

This was approved in a series of model tests in the Water-circulating Tank and Towing Basin at the University of Stellenbosch.

The final proof of the new craft's economy and excellent sea-keeping was delivered by a series of sea -tests on a 5,65m Prototype in the rough sea off Cape Town and the evaluation of the various outboard engines used in the laboratorium and at sea.

Over a period of one year the prototype was successfully tested under various weather conditions from smooth sea to very rough stormy conditions, in wind chop and steep swell waves – showing superior sea-keeping in all conditions.

The popularity of the new craft can be recognized by the appearance of 40 Hysucat-Skiboats, based upon the design of the first prototype, only 1½ years after it's first appearance.

*) Dr. Hoppe is a Naval Architect and Senior Lecturer at the Mechanical Engineering Department of the University of Stellenbosch.

The Hysucat Development

Symbols:

A	Planing area
A_p	Projected chine area
a_s	Area ratio of wetted surface over projected chine area A_p
B_c	Beam over chine of demi-hull
B_{cc}	Beam over chines of total craft
B_{oa}	Beam overall
B_T	Tunnel width or gap between demi-huls
C	Specific fuel consumption of craft in kg or fuel per km
C_1	C per ton of displacement in kg of fuel per km and ton Displacement
C^*	Specific fuel consumption of craft in litre per km and ton
C_2	Specific fuel consumption of craft in litre per km and per ton displacement if specific consumption of engine is related to Hp
C_3	Specific fuel consumption of craft per ton displacement in (1 / sm * t)
C_4	Specific fuel consumption of craft per ton displacement in (kg / sm * t)
C_D	Drag coefficient of foil or drag coefficient of craft in air
C_{Dleg}	Drag coefficient of outboard leg based on wetted cross-sectional area at 25 kn
C_f	Viscous friction resistance coefficient of hull
C_L	Lift coefficient of foil
C_{mot}	Specific fuel consumption of engine in (kg / kW * h)
C^1_{mot}	Specific fuel consumption of engine in (kg/ HP * h)
C_r	Residual resistance coefficient of hull
C_t	Total resistance coefficient of hull

$C_{t,\ h\text{-}f}$	Total resistance coefficient based on the Hysucat resistance
CG	Center of gravity
CP	Center of pressure
d	Water depth in water circulating tank
D	Drag force of foil
D_{leg}	Drag force of outboard engine underwater part (leg)
D_s	Maximum draft of hull at stern when afloat
F_{fuel}	Consumed fuel
F_{nd}	Froude depth number, $F_{nd} = V/\sqrt{g \cdot d}$
F_n	Froude length number, $F_n = V/\sqrt{g \cdot L}$
F_n	Froude displacement number, $F_n = V/\sqrt{g \cdot \nabla^{1/3}}$
$F_{v.f.}$	Fractional weight component of foil at longitudinal position $X_{v.f.}$
$F_{v.st.}$	Fractional weight component of foil at longitudinal position $X_{v.st.}$
g	Gravitational acceleration
h	Water height over foil
HP	Metric horse power ,1 HP = 0,735 kW
K_{corr}	Correlation coefficient of hull
$K_{corr\ tot}$	Overall correlation coefficient of Hysucat equipped with foil
$K_{corr\ h\text{-}f}$	Correlation coefficient of Hysucat hull resistance (foil resistance being subtracted)
K_{fuel}	Cost of fuel o f propulsion plant for a given time period
km	Kilometer, 1000 meter
l	Litre
L	Length of ship hull

L_C	Length over chine
l_c	Chord length of hydrofoil
L_{prot}	Length of the prototype ship
L_{oa}	Length of hull overall
l_m	Mean wetted length of hull at speed
l_{mo}	Mean wetted length of hull afloat
LCG	Longitudinal position of the center of gravity
LCP	Londitudinal position of the center of pressure of the foil or foils
M_{fuel}	Mass of consumed fuel in kg
N_{mot}	Engine speed in r.p.m.
P_{eff}	Effective Power of craft ($R_t * V_s$)
$P_{B,P}$	Brake power of propulsion machinery, for outboard engines measured on propeller shaft
P.C.	Propulsive Coefficient P.C. = P_{eff} / P_B
Q	Torque on outboard engine propeller shaft
R_e	Reynolds number V * L / ?
R_f	Resistance of foil arrangement
R_i	Isolated hull resistance (the resistance measured on model with disconnected foil)
R_r	Residual resistance of hull
R_t	Total resistance of Hysucat hull equipped with foil
s	Hydrofoil thickness
S	Wetted surface of hull at speed or rest
S_{h+f}	Wetted surface of hull plus wetted surface of foil
S_m	Nautical sea-mile, sm = 1,852 (km)
S_t	Steady speed distance traveled by ship in time interval t

t	Steady speed running time interval of ship
t	as a dimension stands for ton, 1 ton = 1000 kg
V, V_S	Ship speed
V_{max}	Maximum speed for which ship is designed
X_{vsf}	Forward attachment point of vertical force to hold demi-hulls in same position as Hysucat with foils
X_{vst}	Aft attachment poin t of vertical force to hold demi-hulls in same position as Hysucat with foils.
X_v	Longitudinal position in % of L_c from transom of the resultant vertical force to hold demi-hulls in same position as Hysucat with foils
a	Angle of inflow to hull
a_D	Angle of deckline with water level
a_f	Angle of inflow of foil
a_h	Angle of inflow to hull bottom near foil attachement
ß	Deadrise angle of demi-hull
?	Ship hull's displacement in mass or weight-force
$?_{prot}$	Prototype ship displacement
$?C_f$	Difference of model-ship friction resistance coefficient
e	Resistance weight force ratio, $e = R_t$ / ?
e_t	Resistance weight force ratio of Hysucat equipped with foil, R_t / ?
e_f	Foil's resistance weigth force ratio D/L
e_{h-f}	Resistance of Hysucat minus resistance of foil weight force coefficient $(R_h - R_f)$ / ?
e_i	Hysucat with disconnected foil measured resistance coefficient (trim and heave position at considered speed is the same as for Hysucat with foil)
e_{h+int}	Isolated hull plus interference resistance, $(R_t - R_f)$ / ?
e_T	Thrust over weight ratio

?	Surface effect of hydrofoil, $K = h/l_c$
?	Scale ratio L/L *
?	Density of water
?	Trim angle at speed
?	Kinematic viscosity of water
∇	Volume of displaced water in m3
$?_p$	Propeller efficiency
*	The star indicates that the marked parameter is a model Parameter
BMI	Bureau of Mechanical Engineering at the University of Stellenbosch

1. *INTRODUCTION*

The abbreviation "Hysucat" is used to define a type a new type of "High Speed Small Craft" and stands for Hydrofoil Supported Catamaran. The basic ideas and the efforts which lead to the development of the first seagoing Hysucat shall be highlighted in the present publication.

After DuCane (1), "High Speed Small Craft" are relatively small but fast ships operating at Froude numbers $F_{nl} = V/\sqrt{g \cdot L}$ larger than unity.

Various different types of such craft are in use and optimized to fulfill their requested task most advantageously. The most popular hull for deep-sea operations is the so called Deep-V-Planning-Hull (1). It has limitations concerning the sea-keeping quality and needs a relatively large propulsion power. The Hydrofoil-Craft improves over both the disadvantages of the Deep-V-Hull but is unpractical as a small craft and extremely sophisticated and therefore costly. Extreme wave conditions also put a limitation on the use of the Hydrofoil-Craft as a deep sea craft.

Hovercraft suffer similar limitations and are very sensitive to strong winds.

In a time of high energy costs "High Speed Small Craft" with low propulsion power and consumption are requested which have acceptable or improved sea-keeping and handling characteristics over the Deep-V-Hull and which can be built and run with relatively low capital investment.

The presently used hull concepts are fully optimized and considerable improvement can not be expected.

A new concept was proposed by Hoppe (2,3), combining a catamaran planing hull with it's well known wave-going qualities and inherent stability with a weight supporting hydrofoil well protected inside the gap of the two demi-hulls, the highly efficient hydrofoil reducing the weight-load on the hulls at speed and with it the resistance of the catamaran. The disadvantage of the usual planing-catamaran, it's high propulsion power requirement in comparison to mono-hulls is eliminated this way.

Keeping in mind that High-Speed-Catamarans have proved to be very successful in rough water off-shore races, larger work-boats of this type with improved sea-keeping and handling in rough seas can be expected. The idea of combining hydrofoil and catamaran is not new and a patent search reveals many essays (4 to 10 and others), which all failed, mainly because the strongly varying trim-stability in the various speed ranges was neglected. This deficiency is eliminated by the new concept (3) which improves trim-stability reserves at speed considerably, making the Hysucat less sensitive to longitudinal weight shifts than the Deep-V-Hull.

To approve the Hysucat Principle several model test series were conducted to show the improvements due to the support hydrofoils. In the first phase, model tests in the water circulating tunnel indicated best foil positioning, resistance improvements and qualitative functioning of the Hysucat in flat water and in waves. To achieve more reliable absolute resistance date several towing tank test series on different Hysucat designs were conducted. The Hysucat Principle kept it's promise and considerable resistance improvements were recorded in all tests, showing that the Hysucat could be more efficient than a Deep-V-Hull in the high speed range. The convincing results initiated the Bureau of Mechanical Engineering at the University of Stellenbosch to finance and develop a seagoing first prototype, a 5,65m Ski-Boat for the sports

fisherman. Considered as a sea-going model boat it was tested and fully approved the Hysucat Principle. It now is in commercial mass production.

2. THE HYSUCAT PRINCIPLE

The word "catamaran" comes from the Polynesian Languages meaning "tied up trees", describing the historical out-rigger or twin-hulled sailing vessels which were developed to perfection and which enabled the Polynesians to spread their civilization over the Pacific Sea (Micronesia, Melanesia, Polynesia, New Zealand and Easter Islands) covering an area larger than Europe and North America combined. Thus, the approval of the catamaran hull for seagoing craft was actually established long before our time.

The catamaran for motorboats, nowadays, is successfully used only for sport or racing craft. In the speed range for usual working boats the catamaran's propulsion power is relatively high because the resistance of the two demi-hulls is increased (by more than 25%) over the one of a comparable mono-hull.

All working boats as Yachts, Fishing Craft, Navy Craft, etc. have to carry a load at relatively lower Froude numbers ($F_{n\nabla} = V/\sqrt{g \cdot \nabla^{1/3}}$)
than the racing craft and the larger engines in the catamaran together with larger fuel storage restrict their use or their payload. To make the work boat catamaran competable it has to have a lower propulsion power requirement which means a lower resistance than the comparable mono-hull. The resistance reduction becomes possible after (2) for the catamaran with a hydrofoil inside the tunnel between two fully asymmetrical demi-planing-hulls which takes up a part of the boat's weight at speed, lift it higher out of the water and this way reduces the overall resistance because the hydrofoil has a much higher lifting efficiency than the hulls.

The efficiency of a hull and a hydrofoil are best expressed by their drag-lift ratio:

$$\mathbf{e = D / L}$$

with e = resistance coefficient, D = dragforce, L = liftforce.

As indicated in Fig. 1 the hydrofoil is considerably more efficient to carry load than the hull at speed. A combination of the catamaran with a hydrofoil, therefore, must improve the craft considerably.

The problem lies only in the right combination of both elements which has to result in reduced overall resistance but still has to produce sufficient transverse and longitudinal stability at all speeds. A further request in any practical boat design is for good sea-keeping and handling characteristics which are also improved by the Hysucat Principle. This becomes clear from Fig. 2 where the velocity vectors of the hydrofoil are indicated when the Hysucat is running through a wave crest.

For planing catamarans in high speed range:

For hydrofoil sections in high speed range near surface:

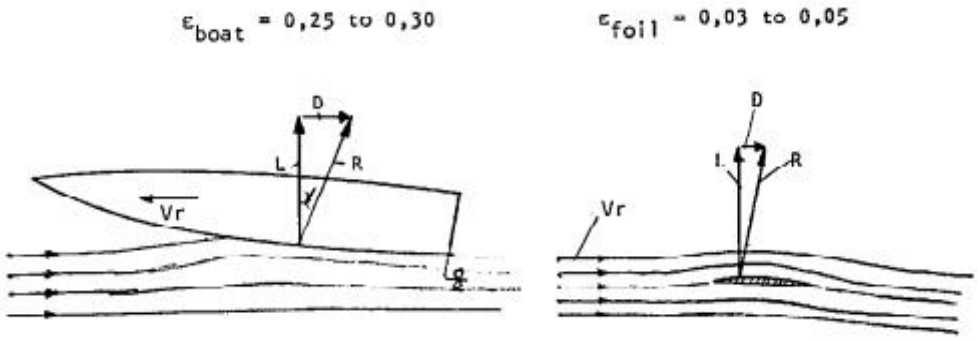

Figure 1.

The hulls are rising abruptly in the wave encounter carrying the hydrofoil with them and creating the vertical velocity component Vvertical. The relative inflow, which is the vector sum of ship speed and vertical velocity, is changed and with it also the incidence angle a_r , which, in this example becomes negative with the result of a reduced hydrofoil lift force. The hulls have to carry more load and follow the wave slope less abruptly with less vehement vertical motions. The hydrofoil, therefore, improves the already good wave-running characteristics of the catamaran by it's damping effect against vertical accelerations in waves.

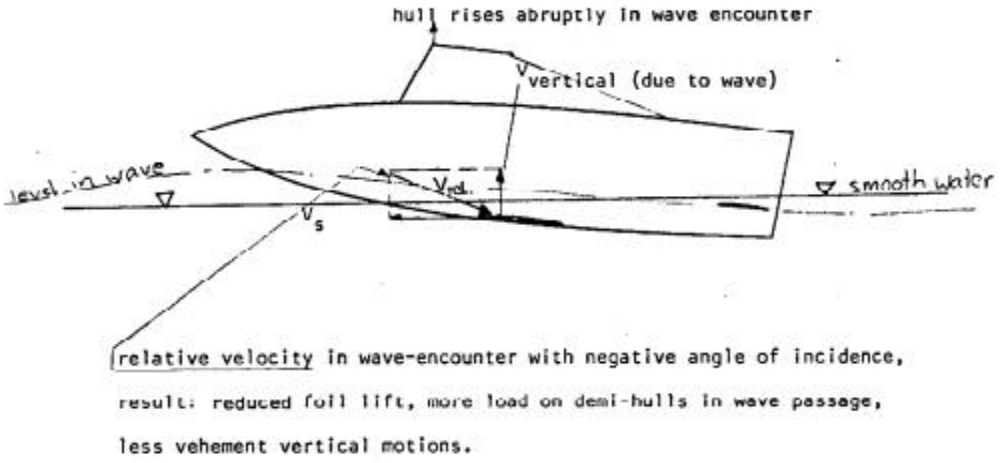

Figure 2.

The Hysucat concept proposed by Hoppe (2) favors a single hydrofoil installation inside the straight tunnel between two fully asymmetrical demi-hulls. The hydrofoil is attached to the keels as deep as possible submerged but still in the protection of the lateral area.

Lengthwise it has to be positioned that the foil's center of pressure (L.C.P.) is in the near vicinity of the longitudinal center of gravity position (L.C.G.) . The shape of the planing hull chine area has a strong influence on the best L.C.P. position for which the resistance is optimal in the full speed range. A hull with broad front chine area and reduced chine beam at the stern has it's best L.C.P. position about 1% to 2% of the chine length L_c behind the L.C. G. position. A typical Deep-V-planing-hull with prismatic hull shape has the best L.C.P. position about 0,5% of L_c in front of the L.C.G. position . On all ships and especially on the smaller boats the center of gravity shifts with changes in load, consumption of fuel or movement of persons. To maintain optimum performance the distance between L.C.P. and L.C.G. has to stay about constant which means controlled shifting of the hydrofoil position or active trim-control devices as stern-flaps or horizontal rudders. This is only possible on larger and sophisticated craft, but then can produce best performance under varying conditions.

The smaller craft "suffer' of more stringend weight shifts but it is not desirable to have complicated trim-control devices. The hull has to take up the right trim in the full speed range automatically. A tandem hydrofoil arrangement which allows the design of a Hysucat with auto-trim-stabilization at speed was therefore proposed by Hoppe (3). Two hydrofoils inside the straight tunnel of a planing catamaran with fully asymmetrical demi-hulls are installed in tandem. A larger mainfoil slightly in front of the center of gravity (L.C.G.) near the keel and a smaller sternfoil in the vicinity of the stern of the boat near the water-level at speed, see Fig. 3.

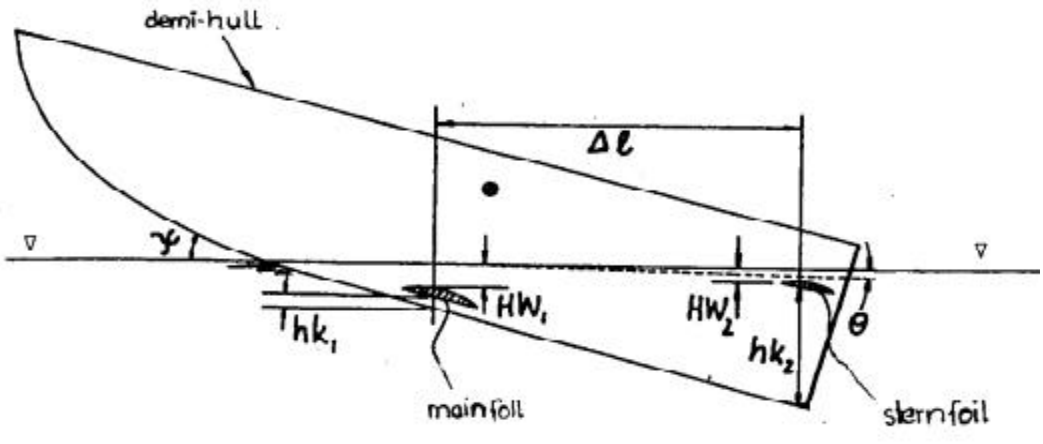

Figure 3.

Both foils approach the water surface with increasing speed and run in the so called hydrofoil surface effect mode which means reduced lift forces due to nearness of the water level. When disturbed, submerged deeper, the foil in surface effect creates strongly rising lift forces which tend to return the foil to the original level of submergence.

This way the hydrofoil's trim stabilization is independent on the angle of incidence a and trim angle ? of the hulls.

The hydrofoils have to be dimensioned to compensate for the reduction of lift in the surface effect and have relatively larger foil area. The foils are arranged that the resultant lift-force of both foils is situated at the best L.C. P. position for the corresponding demi-hulls as determined earlier for the single foil arrangement. The smaller the surface effect ratio ? = HW/ l_c (HW = water height over foil and l_c = foil chord length) the stronger will be the trim stabilization.

However, in extreme surface effect the foil efficiency e_f is reduced and for optimum performance ? should not become smaller than 0,2.

The height of the sternfoil over keel hk_2 (see Fig. 3) determines the boat's trim angle at speed and can be calculated as follows:

$hk_2 = hk_1 + ?1(\tan ? - \tan ?) + k_1 * l_{c1} - k_2 * 1_{c2}$ 1.1

(hk_2 , hk_1 , ?1 being defined in Fig.3; ? being the angle of the waterflow deflection inside the tunnel due to the action of the mainfoil; indices 1 and 2 denoting mainfoil and sternfoil).

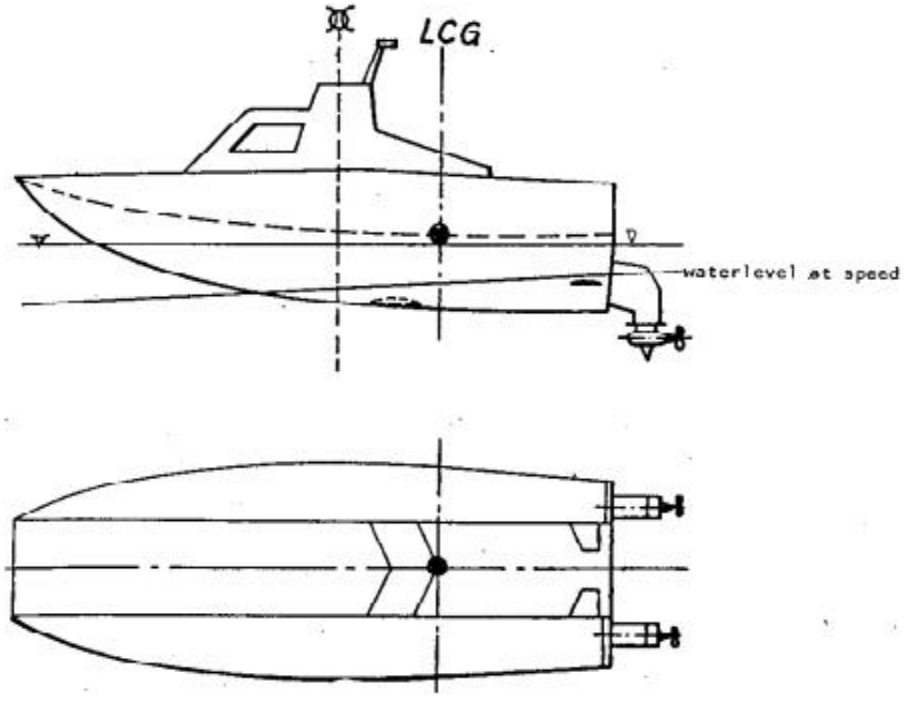

Figure 4.

The principle hydrofoil arrangement after (3) is shown in Fig.4 for a planing catamaran. The mainfoil has sweep and a slight dihedral to allow for smoother penetration of the water-level in waves. The sternfoil consists of two strut foils with sweep and slight dihedral. Strut foils can be built stiffer for the small foil area in request. The foils are dimensioned to carry about 45% of the boat weight at service speed.

3. MODEL TESTS

3.1 Introduction

The advantages of the Hysucat Principle claimed in (2,3) are based on the logical conclusion that the combination of two efficient elements, the catamaran hull and the hydrofoil, will produce a superior "High Speed Small Craft".

The final proof of this assumption will only be accepted when a real sea-going Hysucat has made a successful appearance. The design of a practical Hysucat is requested, which required model testing to establish the unknown hydrodynamic parameters for optimal design.

Sufficient data of Deep-V-Planing craft are available in literature which shall be used as basic starting data and which allows the design of efficient demi-hulls in the envisaged speed range. The most efficient hydrofoil arrangement however, has to be established in model test series with systematical variation of the important parameters involved.

Model testing is the accepted "tool" in new ship design and the only economical way of predicting the resistance and power requirement of the new design proposal. In qualitative tests, which are cheaper, the general functioning of a design proposal as general course holding in flat water and waves, trim at speed, broaching tendencies etc. can be determined and the model eventual re-designed.

The model test results can be correlated to any size of prototype by use of the laws of similitude concerned. However, practical prototype requirements have to be fulfilled and differ considerably with absolute ship size.

It is therefore practical to decide on a real prototype and fix practical design data as displacement, length, beam and service speed. Some model test experience has been gained at the Bureau of Mechanical Engineering at the University of Stellenbosch (BMI) on a 10m (7 t displacement, 40 kn) catamaran built for the Institute of Maritime Technology (ITM). Therefore, a first Hysucat prototype of 10m, 7t, 40 kn was envisaged and outlines and the model of it tested.

The model results could naturally be scaled up and correlated to any larger craft, say of 20m length with a displacement of 56t and a speed of 56,6 knot. As the speed of the prototype also increases with the scale ratio unrealistic speeds are soon reached. A new prototype design is then necessary with own model tests.

A 20m hull with 40 knot service speed would require a completely different foil design to reach the optimum combination in the Hysucat design.

To prove the Hysucat claim the model of a 10m boat was built and tested in the High-Speed-Water-circulating Tank at the University of Stellenbosch. At a later stage a

20m Hysucat with different shape was designed and tested in the Towing Tank of the University of Stellenbosch.

The mono-hydrofoil system as described in (2) was used on the models to prevent the scale effects in these tests with relatively small models to become excessive. The test will reveal the best foil-center of gravity position. With those data available a tandem hydrofoil system after (3) can easily be designed and will be explained in the design of the BMI sea-model.

3.2 Outline Design of a 10m Hysucat

The conditions in the operational area have an important bearing on the hull design. The design proposal is intended for operation under SA sea conditions, which means extreme weather and wave conditions. The most successful high speed small craft for extreme sea conditions is the deep-V-delta mono-hull, having a deadrise angle of 20° to 24° and a prismatic hull over most of its length. The design principles of these craft were chosen as the basis for the demi hulls of the Hysucat design proposal. A corresponding mono hull length-beam ratio of about 5 was anticipated for the demi hulls to reach sufficient buoyancy and good wave-going performance which mostly is not possible for the smaller mono hull craft because of the reduced stability with the high length-beam ratios. The catamaran hull does not suffer stability restrictions, but it must be ensured that sufficient buoyancy at rest at reasonable draft is available (otherwise the length-beam ratio could easily be increased). As the structural costs also increase with length-beam ratio the moderate length-beam ratio for catamaran demi hulls of $L_c / B_c = 9{,}58$ was chosen arbitrarily.

The width of the tunnel between the two demi hulls is dictated by the desired stability characteristics, the performance of the hydrofoil and the transverse structural strength. None of the parameters is absolutely stringent and a reasonable compromise was found for the tunnel width to be approximately twice the chine beam of the demi hulls, finally choosing $2\,B_c / B_T = 1{,}17$. The resultant width over the chine (hulls plus foil) was therefore :

$$B_{ccHYSUCAT} / L_c = 2{,}58$$

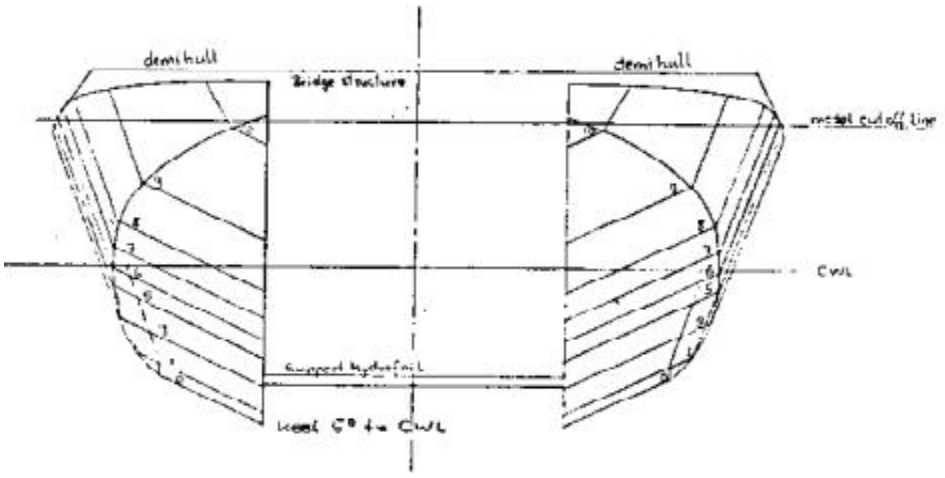

Figure 5. Model of Hysucat 5

To achieve large reserve buoyancy in the foreship to prevent undercutting in very steep waves of critical length (when the trim-oscilations come into reasonance with the wave-of-encounter period) the hull lines were kept extremely full in the foreship and it is advised to keep the tunnel closed up to the front with the forward tunnel ceiling having an increased angle of attack toward the front to take load like a planing area to create lift forces in the case of extremely deep dipping movements, but usually to be free of water contact. This will also prevent spray being carried up in between the tunnel front hulls and being thrown up over the ship superstructure. The front tunnel ceiling should be slightly arched and should have a step near about frame 7, behind which the tunnel ceiling shall remain dry under all service conditions. For the resistance tests it is not necessary to incorporate the tunnel and the superstructure in the model. The stern part of the planing areas of the demi hull was given reduced beam similarly to the Series 62 hulls which allows bringing the center of gravity forward, desirable for ships with inclined shaft propulsion. It further results in the water breaking free from the hull at the chine and reducing wetted surface and there with friction resistance. The hull line drawing of the underwater part of the Hysucat is shown in principle in Fig. 5.

The hydrofoil system (3) was not designed in full detail for this prototype as tests on a mono hydrofoil Hysucat after (2) were envisaged to keep foil scale effects to a minimum. The hydrodynamic performance of the prototype foil was determined theoretically to be able to build the model foil which was chosen for reasons of simplicity initially to be straight and with a circular upper profile section, flat lower surface and a small nose radius. This foil would fulfill the model test requirements where no cavitation limits occur. In a real design case the foil profile section and shape would have to be investigated in more detail to make sure that no cavitation will occur for the variance in incidence angle which will be encountered when the Hysucat operates in waves. The proximity of the foil to the surface has a further influence on the foils performance which needs further investigation for the prototype craft (to be able to optimize the Hysucat design). To improve sea-keeping the prototype foil shall have a slight dihedral and sweep angle. For speeds up to 36 kn subcavitating foils are advisable but speeds over 40 kn necessitate super-cavitating or better super ventilated foils, both of which can also give efficient drag-lift ratios. Such foils have to be investigated as separate items.

The resultant main dimensions of the Hysucat are:

Length overall	L_{oa}	=	10,17m
Length over chine	L_c	=	10,17m
Beam overall	B_{oa}	=	4,68m
Beam over chine of craft	B_{cc}	=	3,94m
Beam over chine of demi hull	B_c	=	1,06m
Tunnel width	B_T	=	1,81m
Maximum draft at stern afloat	D_s	=	0,80m
Design displacement	?	=	7,0 t (max. 9,0 t)

Maximum speed	V_{max}	=	40 kn
Deadrise angle	ß	=	24°

The hull lines drawing of the underwater part, necessary for the model resistance tests, is shown in Figure 5. The optimum center of gravity position is expected to be between 40% and 36% of the chine length form the transom. The positioning of the single foil is expected after preliminary tests to be slightly sternwards of the center of gravity and its best position has to be found in the proposed model tests.

3.3 The Model Hull

Some experience had been gained in previous resistance test in the water-circulating tunnel when scale effects were investigated on a known Deep-V-Hull (11) and in tests on a high speed catamaran hull (12). It was found that a reasonable model size for the water-circulating tunnel is about 0,45m length and 0,3 to 0,6 kg mass. The resistance tests in the water-circulating tunnel are mainly intended to establish qualitative results. However, in (11) and (12) it was found that the predictions were possible in a range of about ±5% which allows the use of the data for preliminary design directly. More accurate and reliable resistance data have to be established later with larger models in the towing tank.

The scale ratio for the Hysucat resistance tests was therefore fixed at:

? = 22,11

which results in the following model dimensions:

L^*_c	=	0,460 m
B^*_{oa}	=	0,210 m
B^*_{cc}	=	0,180 m
B^*_c	=	0,0479 m
B^*_T	=	0,0819 m
D^*_s	=	0,0362 m
?*	=	6,3 N
V^*_{max}	=	4,8 m/s
ß*	=	24°

* *Indicates model data*

The body plan of the Hysucat model is also shown in Fig. 5. Only the underwater part of the Hysucat which is important in the resistance tests, was modeled. The higher parts and the superstructure were excluded. The model was fabricated from very thin aluminium sheets glued with Epoxy Glue, stiffened by five bulkheads and an overlapping deck structure. The two demi hulls were connected to each other with two L-shape aluminium profile beams. The model was painted in yellow Epoxy paint. Figure 6 shows the photograph of the model with the straight foil in the paint tracer tests.

The deck level of the Hysucat model was arranged different from the prototype, the deck on the model being a straight reference plane having a mean angle of about 5° towards the keel line. This allows a quick judgment of the trim angle of the planing surfaces at speed. It was anticipated to run the model hull with a trim angle of about 5° which is near to optimum. In this position the deck will be level with the water surface.

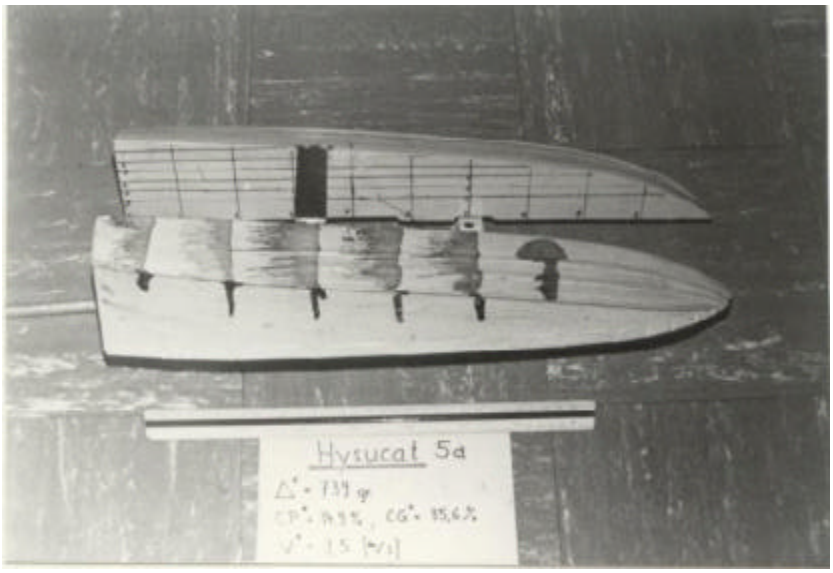

Figure 6. Hysucat model 5a paint tracer test

No turbulence stimulators were fitted as this was found to be unnecessary in the comparative test described (11) due to the high turbulence degree of the water-circulating tunnel. The Hysucat model's spray strakes further discourage laminar boundary layer flow.

Three support hydrofoil models were built, the first being a straight aluminium foil with a chord length of l_c = 13mm, a thickness ratio of s/l_c = 0,15 and a profile section similar to the NACA 16 thickness distribution.

The lower side was kept nearly flat. In preliminary tests it was found that this foil worked reasonably well but flow break-away appeared over about 30% of the suction side. This was expected as the Reynolds numbers for the foils are sub-critical and laminar flow occurrence cannot be prevented. The lift creation of the foil operating

very near to the free surface was found to be not sufficient for the tests on the Hysucat with the higher displacements.

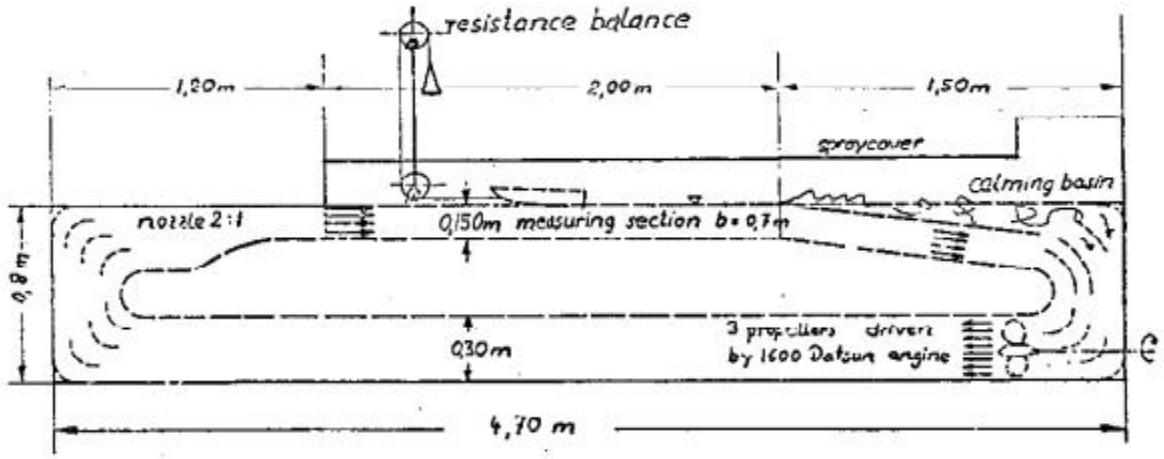

Figure 7. Sketch of Circulating Tank

A second relatively thinner support hydrofoil was therefore made from stainless steel having a chord length of l^*_c = 22mm and thickness ratio of s/l_c = 0,03 and a circular back profile with flat underside and the nose slightly rounded.

The flow break-away area is reduced to about 10% on the suction side. The lift creation of this foil is much stronger and it has to run at a relatively smaller incidence angle a_i = 3° to 3,5° near the free surface. This condition would correspond more closely to prototype conditions where cavitation limitations would require thin foils running at small incidence angles. To investigate the effect of sweep and dihedral on the resistance of the Hysucat a third foil was made with 52° sweep and 15° dihedral. The chord length in flow direction was l_c = 20mm, the profile section being a circular arc with a flat lower side and a slight nose radius; the thickness ratio was s/l_c = 0,1.

The resistance tests of the Hysucat equipped with the first foil are considered to be of preliminary nature and are not included in the present report.

The Hysucat hull without any support hydrofoil was first tested and designated Hysucat 5.

The same hull equipped with the large straight foil (l = 22mm) was designated Hysucat 5a and the Hysucat hull with the swept dihedral foil Hysucat 5b.

TEST FACILITIES

The small high speed water circulating tank with free surface of the Mechanical Engineering Department at the University of Stellenbosch is shown in principle in Figure 7 where also the main dimensions are given. A more detailed description is given in (15) and its reference. For the present test series a contracting top nozzle plate (see Figure 7) was added to reach higher top speeds, over 4,5 m/s, which were necessary to simulate the higher speeds.

The measurement of the model's resistance was achieved with the resistance-balance using weights for part of the resistance force and the fine measurement with a spring balance. An oil damper was provided to reduce vibrations, allowing a steady mean resistance indication at any speed up to 4,5 m/s.

The velocity measurement was achieved by the installed pitot static tube which was calibrated to indicate the mean velocity on the center line of the tank, 15mm under the surface in the cross-section where the model was to be positioned.

3.4 MODEL TESTS IN CIRCULATING TANK

3.4.1 Resistance Tests on Bare Hull

The model hull of the Hysucat as shown in Figure 6 was first tested without the support hydrofoil installed. The resistance was measured over the whole attainable speed range of the water-circulating channel, V = 2 m/s to 4,5 m/s, for three different displacements with a longitudinal center of gravity around 36%. The mean displacement of around 0,7 kg was tested with five different longitudinal center of gravity positions.

The test program is given as follows:

Test Series no.	*Displacement (KG)*	*R* (N)*	*Long. Center of Gravity in % of L_c from transom*
1	0.638	6.25	35.3
2	0.698	6.85	36.3
3	0.825	8.09	38.9
4	0.728	7.13	43.9
5	0.735	7.20	40.0

For full model test results the reader is referred to Hoppe (19).
Fig. 8 shows the resistance coefficient e* plotted over Froude Displacement Number $F_{n\nabla} = V/\sqrt{g \cdot \nabla^{1/3}}$ for the five test series.

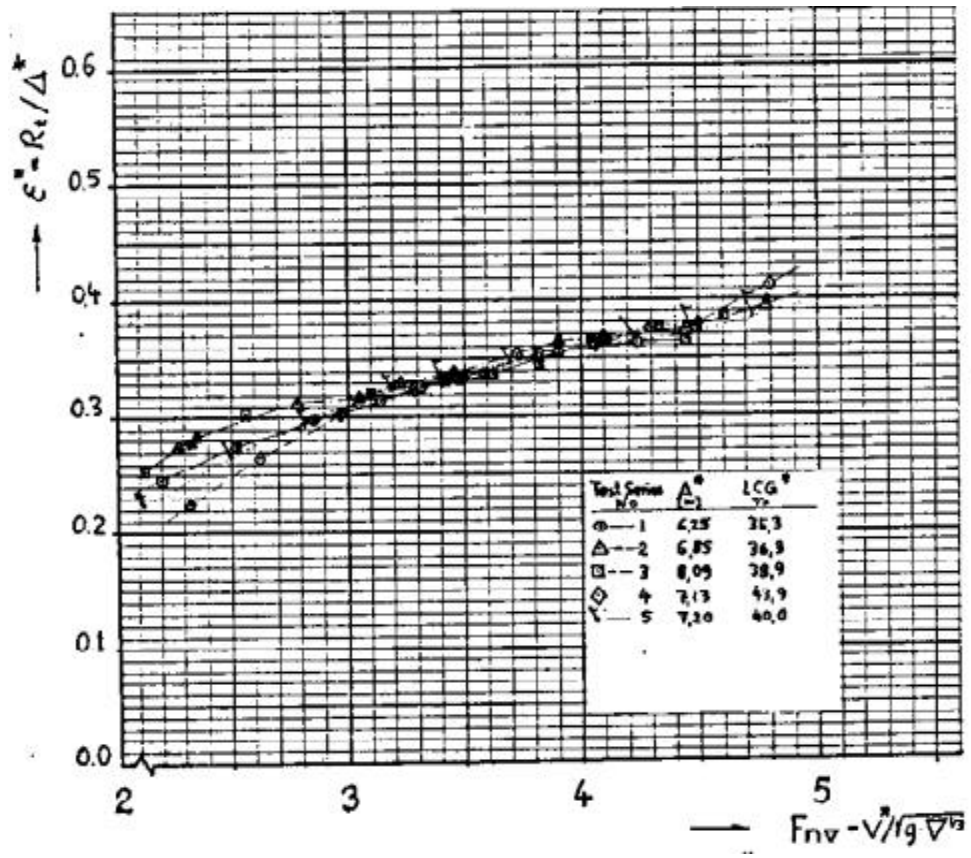

Figure 8: Model ship Resistance Coefficient e *, Hysucat 5, Bare Hull

As can be seen from Figure 8 the resistance-weight ratio e* of the Hysucat 5 hull does not change considerably for different displacements. It shows the typical tendency for shifts in the longitudinal center of gravity LCG*: forward position result in low resistance at low speeds but high values at high speeds and vice versa. The smooth water sea-keeping behavior is strongly influenced by the LCG* position, which, if too far astern, results in heavy porpoising , especially at the higher speeds. This could be expected as the hull then runs at relatively high trim angles and the LCG* positions most forward give the better sea-keeping behavior.

Porpoising was observed on the model in all test series if the speed increased over 3,50 m/s which corresponds to a Froude Number of $F^*_{n\nabla} = 3,9$.

3.4.2 Resistance Tests on Hysucat with Straight Foil

Two different test series were run with the Hysucat hull equipped with the straight foil, shown in Fig. 6. In the first series the foil was fitted to the hull with its longitudinal center of pressure LCP* situated 38,2% of L_C from the transom. The foil spanned the tunnel with the face side slightly higher than the keel (about 3mm) at this position which would give protection against ground contact. These resistance test series were designated number 6 and 7.

For the resistance test series numbers 8 and 9 the foil was shifted slightly aft and fixed with its center of pressure LCP* situated 34,9% of L_C from the transom. The foil was positioned slightly deeper with the flat face side about 2mm deeper than the keel at this position. The angle of the foil with the deck-level-line a_D was arranged to be 1,5° for the test series numbers 6 to 7. In the test series 8 and 9 the angle was increased to 2,6° to impose a heavier load on the foil. Every test series covered the whole attainable speed range of the water-circulating tunnel. The test program is given as follows:

Test Series no.	***Displacement (KG)***	***R* (N)***	***LCP* % of L c***	***LCG* % of L_C***	***a_D (°)***	***Foil Vertical Position***
6	0.736	7.22	38.2	38.8	1.5	Face side flush
7	0.647	6.35	38.2	38.0	1.5	With keel
8	0.645	6.33	34.9	35.6	2.6	Face side 3mm
9	0.748	7.33	34.9	35.6	2.6	Higher than keel

The measured data are plotted in the graphs, Figure 9, in form of the dimensionless model resistance-weight ratio e* over Froude Number F^*_{VI} . A typical resistance test at a speed of 3,8 m/s with the Hysucat 5a (with straight foil) was photographed and is shown in Figure 10 together with a photograph of the hull without the foil under nearly similar conditions. The lower trim angle at speed and the strongly reduced wake behind the model with the foil are made visible. The model (Hysucat 5a with straight foil) resistance coefficients for the various loads, center of gravity and center of pressure conditions appear in a narrow band over the Froude number.

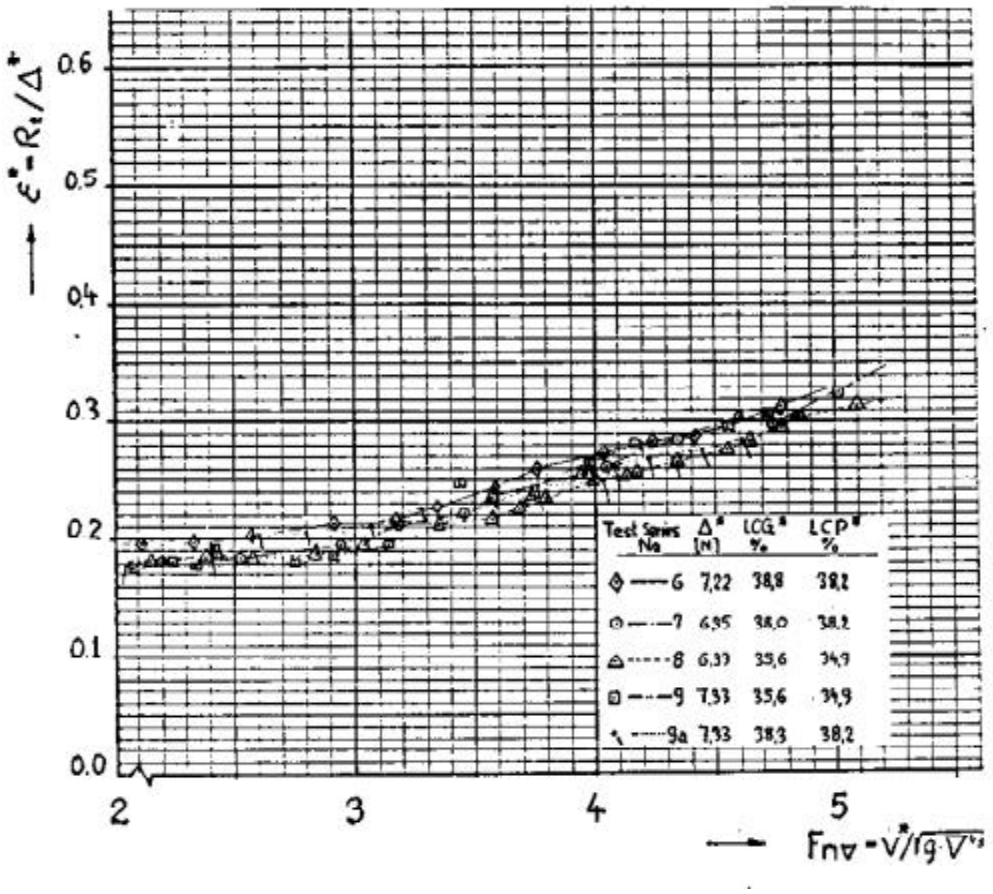

Figure 9: Model Ship Resistance Coefficient e*, Hysucat 5a with Straight Foil

The absolute values of the resistance coefficient are between about e* = 0,2 to 0,3 and are strongly reduced compared with the values of the hull without foil, the improvement being different for the various speeds, but between 35% and 45%. The best improvements are reached for Froude Numbers in the range of $F^*_{n\nabla}$ = 3 to 4. All the tested design conditions present successful Hysucat hull parameters (?* , LCG*, LCP*). The possible improvements on the prototypecan be determined after the correlation calculations have been performed.

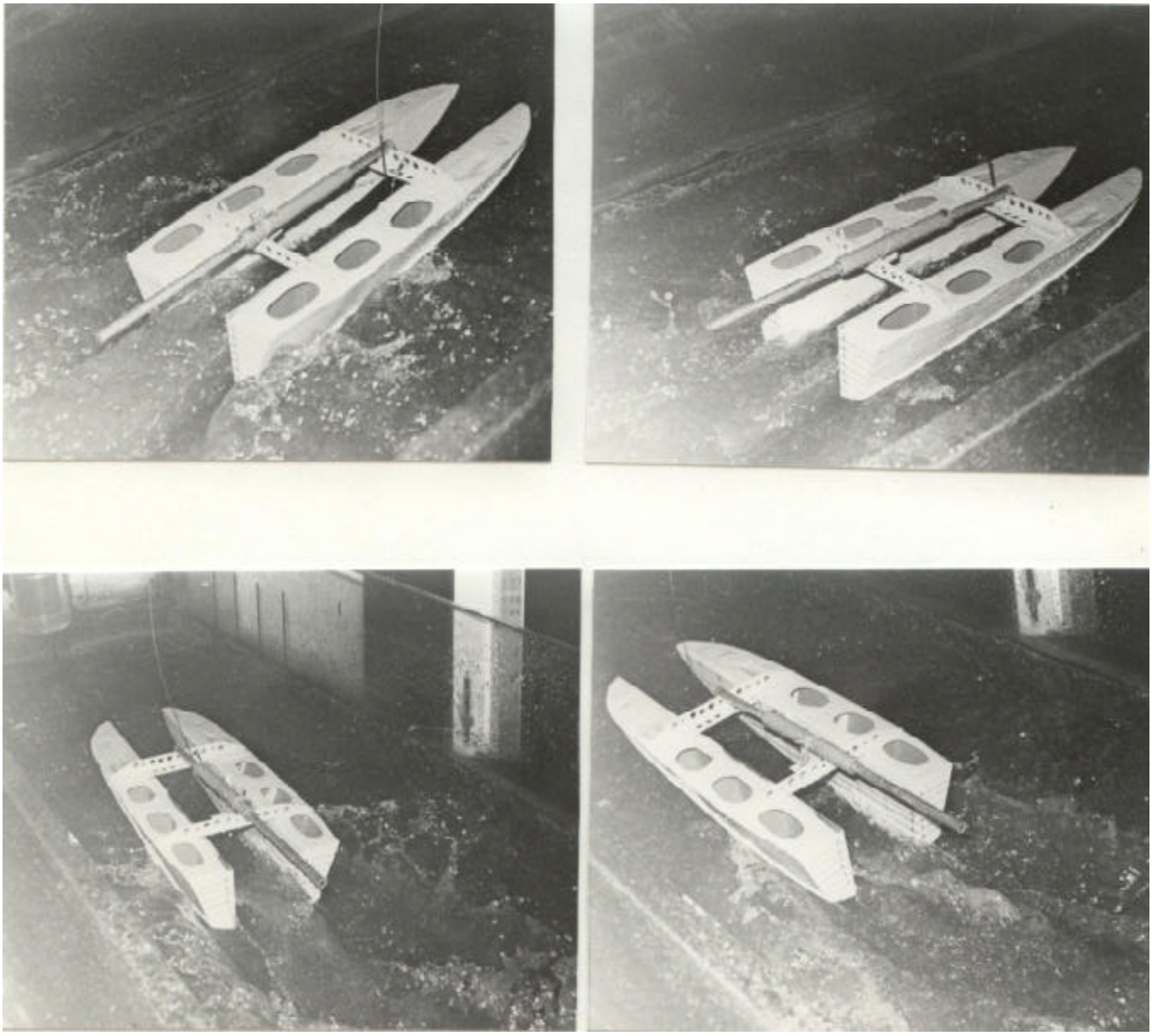

Without hydrofoil
Hysucat 5

V* = 3,5 m/s, ? * = 768 gr,
CG* = 40%

With hydrofoil
Hysucat 5a

with large straight Foil in tank test
V* = 3,8 m/s, ? * = 729 gr,
CP* = 34,9%, CG* 35,6%

Figure 10

3.4.3 Resistance Tests on Hysucat with Swept Foil

The Hyscuat 5b equipped with a support hydrofoil which has dihedral and sweep was investigated mainly because t is believed to improve sea-keeping in waves and to provide easier deflection of floating objects in the sea which might be struck by the foil. The influence of dihedral and sweep on the resistance was therefore intended to be measured in the following resistance test series.

The foil shape and design was explained before and a photograph in Figure 11 shows the configuration. The longitudinal center of pressure LCP* was arranged to be at 34,4% of L_c from the transom for the three test series, 10,11, an d 12.

The foil arrangement on the Hysucat hull is shown in Figure 11. The foil was fixed to the hull via two bearing bolts which allowed the angle of incidence to be changed to any desired angle by changing the middle strut length. To prevent any influence of the middle strut on the resistance it was then taken away for the following tests after the foil was glued to the hull with an angle of $a_D = 3°$. The test program is given as follows:

Test Series no.	***Displacement (Kg)***	***R* (N)***	***LCP % of L_c***	***LCG% of L_c***	***a_D (°)***	***Foil Vertical Position***
10	0.584	5.27	34.4	35.3	3	Foil tip line
11	0.698	6.84	34.4	36.0	3	flush with
12	0.826	8.09	34.4	37.3	3	keel line

The results of the resistance test series 10 to 12 are given in graphical form in Figure 12, where the dimensionless model resistance coefficient e* is shown as a function of the Froude number $F^*_{r\nabla}$. In general the model resistance coefficients e* are similar to those for straight foil arrangements, the swept foil e* being slightly higher (~15%) at lower speeds up to $F^*_{n\nabla} = 3$ and lower (~10%) at maximum speeds. Paint tracer tests on the swept foil at a speed of 3,5 m/s indicate a flowbreak-off of about 30% on the suction side.

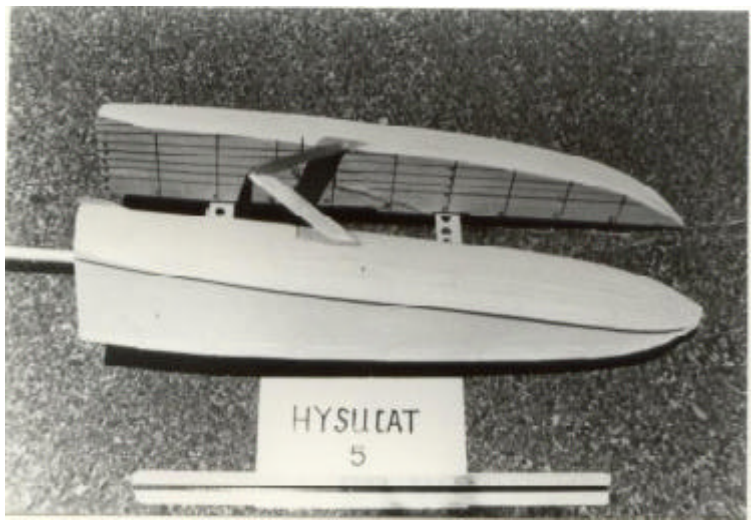

Figure 11: Hysucat 5b with swept foil

This effect is most probably due to laminar flow occurrence and indicates a relatively high foil resistance. A similar tracer test was done for the straight foil at V* = 3,5m/s indicating a much smaller flow break-off area (~10%), most probably due to the lower thickness ratio of the straight foil and the less disturbed flow. From this it could be expected that the straight foil arrangement would result in lower model resistance which is the case only in the lower speed range. The result indicates that the swept dihedral foil in the prototype case will be most probably superior to the straight foil. The observation of the flow over the foil indicates that the swept dihedral foil gives much less disturbance and forward spray than the straight foil once the foil is very near the water surface or breaking the surface. The swept dihedral foil at extreme speed then shows a partly ventilated suction side.

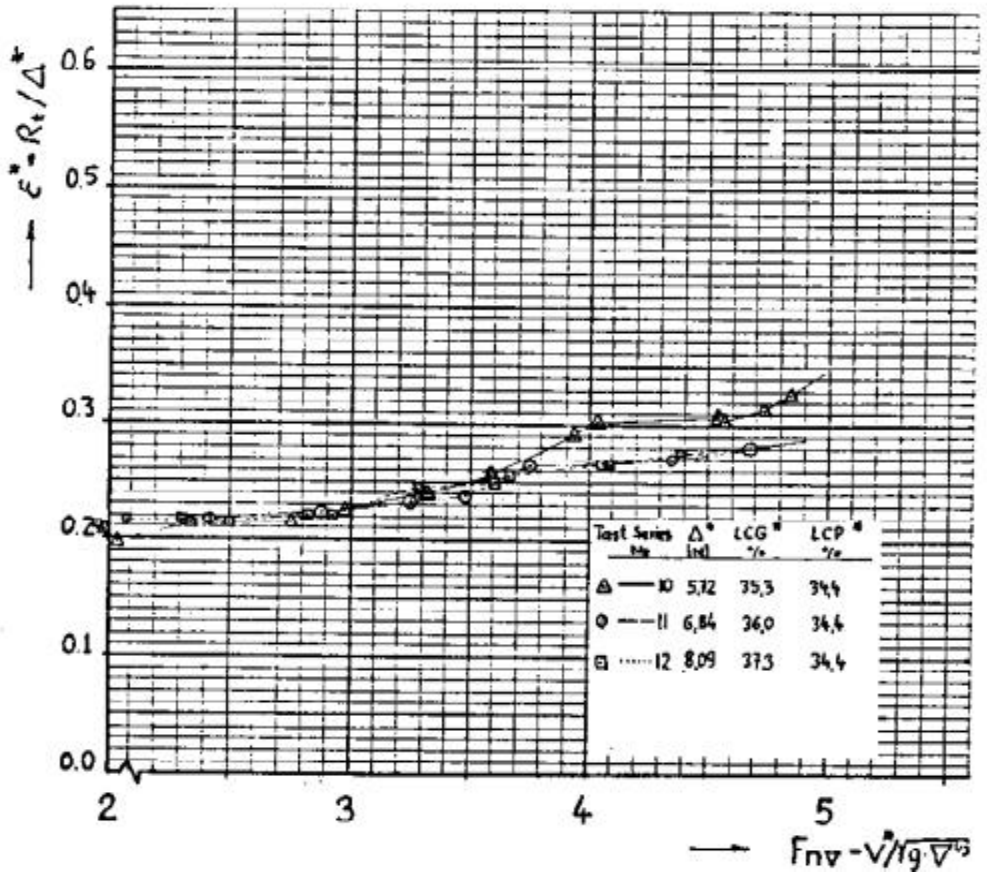

Figure 12: Model Ship Resistance Coefficient e*, Hysucat 5b with Swept foil

In conclusion it can be said that the model resistance tests on the swept foil do not indicate a strong resistance penalty but rather an improved resistance in the prototype case. Tests on larger models with higher foil Reynold Numbers are desirable. As the resistance test results are quite similar for both foil arrangements the correlation calculation will be conducted only for the straight foil arrangement.

3.4.4 Wetted Surfaces and Lengths

For the correlation of the measured model hull resistance test results to a full scale boat the wetted surface area of the hull and the mean wetted length at speed must be known. It was decided to correlate the resistance test results of the test series 8 to a prototype ship of about 10m length and 6,9 t displacement (V_{max} = 40 kn).

A test series was prepared to determine the wetted surface areas of the Hysucat 5a with the straight foil under the same conditions as in test series 8 (?* = 6,33 N, LCP* = 34,9%, LCG* = 35,6%) for five different speeds covering the possible speed range:

V* = 2,40; 2,80; 2,35; 3,68; 4,20 m/s

The wetted surface areas were determined by aid of the paint tracer test described in (11). An example of the paint streak lines is shown on the photograph in Figure 6. The wetted surface was worked out on the model directly after each run by adding up all the single hull surface elements indicated by the trace lines to have been in contact with solid water (defined in reference (13).

The results are given in Table 1:

V* m/s	Wetted Surfaces (m^2)	Wetted mean length (m)	S^*/S_D^*	l_m^*/l_{mD}^*
0	$647,4.10^{-4}$	0,382	-	-
2,40	$325,6.10^{-4}$	0,261	0,504	0,683
2,80	$318,1.10^{-4}$	0,254	0,491	0,665
3,25	$347,1.10^{-4}$	0,251	0,536	0,657
3,68	$396,2.10^{-4}$	0,281	0,612	0,736
4,20	$353,0.10^{-4}$	0,276	0,546	0,723

Δ^* = 6.33 (N) LCG* = 35.8 LCP* = 34,9 $\alpha_\Box$ = 2,6°

Table 1: Wetted surface and mean Lengths in Test Series 8

3.4.5 Foil and Hull Load Distribution

For the prediction of the prototype resistance of the Hysucat hull the weight load which the support hydrofoil will support in each specific case has to be known as the correlation calculation has to be performed for hull and foil as separate units but with consideration of the interference effect of demi hull to demi hull and foil. It was tried to calculate the foil lift considering its angle of attack towards the inflow when installed on the Hysucat, but he result was unsatisfactory as the interference effect hull-foil and the nearness of the foil to the water surface could not be properly accounted for.

It was therefore decided to measure the foil forces and interference effect by running the Hysucat model under the Test Series No.8 conditions in separate test runs keeping the speed constant with the straight foil installed and in the same trim and heave position without the foil, measuring the resistance and the vertical forces necessary to keep the Hysucat without foil in the same position as with the foil at speed.

This test series (no.13) could be performed by installing a vertical plane plank over the longitudinal center line of the model in the water-circulating tunnel and fixing the position of the Hysucat model with the foil installed by two thin vertical ropes, one near the bow and one near the stern in the longitudinal center plane of the model. The two vertical lines were fixed to the plank at a specific speed to hold it in position as a double pendulum arrangement. The model resistance was then measured and recorded and then the foil removed from the hull. By applying a towing force via a spring balance to the model without foil it was returned to exactly the position where it had been measured with the foil, the pendulum ropes then being exactly vertical. The recorded resistance of the towing force is the isolated hull resistance without foil and interference effect called R^*_i. It was expected that this resistance would be lower than the model-with-foil-resistance R^*_t, but this was not the case. As can be seen from Table 2, R^*_i is nearly the same as R^*_t in the lower speed range. This indicates that the resistance improvement due to the interference effect of the foil on the hull is in the same order and stronger than the model foil resistance. It becomes clear that the interference effect foil-on-hull plays an important role in the resistance improvement of the Hysucat hull.

In return, there is an interference effect hull-on-foil which could not be measured in the present test set-up. The results of Test Series 13 are given in Table 14 including model speed V*, Hysucat 5a model with straight foil resistance R^*_t and its coefficient e*, the vertical pendulum rope forces forward $F_{v.f.}$ and near stern $F_{v.st.}$, the isolated hull without foil resistance R^*_i and its coefficient e_i, the sum of the vertical forces to hold the hull without foil in position, F_v, and its percentage towards the boat weight and X_v, its longitudinal position in percent of L^*_c, the angle of incidence of the foil a_f and the angle of incidence of the hull bottom area near the foil attachment (bottom slightly curved).

The test results in Table 2 show that the foil takes up about 43% of the displacement weight and is (astonishingly) nearly constant over the investigated speed range. The resultant vertical F_v is not positioned at the foils pressure center, but in all tested cases slightly aft of it. This is a result of the foil-on-hull interference effect. The trim angle a_n and foil incidence angle a_f are also nearly constant in the measured speed range. The strong tendency of the Hysucat to hold the trim angle constant was observed in all tests and indicates a completely different behavior than observed on

usual deep-V-craft. This may be another reason for the much lower hump resistance of the Hysucat compared with other planing craft and hydrofoil boats.

The model hydrofoil was isolated from the model boat and tested in the water-circulating tunnel. To simulate the side wall effect, when installed inside the Hysucat tunnel, two end plates were fitted. Lift-force and drag-force measurements were conducted for one constant angle of attack of 3,8° (as mainly used in model arrangement), three different speeds of 3,75 m/s ; 3,26 n/s ; 2,96 m/s were used, resulting in the respective Reynolds numbers of $R_{e1} = 0{,}83 * 10^5$, $R_{e2} = 0{,}72 * 10^5$, $R_{e3} = 0{,}65 * 10^5$. For various constant loads the water heights over the hydrofoil were also recorded. The result of the isolated foil test is shown in Fig. 14 in form of the drag-lift ratio plotted over the water height above the foil (h). Fig. 13 shows the variation of the drag coefficient C_D and the lift coefficient C_L with water-height above the foil.

Test No.	V* m/s	$F^*_{n\nabla}$	R^*_t (N)	ϵ_t*	F^*_{vf} (N)	$F^*_{v,st}$ (N)	ΣF_v (N)	F_v in % of Δ	X_v in %	R^*_1 (N)	ϵ_1*	α_f (°)	α_h (°)	h_{mm}
0	0	-	-	-	-	-	-	-	0	0	0	- 3,12	2,21	-
1	2,40	2,61	1,137	0,179	0,441	2,254	2,695	42,5	31,84	1,137	0,179	+ 3,10	+ 5,83	27
2	2,80	3,04	1,225	0,193	0,588	2,352	2,940	46,4	34,71	1,294	0,204	+ 3,48	+ 6,21	24
3	3,20	3,53	1,401	0,221	0,343	2,548	2,891	45,6	28,30	1,431	0,226	+ 3,48	+ 6,21	18
4	3,60	4,10	1,558	0,246	0,392	2,352	2,744	43,3	30,21	1,617	0,255	+ 3,48	+ 6,21	13
5	4,20	4,56	1,775	0,272	0,490	2,303	2,793	44,0	32,77	1,813	0,286	+ 3,48	+ 6,21	8

Longitudinal positions of vertical ropes $X_{v,st}$ = 85,25 mm, X_{vf} = 44,0 mm from transom

Δ* = 6,33 (N) LCB* = 35,6% LCP* = 34,9% α_f = 2,6° against deck level line

Table 2: Test Series No. 13 foil and hull load distribution, Test Series 8 conditions

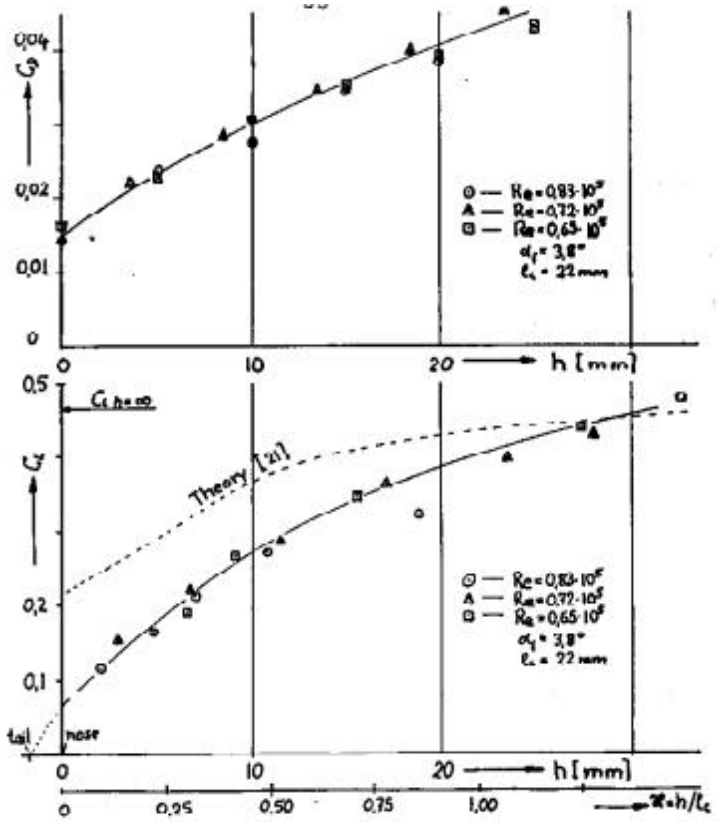

Figure 13: Drag and Lift Ratios in Surface Effect of Isolated Model Foil with Endplates

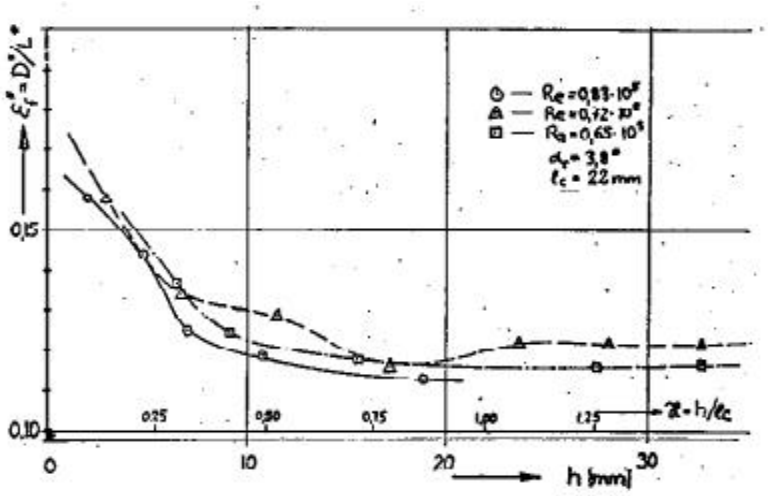

Figure 14: Drag-lift Ratios of Isolated Model Foil with Endplates

3.4.6 General Sea-keeping of Hysucat Model:

The smooth water sea-keeping of the Hysucat model was observed during all test runs and concerns mainly the directional stability or course holding ability and the tendency to porpoising, the trim at speed and softness of ride. Further tests were conducted on the model in regular head waves in the water-circulating tunnel in comparison with a successful deep-V-hull described and tested in (11).

A short summary of the observations shall be given only:

The Hysucat model without the hydrofoil "suffered" strongly of porpoising which was considerably improved when the hydrofoil was mounted but it still shows a light tendency to porpoising at top speed if the longitudinal center of gravity LCG* is positioned excessively aft. The porpoising tendency of the heavier loaded hull appears already at relatively lower speeds. The intensity and frequency of the porpoising motions increase with rising speed. The lowest resistances are measured for LCG* positions slightly forward of the ones for which porpoising starts. Once porpoising is observed on the model the measured resistances are higher than without it. Porpoising has to be prevented and conditions where it appears strongly are excluded in the present report. The LCG* positions in this report are chosen as to avoid strong porpoising. The longitudinal center of pressure LCP* of the foil has to be positioned slightly aft of the LCG* position for freedom of porpoising. If porpoising in a specific case may appear the distance between LCG* and LCP* has to be increased by either shifting LCG* forward or LCP* sternwards. Should the distance between these two points become excessively large, the resistance on the model increases because the foil imposes a head-down-trim onto the hull which then runs at too low incidence angles which increases the resistance especially at the higher speeds. It is seen that the proper positioning of LCP* is of utmost importance and can be used to achieve desired hull behavior.

For all the tests reported here the model showed excellent directional stability and the rudder-like stern plates visible on the lower photograph in Figure 11, were unnecessary and could be removed. In other tests slight yaw oscillations could be observed when the LCG* position was extremely forward, but his was in any case an unexceptable condition as the resistance of the Hysucat is then higher than the bare hull resistance in the high speed range. The trim of the Hysucat model at speed was observed in all tests to be nearly constant over the whole speed range which is quite different from usual planing craft. Also the excessive trim near the so-called "hump resistance" was not observed from which it could be concluded that it is much easier and requires less power reserves to bring the Hysucat craft into the planing state. This is a significant advantage as all deep-V-planing craft and hydrofoil craft require a high power reserve at this low speed and fixed pitch propellers are often not able to perform well at hump speed as well as top speed, resulting in a strongly reduced top speed. Therefore it is believed that the design of the propulsion system of a Hysucat craft would be much easier and cheaper than on hydrofoil or deep-V-planing craft.

The Hysucat model shows a much softer ride, but still produces strong transverse stability at speed and even when listed slightly it runs straight and steady. The vertical heave and trim motions of the Hysucat which result from disturbances in the water-inflow or from small waves are strongly reduced compared with the hull without foil. In head waves the Hysucat also shows softer reaction motions, but naturally follows the movement of larger waves in a similar way as the tested deep-V-hull. Strong motions with deep dipping of the bows are observed for Hysucat and deep-V-hull in a very similar way at wave lengths near to the ship lengths. The survivability of heavy seas seems to be about similar for both models and no dangerous behavior was observed on the Hysucat model.

In long waves at high speed the Hysucat model shows a greater tendency to "fly" out of the water when a wave crest is passed. The sudden lifting forces under the bow tend to lift the bows, but in the meantime the foil produces higher lift forces which in certain critical conditions lead to the model flying free with about constant trim angle. The re-entry after the crest has passed is smoother for the Hysucat with the swept foil. The comparable deep-V-hull shows similar tendencies, but not nearly as strong and much more quickly experiences the bow-down-movement when the end of the boat goes through the crest. This special behavior observed on the Hysucat model needs more investigation as at this stage it cannot be said if it is of advantage or disadvantage.

The use of the tandem hydrofoil system as proposed in (3) will change this behavior, which is typical for the mono-hydrofoil system only. A Hysucat after (3) will behave more like a deep-V-hull if the sternfoil is large in relation to the mainfoil. Hysucats with relatively small sternfoils will show a trim behavior at speed in waves between the deep-V-hull and the mono-hydrofoil Hysucat. The dimensioning of the tandem-foil system (3)can be used to reach any desired behavior at speed in waves.

In summary it can be said that the Hysucat craft will show a similar behavior in head-seas as a deep-V-craft but with lower accelerations and a smoother ride. It will have better sea-keeping behavior than the hull without the foil. Directional stability is good and no broaching tendencies could be traced.

3.5 Model to Ship Correlation

3.5.1 Theoretical Background

As for displacement ships the model resistance may be split up into a resistance caused by frictional forces along the wetted surface and the residual resistance which in case of a planing craft is caused mainly by the drag forces induced by the planing bottom surface (20). The lifting forces are equal to the weight of the ship when fully planing. The lift forces are proportional at $A * V^2$

With A = area of planing surface
V = speed of boat

Similarity between model ship and prototype is reached when the equilibrium condition; boat weight equal lift forces, applies:

$$\frac{\Delta}{A.V^2} = \frac{\Delta^*}{A^*.V^{*2}} \qquad \ldots\ldots\ldots\ldots 1$$

or

$$\frac{\Delta}{\Delta^*} = \frac{A.V^2}{A^*.V^{*2}} \qquad \ldots\ldots\ldots\ldots 2$$

In a dimensional analysis follows that:

$$\frac{\Delta}{\Delta^*} = \frac{L_s^3}{L_s^{*3}} = \lambda^3 \qquad \ldots\ldots\ldots\ldots 3$$

with L_s = significant ship length and
L_s^* = the corresponding model ship length,
? = L_s / L_s^* , the scale ratio

The surfaces A and A* are in the relation:

$$\frac{A}{A^*} = \frac{L_s^2}{L_s^{*2}} = \lambda^2 \qquad \ldots\ldots\ldots\ldots 4$$

so that for equation 4.1 results:

$$\lambda^3 = \lambda^2 \cdot \frac{V^2}{V^{*2}}$$

or

$$V^* = \frac{V}{\sqrt{\lambda}} \qquad \ldots\ldots\ldots\ldots 5$$

The residual resistance of the model has to be scaled up in the ratio $?^3$ after the frictional resistance has been deducted from the measured model resistance which is the same procedure as for displacement ships. However, the wetted surface of the planing craft changes with speed and trim and has to be measured on the model as well.

3l.5.2 ***Development of the Correlation Factor***

Froude's law of comparison may be stated in a modern form for planing craft in the following way. Two geometrically similar planing hulls are run at the same Froude number which may be based upon a significant length dimension L_s

$$F_n = \frac{V}{\sqrt{g \cdot L_s}} = \frac{V^*}{\sqrt{g \cdot L_s^*}} \qquad \ldots\ldots 6$$

As the length of the planing hull in touch with water changes with speed and trim, it is usual to base a significant length dimension on the displacement volume alone:

$$L_s = \nabla^{1/3}$$

which leads to the so called Froude-displacement-number

$$F_{n\nabla} = \frac{V}{\sqrt{g.\nabla^{1/3}}} = \frac{V^*}{\sqrt{g.\nabla^{*1/3}}} \quad \ldots\ 7$$

Running at same Froude numbers the residual resistance of model and ship are similar and can be correlated by Froude's law:

$$R_r = R_r^* . \lambda^3 \quad \ldots\ 8$$

with other words the residual resistance coefficients

$$C_r = C_r^* = R_r / \frac{\rho}{2} . V^2 . S_c = R_r^* / \frac{\rho^*}{2} . V^{*2} . S_c^* \quad \ldots\ 9$$

are the same for ship and model.

The model's friction resistance is determined by use of the smooth -turbulent Model-Ship-Correlation-Line proposed by the ITTC 57

$$C_f^* = 0{,}075/(\text{Log } R_e^* - 2)^2$$

With C^*_f = friction coefficient and $R^*_e = V^* . L^*_m / ?^*$ and results in :

$$R_f^* = C_f^* . \frac{\rho^*}{2} . V^{*2} . S_c^* \quad \ldots\ 10$$

with S^*_c = wetted surface of hull in contact with solid water after (13).

From equations 9 and 10 it is clear that the wetted surface S* has to be determined accurately and that the occurrence of laminar flow has to be prevented as C^*_f is valid only for turbulent flow.

The model residual resistance is then the measured model resistance minus the friction resistance after 10.

$$R_r^* = R_t^* - R_f^* \quad \ldots\ 11$$

and for 9 follows:

$$C_r^* = (R_t^* - R_f^*)\frac{\rho^*}{2} V^{*2} . S_c^* \quad \ldots\ 12$$

which is equal to:

$$C_r = R_r \Big/ \frac{\rho}{2} V^2 . S_c$$

from which results :

$$R_r = (R_t^* - R_f^*) . \frac{\rho}{2} V^2 . S_c \Big/ \frac{\rho^*}{2} . V^{*2} . S_c^* \quad \ldots\ 13$$

Taking into account the different densities of model test water and sea water, acceleration of earth g assumed constant, equation 8 becomes:

$$R_r = R_r^* . \lambda^3 . \frac{\rho}{\rho^*}$$

and equation 13 with equation 10 results in:

$$R_r = \frac{\rho}{\rho^*} . \lambda^3 (R_t^* - C_f^* . \frac{\rho^*}{2} . V^{*2} . S_c^*) \quad \ldots\ 14$$

which contains only model data.

The frictional resistance of the prototype ship is:

$$R_f = (C_f + \Delta C_f) . \frac{\rho}{2} . V^2 . S_c \quad \ldots\ 15$$

with $?C_f$= roughness allowance which accounts for the relatively rougher surface of the prototype against the smooth model.

The term $\frac{\rho}{2}.V^2.S_c$ equation 15 is in dimensional form a force and it can be transformed by Froude's law to:

$$\frac{\rho}{2}.V^2.S_c = \lambda^3.\frac{\rho^*}{2}.V^{*2}.S_c^* \quad .... \quad 16$$

The total resistance of the prototype ship is the sum of the prototype residual and frictional resistance

$$R_t = R_r + R_f$$

which follows with the equations 13, 15 and 16 to

$$R_t = \frac{\rho}{\rho^*}.\lambda^3\{R_t^* - \frac{\rho^*}{2}.V^{*2}.S_c^*(C_f^* - C_f - \Delta C_f)\} \quad .... \quad 17$$

The term $(C_f^* - C_f - \Delta C_f)\frac{\rho^*}{2}.V^{*2}.S_c^*$ is called the friction deduction. It is the force of the relatively higher model skin friction.

The resistance of a planing craft is usually presented in dimensionless form as the resistance-weight force ratioe,

$$\varepsilon = R_t/\Delta \quad .... \quad 18$$

with ? = weight force of the displacement.

From the equations 17 and 18 follows:

$$\varepsilon = \varepsilon^*\{1 - \frac{\frac{\rho^*}{2}V^{*2}.S^*(C_f^* - C_f - \Delta C_f)}{R_t^*}\} \quad .... \quad 19$$

assuming $\rho/\rho^* = 1$.

With $C_t^* = R_t^*/\frac{\rho^*}{2}.V^{*2}.S_c^*$ it becomes:

$$\varepsilon = \varepsilon^*(1 - \frac{C_f^* - C_f - \Delta C_f}{C_t^*}) \quad .... \quad 20$$

The term in the brackets is called the correlation factor k_{corr}

$$\varepsilon = \varepsilon^*.k_{corr} \quad .... \quad 21$$

For the smaller planing craft as investigated in the present thesis the roughness allowance $?C_f$ can be assumed after (13) to be zero for carefully worked surface conditions and then:

$$\Delta C_f = 0 \qquad \ldots\ 22$$

The correlation factor k_{corr} is:

$$k_{corr} = 1 - \frac{C_f^* - C_f}{C_t^*} \qquad \ldots\ 23$$

With C^*_f being the model's friction coefficient after ITTC 57:

C_f being the prototype friction coefficient after ITTC 57

$?C_f$ being the roughness allowance, assumed zero for the smaller boats with high surface quality

and C^*_t being the model's total resi stance coefficient based on wetted area at speed.

k_{corr} becomes unity when model and ship are of equal dimensions as $(C_f^* - C_f)/C_t^*$ is then zero. The smaller the model size the larger the term $(C_f^* - C_f)/C_t^*$ becomes. For the 2.6m long Series 62 models (13) it was about 0, 14, for the 0,45m model of a deep-V-hull tested in (11) it is up to 0,44.

As this value is based upon the measurements of the model resistance, the model speed and the model's wetted surface it becomes clear that the correlation becomes much more sensitive to inaccuracies in the measurements for the smaller models. Especially the measurement of the wetted surface of the hull in touch with solid water is relatively inaccurate and makes the correlation for the small models comparatively much less reliable than for the larger models.

A error of +10% in the determination of the wetted surface would result in a resistance prediction error of

$$\frac{1 - 0,14}{1 - 0,14*1.1} = \frac{0,86}{0.846} = 1,0165 \triangleq 1,65\%$$

for the 2,6m long models and

$$\frac{1 - 0,44}{1 - 0,44*1.1} = \frac{0,56}{0,516} = 1,0853 \triangleq 8,53\%$$

for the 0,45m long models for the predicted prototype resistance ratio e of a ship with a displacement of 16 t.

The testing of many different small models in the water-circulating tunnel allows the collection of experience data concerning the correlation factor k_{corr} which is very useful for future work.

3.5.3 Prototype Bare-Hull Resistance

The correlation factor k_{corr} for the Hysucat hull without the foil installed is assumed to be similar to the ones measured and calculated on the IMT -catamaran hull (12) of similar size, which even compares relatively well with the correlation factor for a monohull with similar model dimensions and scale ratio ? as tested in (11). Both models have the same length and approximate displacements and the same scale ratio and were tested in the same water -circulating tank. The correlation factor k_{corr} of the IMT -catamaran hull tested for various displacements and longitudinal centers of gravity LCG* is shown in Figure 15. The correlation factor varies slightly with displacement and is smaller for the longitudinal center of gravity most forward (40%). As it was not the objective of the present test series to investigate the bare hull catamaran resistance which is needed only for comparison reasons to indicate the improvement gained by the Hysucat principle and wetted area tests are extremely time consuming, the bare hull resistance coefficients were correlated with a mean correlation factor k_{corr} taken from (12) and shown in Figure 13. The mean correlation factors employed are given in the graph in Figure 14, which is used to compute the bare-hull resistance of the 10m design proposal catamaran. The resistance coefficients of this prototype are presented in graphical form for the Test Series 1 to 5 in Figure 17.

For comparison reason the resistance coefficient of a deep-V-monohull of 16t (? * = 4,24 N, L_c = 0,45m) is plotted on the same diagram and gives a good impression of the catamaran's much higher resistance coefficient.

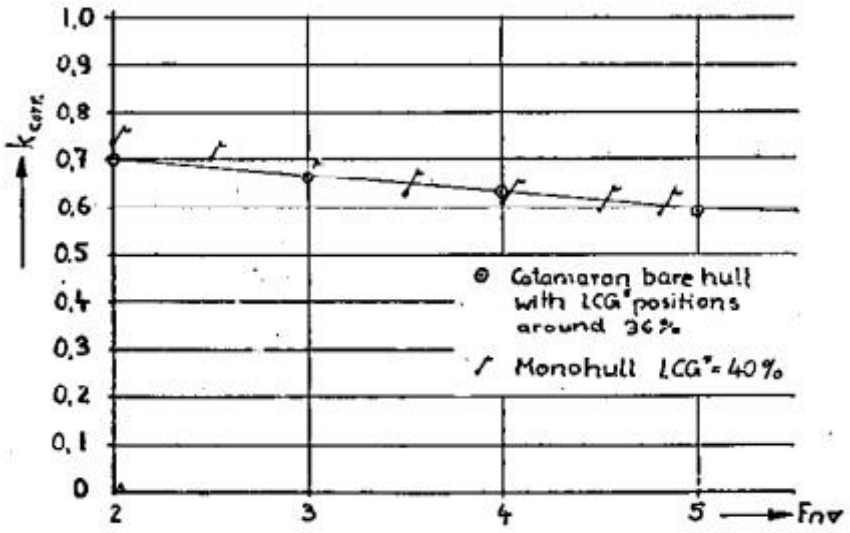

Figure 15: Prototype Hysucat Resistance Predicion

A straight forward correlation calculation as used on the bare hull (12) seems not to deliver sufficient accurate and reliable resistance predictions for the Hysucat as the specific planing hull bottom loads are much lower than the loads on the support hydrofoil. In the present test the occurrence of laminar flow on the hydrofoil, which has a Reynolds number of $R^*_{e\,foil} = 0{,}88.10^5$ at maximum speed, cannot be ruled out and has been taken into account. Laminar flow over the hydrofoil will reduce the friction resistance but increases the profile's drag as the laminar flow breaks off more easily at places of profile curvature with positive pressure gradient (suction side) which increases the drag (especially for larger angles of attack) and reduces the lift. Foil areas with flow break-away appearance were traced with the aid of paint tracer tests which are described in chapter 5.3.

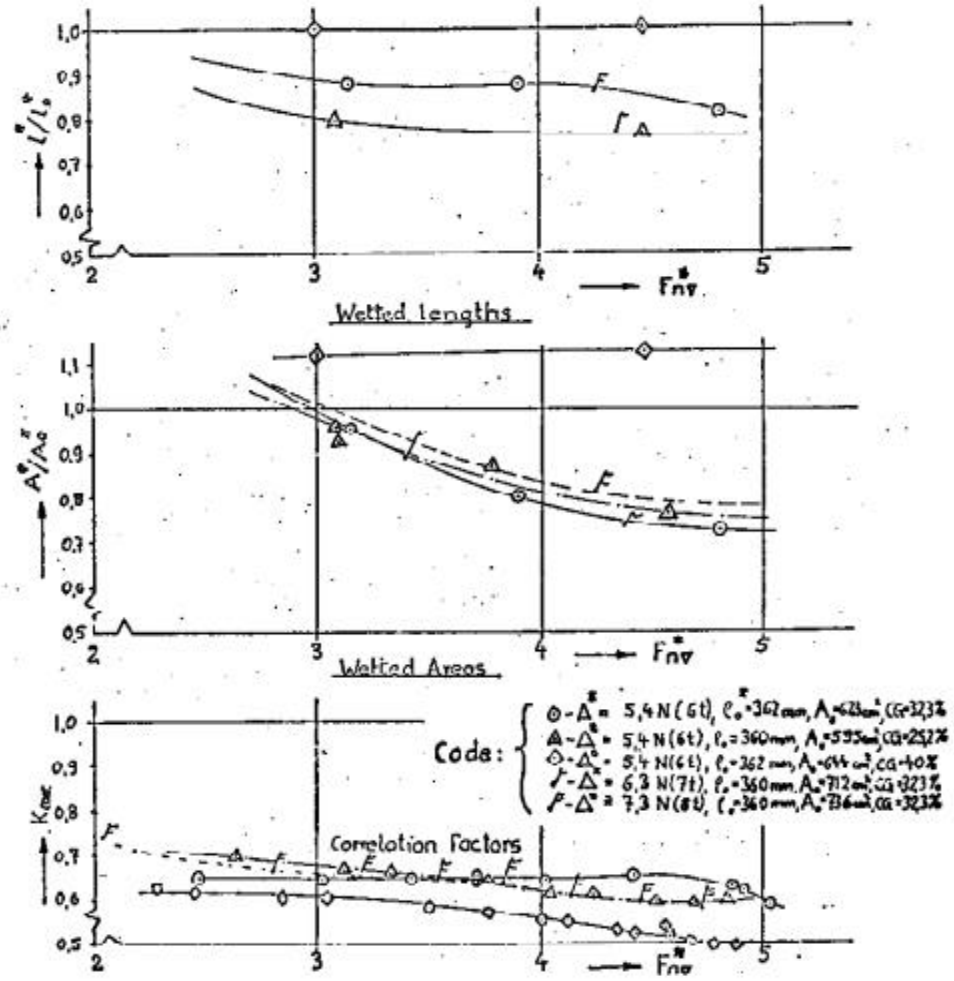

Figure 16: Correlation Factors for 0,45m IMT Catamaran, Reference (2).

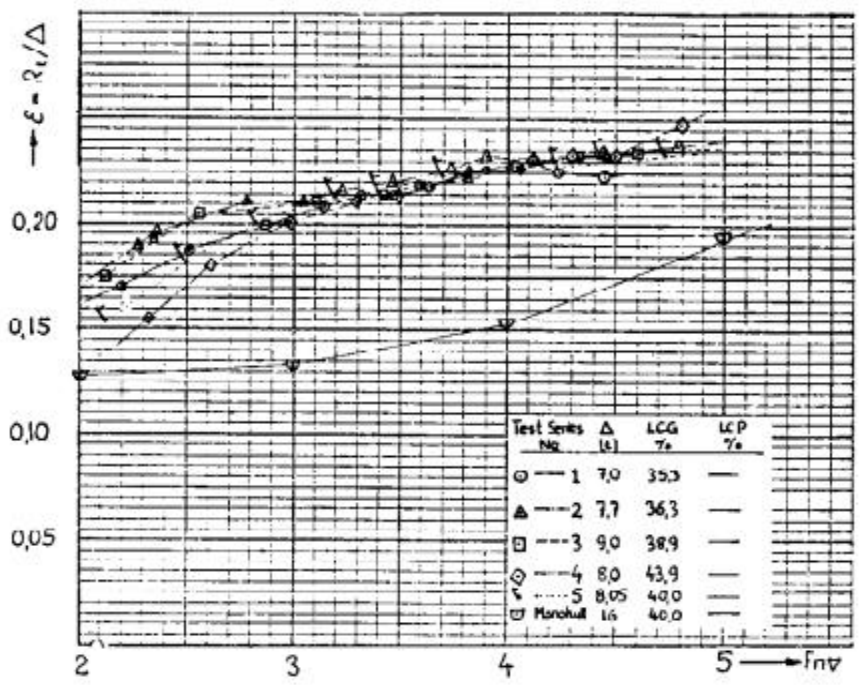

Figure 17: Ship Resistance Coefficient e, Hysucat 5 (10 m), Bare hull

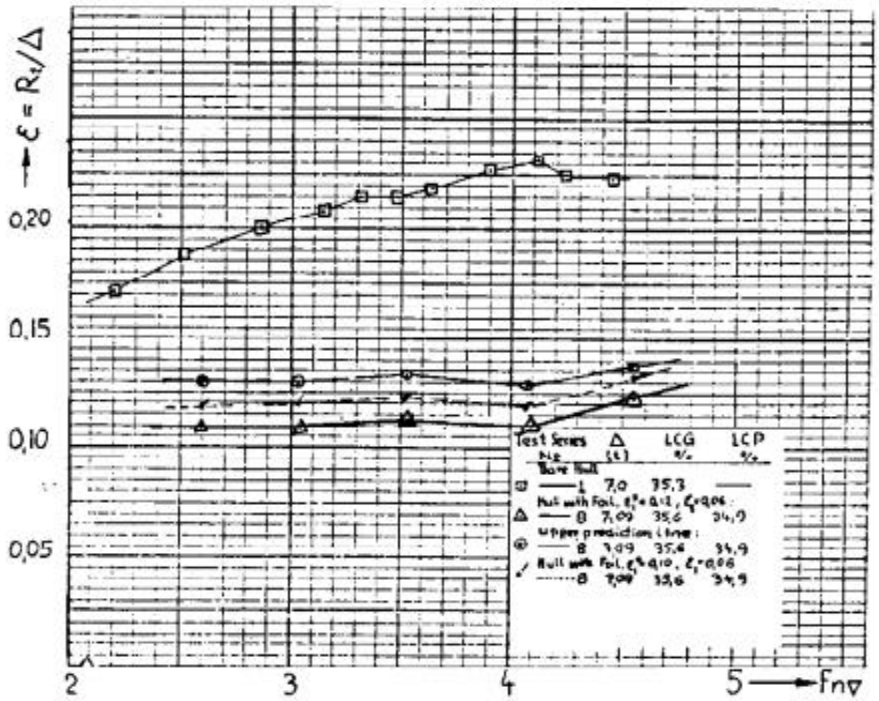

Figure 18: Ship Resistance Coefficient e, Hysucat 5 (10 m), with and without Foil, Test Series No. 8

However, to establish an upper limiting curve of the Hysucat resistance a straight forward correlation calculation will be tried assuming laminar flow over the hydrofoil but neglecting the increased form drag. The friction coefficient of the model hull for turbulent flow at a Reynolds number of about $R^*_e = 1.10^6$ is very much the same as the laminar friction coefficient of the foil with a Reynolds number of $R^*_{e\,foil} = 0{,}8.10^5$ which also is about valid for both corresponding friction coefficients of the prototypes (see friction line in (14), chapter 7, Figure 3.) This means that the friction differences between the model and prototype of hull and foil are nearly the same, which allows a combined treatment. As the laminar flow foil form drag on the model is neglected, it can be assumed that this prediction will result in too high prototype resistance predictions and it can be regarded as an upper prediction resistance line, the real prototype resistance being somewhat smaller. This will be worked out in more detail later.

Test No.	V^* m/s	$F^*_{n\nabla}$	S^*_{H+F} m^2	ℓ^*_{st} m	$R^*_e.10^{-6}$	$Re.10^{-6}$	$C^*_f.10^3$	$C_f.10^3$	$\Delta C_f.10^3$	$\frac{\rho}{2}.V^{*2}.S^*_{H+F}$	R^*_t (N)	$c^*_t.10^3$	K_{corr}	e^*	e
1	2,40	2,61	$361.2.10^{-4}$	0,281	0,626	84,60	5,203	2,222	2,981	104,03	1,137	10,93	0,727	0,179	0,130
2	2,80	3,04	$363.2.10^{-4}$	0,354	0,791	73,37	5,055	2,180	2,875	138,45	1,225	8,85	0,675	0,183	0,190
3	3,25	3,53	$382.2.10^{-4}$	0,251	0,818	84,20	4,902	2,136	2,765	201,85	1,401	6,94	0,601	0,221	0,133
4	3,68	4,10	$431.2.10^{-4}$	0,281	1,034	106,70	4,654	2,064	2,590	281,87	1,558	5,54	0,515	0,246	0,127
5	4,20	4,55	$388.2.10^{-4}$	0,276	1,159	119,60	4,541	2,030	2,511	342,39	1,725	5,04	0,502	0,272	0,137

Laminar flow assumed over foil, foil form drag of model neglected

Δ = 7,10 t LCG = 35,6% LCP = 34,0% λ = 22,22 L_{prot} = 10 m

Table 3: Straight forward Correlation Calculation on Hysucat 5a with Foil (giving upper resistance prediction line)

The correlation calculation for resistance Test Series No. 8 is given in Table 3 and the resultant prototype resistance coefficient e plotted over the Froude number is shown in Figure 18, from which the considerable resistance reduction due to the support hydrofoil becomes clear. This reaches a maximum of 41% at $Fn\nabla$ = 4 and in reality will be more when the model foil's increased form drag is considered. It is interesting to note that even at relatively low Froude numbers considerable improvements are achieved, which indicates that the so-called resistance hump will also be lower (which cannot be tested in the present supercritical water-circulating tank).

3.5.4 Separate Correlation Calculation

A more reliable resistance prediction from the measured model data is possible when the Hysucat hull and the support foil are treated as separate items. To enable this kind of correlation calculation the load and resistance of the support hydrofoil during operation and when attached to the catamaran hull have to be measured, which was assumed to be too complicated at this stage of the investigation with the relatively

small model. However, a good approach is possible by measuring the Hysucat (with foil) resistance, fixing the heave and trim position of the model in the water-circulating tank at speed and then removing the foil and measuring the bare hull resistance in the same hull position, so that the isolated hull resistance minus the foil-onto-hull interference effect are determined. Further, by measuring the vertical forces to hold the bare hull model in the same position at speed as the hull with foil, the lifting forces of the foil plus the foil-onto-hull interference effect were determined allowing a good guess of the lift forces the foil produced. The tests have been described in chapter 3.4.5 and indicate that about 44% of the Hysucat weight is carried by the foil (plus it interference effect on the hulls). The isolated hull resistance was slightly higher than the Hysucat with foil resistance, indicating the importance of the foil-onto-hull interference effect which reduced the Hysucat hull resistance by more than the resistance of the model foil (with endplates) which was measured to be an average $e^*_f = 0{,}12$.

The isolated model hull resistance R_{h+int}. is established for the following correlation calculation by subtracting the model foil resistance R^*_f from the measured Hysucat-with-foil-model-resistance R^*_t which is possible when the isolated model foil resistance R^*_f is known. Measurements of R^*_f with the model foil were conducted, of which the drag-lift-ratios are given in Figure 14 for various speeds, an incidence angle $a = 3{,}8°$, and various depths of sub mergence. For operation very close to the surface the foil's drag-lift-ratios increase, but for depths of more than 30% of the chord length the mean drag-lift-ratio of the model foil is constant and about 0,12. The best measured value was 0,114. The lift reduction due to surface nearness of the tested foil is shown in Fig. 13 and compared to the theoretical value after (21). The discrepancy cannot be explained at this stage but may be influenced by scale effects and water-level quality at speed in the tank.

Test No.	V^* m/s	F^*_{nV}	R^*_t (N)	c^*_t	Measured R^*_i (N)	c^*_i	$F_{v_{foil}}$ %	Hull % Δ	R^*_f (N)	R^*_t-R^*_f(N)	c^*_{h-f}	$S^*.10^4$ m²	t^* (m)	$R^*_e.10^-$
1	2,40	2,61	1,137	0,179	1,137	0,179	42,5	57,5	0,269	0,867	0,238	326	0,261	0,626
2	2,60	3,04	1,225	0,193	1,294	0,204	46,4	53,6	0,294	0,931	0,274	318	0,254	0,711
3	3,25	3,53	1,401	0,221	1,431	0,226	45,6	54,4	0,288	1,113	0,322	347	0,251	0,810
4	3,68	4,10	1,558	0,246	1,617	0,255	43,3	56,7	0,274	1,284	0,357	386	0,261	1.034
5	4,20	4,56	1,725	0,272	1,813	0,286	44,0	56,0	0,279	1,446	0,407	353	0,276	1,159

Table continued

Test No.	$R_e.10^{-9}$	$C^*_f.10^3$	$C_f.10^3$	$\Delta C_f.10^3$	$\frac{\rho^*}{2}V^{*2}.S^*$ (N/m²)	$C^*_{t\ h-f}.10^3$	$K_{corr\ h-f}$	c_{h-f}	Assumed c_f	c_t	$K_{corr\ total}$
1	64,6	5,203	2,222	2,981	93,88	9,237	0,877	0,161	0,06	0,118	0,66
2	73,4	5,055	2,180	2,875	124,66	7,468	0,815	0,159	0,06	0,118	0,61
3	84,2	4,902	2,138	2,766	183,26	6,070	0,544	0,175	0,06	0,123	0,56
4	105,7	4,654	2,064	2,590	269,14	4,766	0,459	0,184	0,06	0,119	0,45
5	119,8	4,541	2,030	2,511	311,35	4,869	0,459	0,197	0,06	0,131	0,48

Δ^* = 6,34 N Δ = 7,1 t L_p = 10 m λ = 22,22

LCG* = 35,6% LCF* = 34,9% D^*/L^* = 0,1 assumed

Table 4: Hull-foil Separated Correlation Calculation, Resistance Test Series No.8

Test No.	V^* m/s	F^*_{nV}	Table 16 c^*_t	Measured R^*_i (N)	c^*_i	$F_{v_{foil}}$ %Δ	$F_{v_{hulls}}$ %Δ	R^*_f (N)	R^*_t-R^*_f(N)	c^*_{h-f}	$\frac{\rho^*}{2}V^{*2}.S^*$	$C_{t\ h-f}.10^3$
1	2,40	2,61	0,179	1,137	0,179	42,5	57,5	0,269	0,868	0,238	89,89	8,661
2	2,60	3,04	0,193	1,294	0,204	46,4	53,6	0,353	0,872	0,257	124,66	6,895
3	3,25	3,53	0,221	1,431	0,226	45,6	54,4	0,347	1,054	0,306	183,26	5,754
4	3,68	4,10	0,246	1,617	0,255	43,3	56,7	0,329	1,220	0,342	268,14	4,582
5	4,20	4,56	0,272	1,813	0,286	44,0	56,0	0,335	1,390	0,392	311,35	4,465

Table continued

With the assumption of a prototype Drag-Lift-Ratio of 0,08

Test No.	$\Delta C_f.10^3$	K_{corr}	c_{h-f}	c_f	c_t	$K_{corr\ total}$	c_f	c_t
1	2,981	0,656	0,1463	0,06	0,1056	0,6123	0,08	0,118
2	2,875	0,588	0,1511	0,06	0,1088	0,5832	0,08	0,118
3	2,766	0,518	0,1589	0,06	0,1139	0,5149	0,08	0,123
4	2,590	0,435	0,1487	0,06	0,1103	0,4484	0,08	0,119
5	2,511	0,438	0,1715	0,06	0,1224	0,4500	0,08	0,131

Δ^* = 6,34 N Δ = 7,1 t L_p = 10 m λ = 22,22

LCG* = 35,6% LCF* = 34,9% D^*/L^* = 0,12 assumed and measured on the isolated foil

Table 5: Hull-foil Separated Correlation Calculation, Resistance Test Series No. 8

This allows the separate correlation calculation to be conducted. The prototype is a 10 m, 7,1 t, 40 knot boat, which means that the scale ratio is ? = 22,22. The correlation calculation for the Test Series 8 is given in Table 5 and contains the following steps:
The Hysucat model resistance (with foil) R^*_t is used as the starting point from which the resistance of the model foil R^*_f is subtracted employing the measured model drag-lift-ratio $e^*_f = 0{,}12$, see Fig. 17 (for comparison reasons a similar calculation with $e^*_f = 0{,}10$ is given in Table 4) and proportion of weight taken up by the foil. The remaining resistance $R^*_t - R^*_f$ is the isolated hull resistance including the interference effect of the foil-on-the-hull (named $e^*_{h+int.}$) , which is correlated corresponding to equation (20) and gives the resistance of the hull (with interference effect) of the prototype e_{h+int} . In proportion to the weight component it supports, the prototype foil resistance e_{foil} , assumed conservatively with $e_{foil} = 0{,}06$ (L/D =17), is added, giving the total prototype Hysucat resistance coefficient e_{tot} which is plotted in the diagram in Figure 16 in comparison to the resistance coefficient of the catamaran without foil. Also given in Tables 4 and 5 are the total correlation factors K_{corr} for the Hysucat Test which can be used with good approximation to correlate the other model test series with the Hysucat model (which is left to the interested reader.)

The diagram in Figure 16 also contains the "upper resistance prediction curve" developed previously in the straight forward correlation calculation which gives a resistance prediction which is about 12 to 19% higher, bus shows otherwise similar tendencies. The diagram in Figure 16 shows the tremendous resistance improvement due to the support hydrofoil which is apparent in the full speed range and reaches a maximum near the design speed ($Fn_\nabla = 4{,}2$) where it is 45,8%. At a Froude number of $Fn_\nabla = 3$ (V = 23,8 kn) it is still 45,8% and drops slightly for the lower Froude numbers. The resistance hump of the Hysucat cannot be measured in the full speed range in the utilized facility, mainly because of standing waves at Froude depth numbers around unity and of stronger laminar flow influence. However, the indication is given in Figure 16 that the resistance hump is also reduced strongly due to the trim reducing effect of the support hydrofoil. This is a special advantage for cruising speed conditions and allows a much more economical operation of the craft as compared to usual hulls and further eases the propeller design allowing a fixed pitch propeller to be used for all operation conditions. The resistance coefficient e of the present case shall be compared with the resistance coefficients of other conventional ship hulls to allow the judgment of the resistance quality of the Hysucat principle in the following chapter.

3.5.5 Comparison with other Craft

The resistance tests on the Hysucat hull indicate that the resistance of a high speed catamaran hull can be improved considerably. This is not sufficient for a general evaluation of the new hull concept as catamaran hulls are known to have a relatively high resistance and are not in general use.

The Hysucat resistance has to be compared to the conventional craft in daily use as Displacement Hulls, Sea-going Planing Hulls, Hydrofoil Craft, Hover Craft, etc., for which Tendency Curves were published by the Baron Hanns von Schertel (16). These Tendency Curves consist of resistance coefficient curves ($e = R_t / ?$) plotted over the

Froude-length-number $F_{n\ell} = V/\sqrt{g \cdot L}$, indicating the range of possible resistance for the various craft. As the Froude-length-number Fn? is meaningless for hydrofoil craft once they are foil borne the bands of curves for the various craft were plotted over the Froude-displacement number $F_{n\nabla} = V/\sqrt{g \cdot \nabla^{1/3}}$ which is mostly used to plot planing craft resistances and which is shown in Figure 19. The plot was derived by use of the typical displacement-length ratios $\sqrt[3]{\nabla}/L$ for the various type of craft involved which are around 0,39 for displacement ships, 0,44 for Deep-V-Planing Craft and 0,39 for Hydrofoil Craft. For completeness the typical "resistance hump" of a 41 knot Hydrofoil Craft, taken from (17), and the resistance coefficients by the new generation of Dee-V-Planing Hulls developed by the Abeking and Rasmussen Shipyard in Bremen, Germany, the SAR 33 and SAR33S, are also included.

The Hysucat hull-resistance coefficient curve (excluded air resistance) as derived from the Test Series No. 8 is plotted on the same diagram, Figure 19, from which it becomes clear that it falls well within the band of Hydrofoil Craft Tendency Curves. The Hysucat resistance is much lower than for Displacement Ships and Deep-V-Planing Craft in the speed range $F_{n\nabla}$ = 2 to 4,5. As its design speed of $F_{n\nabla}$ = 4,2 it competes well with the best Hydrofoil Craft.

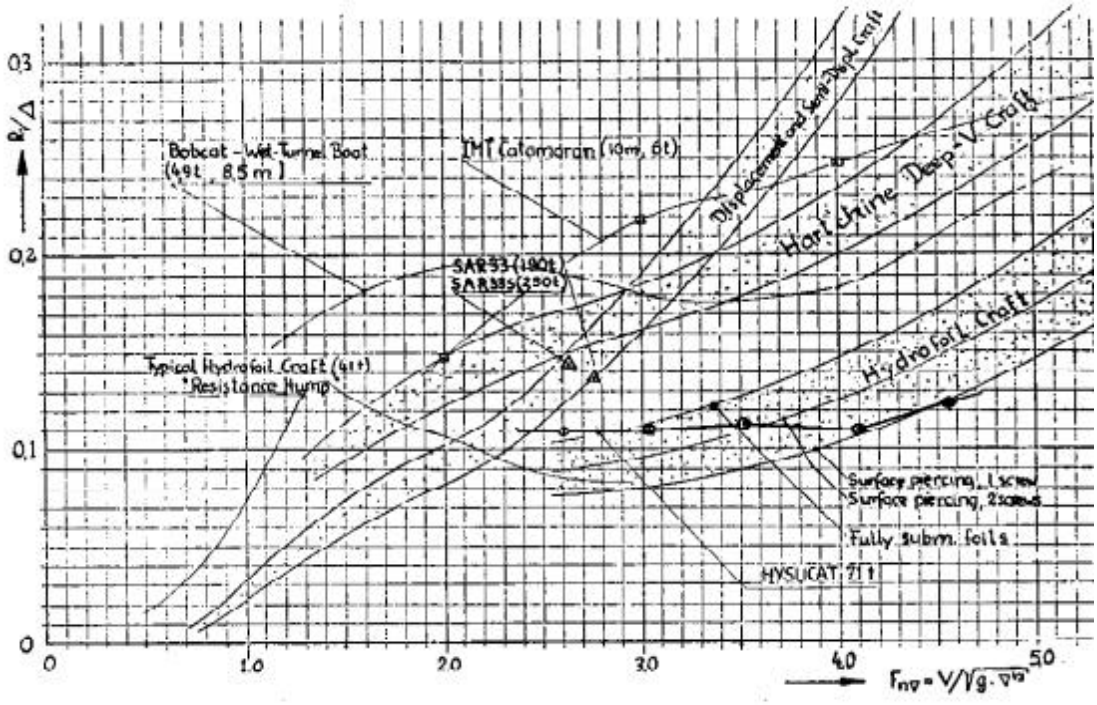

FIGURE 19: Resistance Coefficients e of Sea Craft

It may be remembered that the Hysucat resistance curve is applied to one design only and is not optimal at lower than design speeds. The Hydrofoil Tendency Curve was developed for optimal conditions at any speed. In other words, if a Hysucat Craft had to be developed for lower speeds, say $F_{n\nabla}$ = 3, then the design speed resistance would be lower than for the presently investigated hull and again would compare well with hydrofoil resistance data. The hump resistance is expected to be lower than for the Deep-V-Planing-Hull and the Hydrofoil Craft, but this needs further investigation.

The low resistance of the Hysucat in comparison with conventional hulls seems to be surprising, but can be explained by the efficient way the support hydrofoil carries a part of the ship weight and the positive interference effects between foil and demi-hulls. It can be expected that by systematical optimization the Hyscuat hull can still be improved considerably.

3.6 Towing Tank Tests

3.6.1 General

The previous model tests are mainly considered in a qualitative sense to show which improvements can be expected due to the support hydrofoil arrangement. For design optimization more accurate and reliable data are required which were established in several Hysucat-model-test-series in the towing tank of the University of Stellenbosch (92m long, 4,65m wide and 2,65m deep) with larger models of 1,2m to 1,5m lengths. Most of these tests were conducted in the frame of B.Sc-Thesis work (22, 23, 24, 25, 26,). The main results for the corresponding design conditions are reported in the following to establish more complete Hysucat tendency curves.

3.6.2 20m Hysucat

A 20m Hysucat design was outlined by Smit (22, 23) as a sea-going High Speed Interceptor of 40 knot. The total displacement, fully loaded was estimated to be ? = 65 t for a hull built in aluminium. The hull was based on the Hysucat 5 as a starting shape but was simplified to allow for easier construction in aluminium with a minimum of double curvature in the hull plating. The maximum deadrise of 25° was applied for soft wave-going. The tunnel width was slightly reduced (14%) in relation to the Hysucat 5 shape in order to improve transverse structural strength which poses a major problem in the design of the larger craft and especially for the hydrofoil spanning the tunnel. A slight reduction in hull performance can be expected compared to the Hysucat 5 shape due to the narrower hydrofoil and less slenderness of the demi-hulls. The main dimensions are as follows:

ℓ_c	=	20,0m	
B_{max}	=	10,8m	
B_{tunnel}	=	3,2m	
$B_{c\ demihull}$	=	1,7m	
$\ell_c/2B_c$	=	5,88	(comparable mono-hull ratio)
Δ	=	65 t	
V_{max}	=	40 knot	

Two parent models were built, one in a scale of ? = 17,6 for towing tank tests and a smaller one in a scale of ? = 44,44 for tests in the water-circulating tunnel. The larger model, designated Hysucat 6b, is shown on the photograph in Figure 20, and

at corresponding design speed in the towing tank in Figure 21. Figure 22 shows a photograph of the constant speed towing winch developed for these tests. The resistance test results and correlated predictions for the prototype are reported in (22, 23) for various displacements, longitudinal center of pressure positions (LCP). The influence of turbulence stimulation was found to be important and therefore the final design condition was re-tested at a later stage with careful turbulence stimulation. The results of the re-test are given in the diagram in Fig. 23, together with the design conditions, containing the model- and correlated resistance coefficients e, the reduced wetted surface ratios S_{speed} / S_{rest} and length ratios $?_{speed}, / ?_{rest}$, as well as the correlation coefficients k_{corr}.

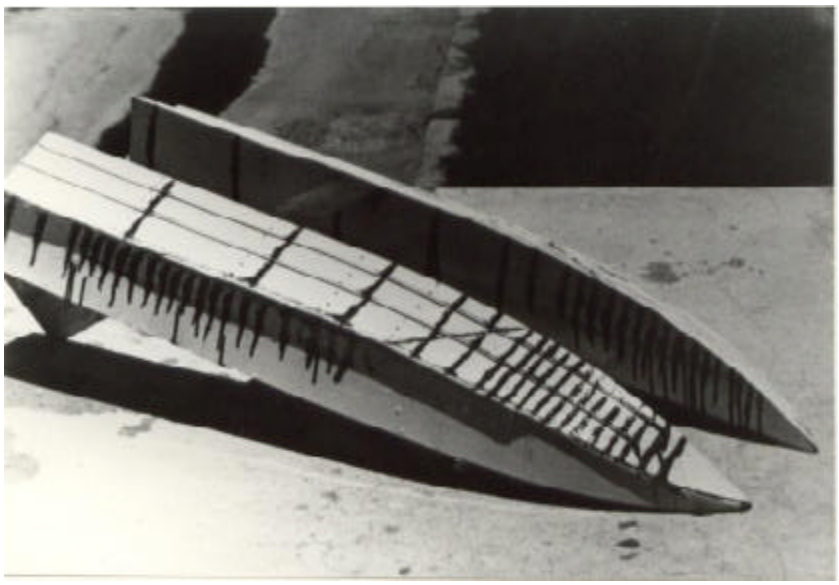

Figure 20

Figure 21

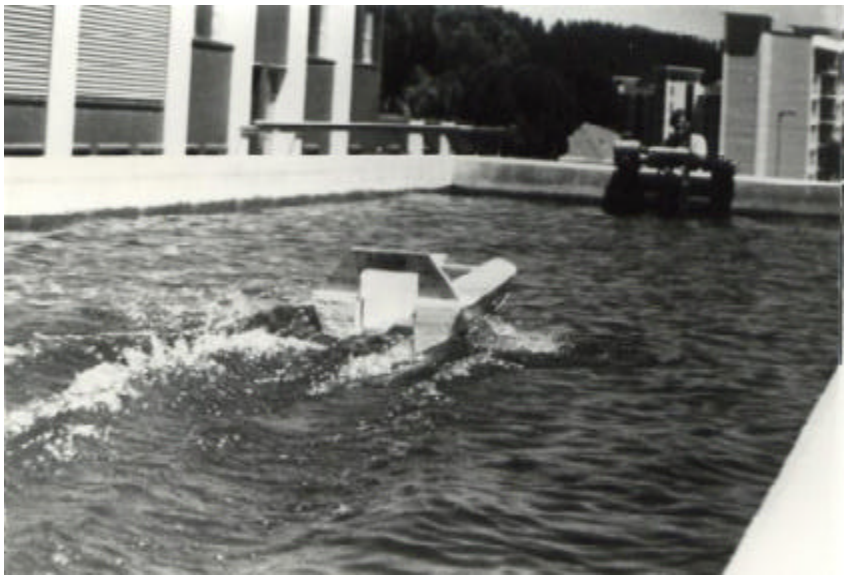

Figure 22

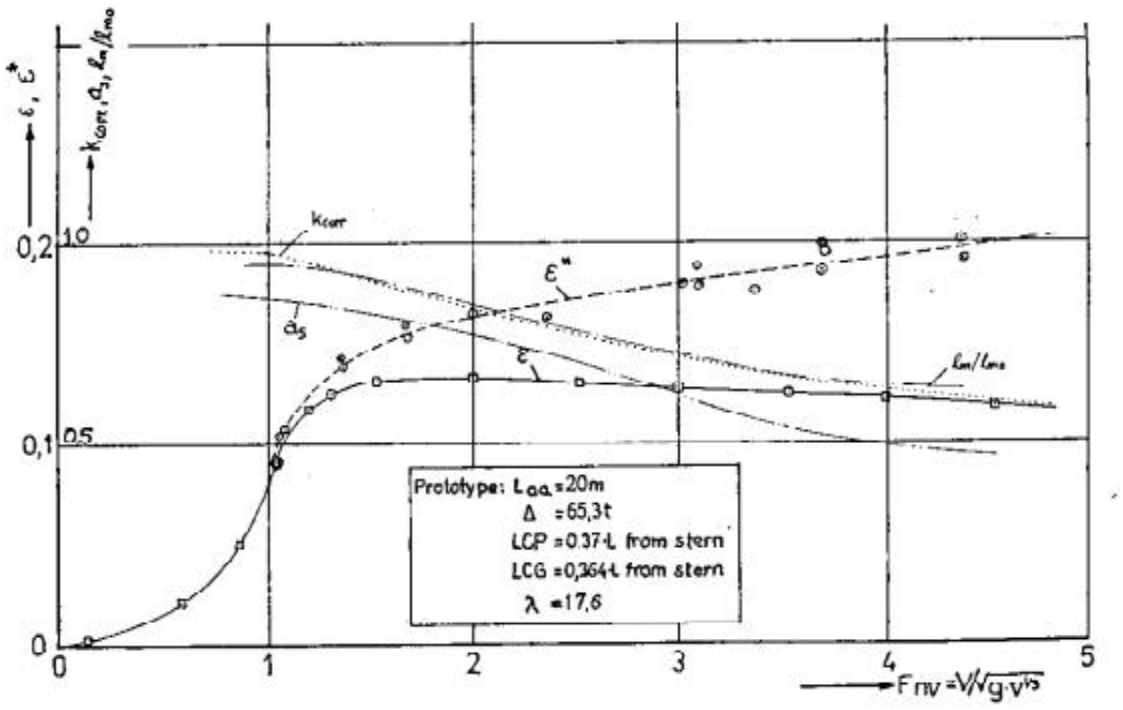

Figure 23: Resistance Coefficient e for Hysucat 6b

A problem was encountered with the constant speed towing winch concerning the resistance measurements which showed fluctuations due to the elasticity of the towing cable, which had to be very thin to create a high cable stress which would allow it to leave the water at an early stage. In the first test series the measuring distances were too short (50m) to allow the Hysucat model to rise and establish constant flow conditions. It was found, that, with extended running lengths and lower accelerations the Hysucat 6b resistance was considerably lower at the end of the run. These test results with the model in a "balanced flow state" are given in Figure 23, and give the steady flow resistance of the Hysucat 6b in the design condition.

The 20m Hysucat prediction is compared in Figure 26 with the other model test results and with ship tendency curves, taken from (6). The Hysucat 6b has a slightly higher hull resistance coefficient than the Hysu cat 5 hull, as expected, but, also shows a considerable improvement against the bare hull resistance and against conventional hulls.

3.6.3 30m Hysucat

A 30m Hysucat design with an operational open-sea-speed of 32 knots and displacement of maximal 190 tons was outlined by Fourie (24). This craft operates at Froude numbers considerably lower than the previous models an falls in a Froude number range up to F_∇ = 2,2, for which the Deep-V-Planing hull is not any more favourable and the Semi-Displacement hull delivers the best results.

As many of the larger sea-going craft designs falls into this range it is of special interest, to see, if a Hysucat design can deliver a competable craft.

Taking into account the lower Froude number the design of the demi-hulls had to be more slender than the previous models with sharper bow sections and reduced beam astern. The basic parent model was similar to the Series 62 hull 115 but with increased deadrise and altered bow sections (no semi-displacement hull shape was env isaged at this stage for constructional reasons).

The mono-hydrofoil was designed to carry 60% of the total weight at the design speed and required a relatively larger span and chord length than the previous models. A model of the underwater part of the hull in a scale of ? = 1/20 was built with the following dimensions:

	ℓ_c	= 1,500m
	B_{max}	= 0,684m
	$B_{c\ demihull}$	= 0,119m
	D_{tunnel}	= 0,302m
	$\ell_c/2B_c$	= 6,3 (comparable mono-hull ratio)
Dead-rise β		= 25°
test range Δ		= 15(kg) to 24(kg)
hydrofoil	ℓ_c	= 0,160m
	b	= 0,362m

The model hull is shown in Figure 24.
Various loads, longitudinal center of gravity positions and longitudinal center of pressure conditions were tested and reported in (24). The speed measurements, as reported in (24) contained a transfer fault which necessitated a re-test.

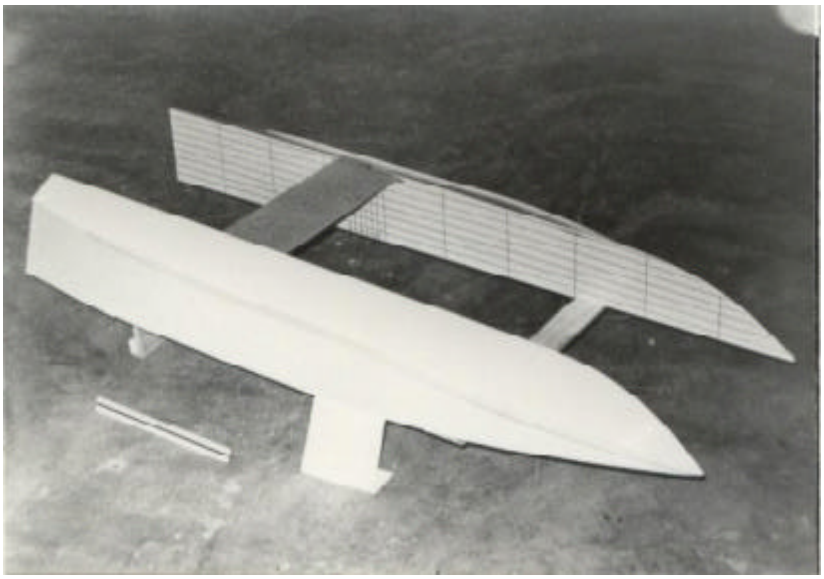

Figure 24

The corrected and re-tested resistance in the design conditions is given in Figure 25 for model and prototype. The resistance predictions in the design condition is compared in Figure 25 with other craft and ship tendency curves from which it becomes clear that a low Froude number Hysucat is well feasible.

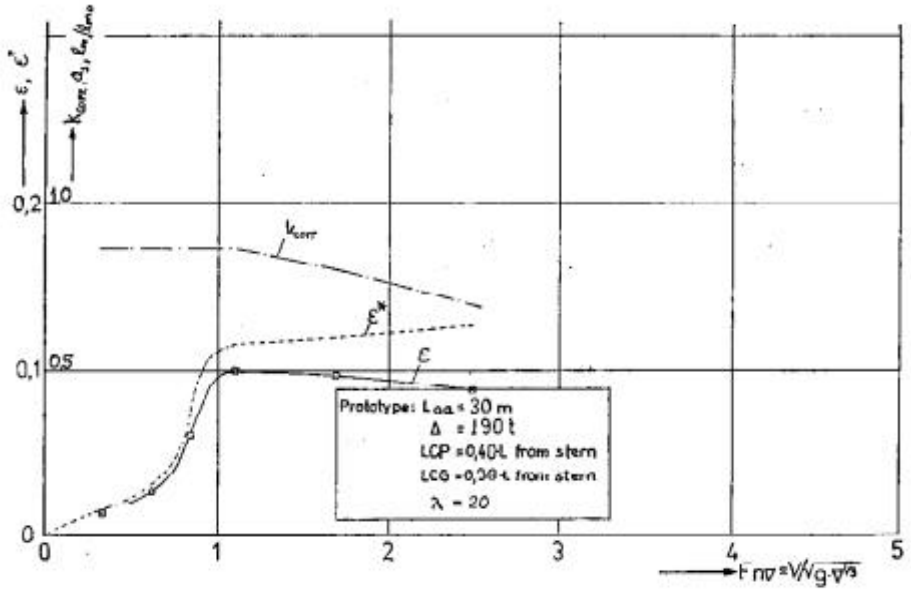

Figure 25: Resistance Coefficient e for Hysucat 7

3.6.4 Tendency Tests

Several smaller resistance test series with the existing Hysucat models were executed to investigate the influence of the hydrofoil size and shape on the total resistance. The model Hysu cat 5 was equipped with different hydrofoils, one having double chord length the one of the Hysucat 5a tests at equal tunnel width, and a second hydrofoil with the same chord length as on Hysucat 5a but with double span width.

The models with double hydro foil area rose out of the water at relatively lower speeds until the top surfaces were running dry at high Froude numbers. The correlated resistance prediction for a 10m prototype with double chord length gave similar resistance coefficients as the Hysucat 5a. The model with double span width showed an improvement resistance coefficient of about 10% in the full planing stage. The hump resistance could not be determined in these water-circulating tests.

In a further test series the mono-hydrofoil of the Hysucat 5a model was replaced by a tandem hydrofoil system corresponding to (3). The resistance prediction was very close to the original one, slightly higher (~5%), but this was thought to be due to foil scale effects. At very high Froude numbers $(F_{n\nabla} \geq 4{,}2)$ the resistance was slightly higher with the tandem hydrofoil system. Directional stability was excellent and no porpoising was observed in the full speed range.

Pietersen (25) investigated a tandem hydrofoil system with 24° dihedral for a 20m Hysucat in towing tank tests.

Resistance improvements similar to (23) were reached for certain foil arrangements but considerable problems due to insufficient directional stability were experienced.

Figure 26 shows the model used by Pietersen (25).

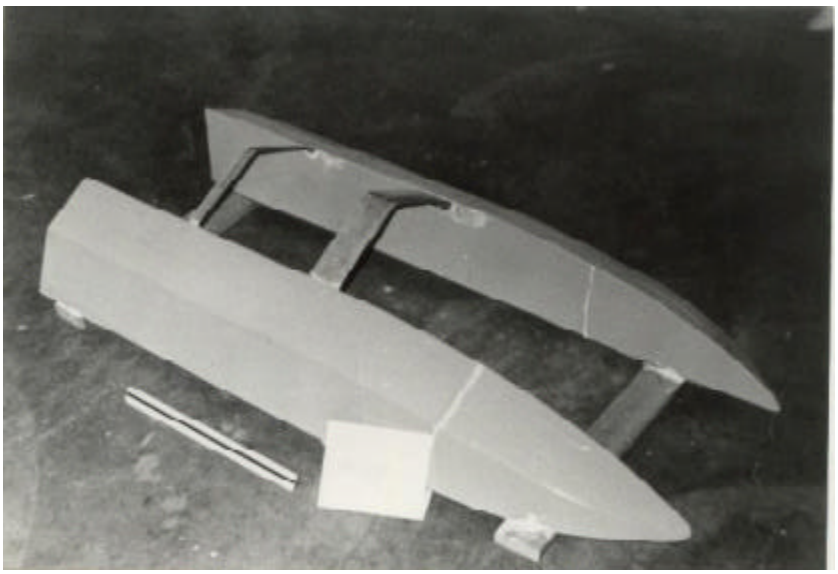

Figure 26: Hysucat Model 6 with Dihedral foils

3.7 Evaluation of the Hysucat Principle after Model tests

The present model tests have proved that the new hull concept, the Hysucat, achieves the expected resistance improvements against high speed planing catamaran and planing mono-hulls which were measured to be in the order of 40%. For comparison reasons the main test results on the various Hysucat test series are shown in Fig. 26 against the background of ship tendency curves, Displacement Craft, Hard chine Deep-V-Craft, Semi-Displacement Craft and Hydrofoil Craft. The investigated model hulls were straight forward designs and by further systematical research in design optimization the new hull concept may be further improved. It was found that a load distribution of about 45% on the foil and 55% on the hull results in a craft with sufficient stability and good sea-keeping quality. The Institute for Maritime Technology (IMT) has equipped their 5m sea model catamaran "Dolomini" with a support hydrofoil and test have confirmed in principle the resistance reduction as measured in the model tests. Further it was found that the sea model showed a much "softer ride in waves" and o problems in sea-keeping. Against the catamaran-without-foil it was observed that the one with the foil had no problems to overcome the resistance hump whereas the hull without foil had to be trimmed to overcome the resistance hump. This confirms the observation on the model with the reduced hump resistance.

Model tests with the Hysucat model in the water-circulating tank in severe head waves at high speeds showed that the craft compares well with a Deep-V-Planing model of approved design (18) which was run simultaneously. The Hysucat model with a mono-hydrofoil could stand similar conditions as the mono-hull in the severe sea "survival test" and its tendency to keep the trim angle constant sometimes leads to a phenomenon not observed on the mono-hull which consists of a kind of an "over-flying movement" once a strong wave crest has struck the craft at speed. The whole model tends to lift itself out of the water without taking up extreme trim angles and seem to "over-fly" the wave crest and following through without showing dangerous bow dipping at landing. The phenomenon can be explained by the fact that once the approaching wave is increasing the trim angle suddenly, the angle of attack on the foil and hull are also increased with the result that much larger lift forces are suddenly created, which tend to lift the boat out of the water. This phenomenon needs further investigation to establish if it has positive or negative effects under various practical conditions.

The smooth water sea-keeping of the Hysucat is mainly determined by the demi-hull shape and the position of the foil's longitudinal pressure center LCP in relation to the longitudinal center of gravity LCG of the boat. LCP for the investigated demi-hull shape has to be slightly behind LCG (~0,5 to 2%) . For LCG positions further forward lower trim angles at speed were observed with resultant resistance increases and LCG positions much further astern resulted in porpoising motions at higher speeds especially for the heavier models. The resistance was minimal for conditions just before start of porpoising.

The course holding quality of the Hysucat 5 model was excellent in all tests. However, in another test series, not included in the present report, in which it was tried to reduce the wetted area at speed by introducing a vertical step behind the foil on the vertical tunnel sides of the demi-hulls, the model showed strong course holding instabilities with the result of strong yaw motions of the model in the water-circulating tunnel.

This method of reducing wetted area on the Hysucat 5 hull had to be abandoned but may be successful on different hull designs with better original course holding stability.

It was found in the model tests with the Hysucat resistance at design speed compares well with the resistance of Hydrofoil Craft. However, the mode of operation of the Hydrofoil Craft is completely different from that of the Hysucat one and comparison would be fruitless. The Hysucat is better seen as an improvement for planing craft. Its advantages are more in the field of easier and cheaper construction and the development of new craft. The sea-going Hydrofoil Craft needed about 50 years development and resulted in a very complicated and expensive construction mainly due to stability and sea-keeping control problems.

The Hysucat craft can be designed and built with reasonable success without requiring much development and will result in a much cheaper craft compared with usual planing hulls, but being much more economical (construction and running costs).

However, it still offers some advantages even against a Hydrofoil craft: The Foils of the Hysucat do not penetrate deeper than the hull or the propeller and therefore the Hysucat can operate in much shallower water in its full speed range, it can easily be launched from slipways or beaches and loaded on a trailer, damage to foils during operation has less serious effects and the craft still remains operational, it offers a low target profile as a warship. In extreme wave conditions the Hydrofoil Craft has to remain waterborne and all its advantages are lost, being a platform with unacceptable motions and accelerations and hardly maneuverable. The Hysucat craft will also have to slow down in severe seas but still shows better sea-keeping in these extreme conditions due to the catamaran concept and the relatively slender demi-hulls, the slow and high speed operation not being so distinctly different for the Hydrofoil Craft. The design of the propulsion system of a Hysucat (being in principle similar to Planing Craft System), is simpler, cheaper and more efficient than for a Hydrofoil Craft with the propellers deep down near the foils necessitating long inclined shafts or long ducting for waterjet systems.

The question for which kind of sea craft the Hysucat concept could be used with advantage, is difficult to answer so long as no practical experience has been gained with the new type of craft. The advantageous speed range of the Hysucat is between the Froude displacement numbers of

$$F_{n\nabla} = 2{,}0 \text{ to } 5{,}0 \qquad \ldots\ldots\ldots (31)$$

for the presently tested hull shape and could be valid for larger Froude numbers if especially designed for it. This makes the Hysucat concept interesting for the smaller sea-going high speed craft which are usually planing or semi-planing craft.
For operations in areas with less severe wave conditions or for short time operations in deep sea conditions the Hysucat concept offers advantages for small fast craft (say 6 to 8m) which are relatively heavily loaded, but for long duration deep sea operations the sea-keeping quality of only larger craft is acceptable which is estimated to be at minimum in the range of craft of 15m to 18m. The Hysucat Craft could be built in larger sizes than the Hydrofoil Craft as the load could more easily be distributed over numerous support foils and the hull structure would be lighter than for the Hydrofoil Craft with its four “point –loads” from the foils which have to carry the whole weight of the craft. However, the propulsion power requirement for the very large high speed craft will become excessive (a 50m Hysucat with a weight of

800t at 40 kn would require about 44 300 HP propulsion power) and there is a reasonable upper limit for the Hysucat craft, which is estimated for foreseeable practical applications to be with craft of around 30 to 40m.

A reasonable Hysucat craft of about minimum size for open sea operations under South African conditions is thought to be around 17m length, 35 t weight and 40kn maximum speed, and would require about 2200 Hp propulsion power.

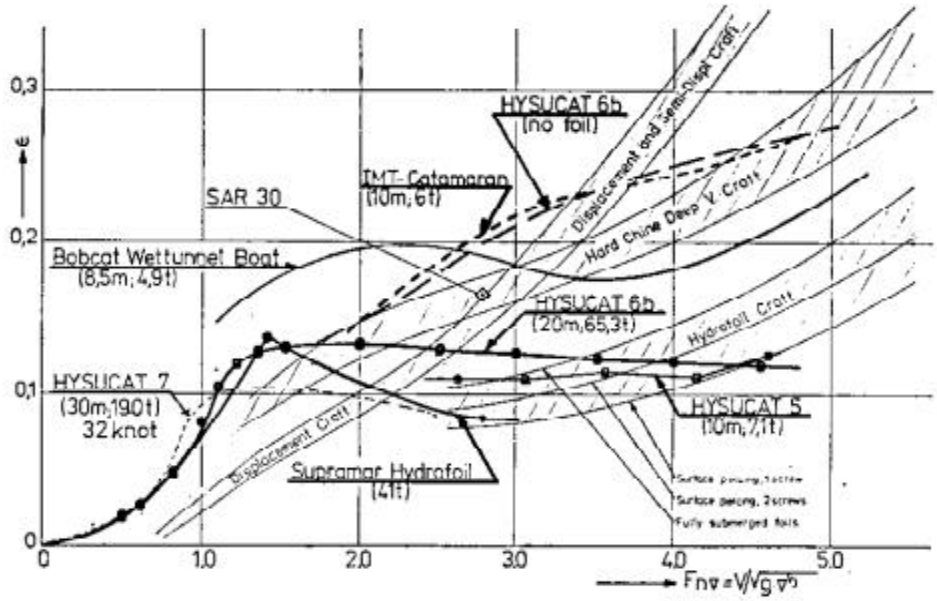

Figure 27: Resistance-Displacement Ratios of Sea Craft

4. *Propulsion of the Hysucat*

4.1 Propulsion System and Power requirement

The installation of the propulsion power system for the Hysucat causes no special problems and similar installations as used in Deep-V-Planing hulls are directly applicable. For the smaller craft up to about 8m the use of twin outboard engines is favourable for reasons of low capital costs, extended range, simple installation, easy handling and excellent maneuverability.

The fuel consumption in small craft is of low priority and the high specific consumption of the two-stroke-cycle outboard engine is accepted. For larger craft up to about 12m with longer running periods the fuel consumption becomes of utmost importance and inboard petrol or Diesel engines are preferred. The use of twin inboards outboard systems with Z-drive are efficient and result in highly maneuverable craft with power trim. For the fast craft the use of jet propulsion systems becomes competable with the advantages of low draft, less vulnerable propulsion parts and high maneuverability. For the larger craft the direct coupled Diesel engine and jet propulsion system look attractive and efficient. The demi-hulls are rather slender and Diesel engines with upright cylinders in line arrangement are

preferable to allow for sufficient working space around the engines inside the demi-hulls.

For larger and extremely fast craft gas turbines in combination with jet propulsion systems or surface propeller arrangements (Arnison drive) are interesting. With the resistance coefficients known from model tests the required propulsion power of the various Hysucat designs can be estimated under the assumption of appropriate propulsion coefficients

$$P.C. = P_{eff}/P_B \qquad 4.1$$

known from Deep-V-Planing hulls.

P.C. is the overall propulsion efficiency and includes propeller efficiency, propeller arrangement efficiency, wake and thrust deduction, propulsor appendage drag and trim influence of propulsor on craft.

P_B is the shaft brake horse power of the engines and P_{eff} is the effective power,

$P_{eff} = V_s * R_t$, V_s = ship speed and R_t = total resistance of the craft.

The required power of the propulsion engines is determined as :

$$P_B = P_{eff}/P.C. \qquad 4.2$$

and

$$P_B = R_t\{N\} \cdot V_s\{m/s\}/(1000 \cdot P.C.) \ \{kW\} \qquad 4.3$$

and with the use of the resistance coefficient e

$$P_B = \varepsilon \cdot \Delta \cdot V_S/1000\ P.C.\ \{kW\}, \qquad 4.4$$

with ? in Newtons.

The propulsive coefficient P.C. for fast planing craft with subcavitating propellers can be estimated from data given by DuCane (1) and is about 0,48 to 0,56, depending on speed, propulsion machinery and transmission system used.

The hull propulsion power requirement of the 10m Hysucat tested under (3) with a displacement of 7,1 t at 36 knot (Fr∇ = 4,27, e = 0,12 from Fig.18) follow with P.C. = 0,49 from (1, page 414) to:

$$P_B = 0,12 \cdot 7,1 \cdot 1000 \cdot 9,81 \cdot 36 \cdot 0,5145/1000 \cdot 0,49$$

$$P_B = 316\ \{kW\} \triangleq 430\ (HP\ metric)$$

An addition for wind resistance and eventual for bad weather is necessary but would apply to the comparison craft as well.
In comparison to this, the same catamaran without the support foils has a resistance coefficient of e = 0,224 (Fig. 18) and a propulsive power requirement of

$$P_B = 0{,}224 \cdot 7{,}1 \cdot 1000 \cdot 9{,}81 \cdot 36 \cdot 0{,}5145 / 1000 \cdot 0{,}49$$

$$P_B = 590 \text{ (kW)} \triangleq 802 \text{ (HP)}$$

The Hysucat principle brings, thus, an improvement of 46%:

(802 HP ≙ 100%

430 HP ≙ 53,6%).

The fuel consumption is proportional to the power requirement (which is proportional to the resistance) and will be reduced by 46% as well. This has a significant influence on the ship design as less fuel weight is necessary for the same range.

If the above 10m Hyscuat is compared to a conventional Deep-V-Mono-hull of the Polycat-Series (18) with e = 0,20 at $Fn\nabla = 4{,}27$ the power requirement becomes:

$$P_B = 0{,}20 \cdot 7{,}1 \cdot 9{,}81 \cdot 36 \cdot 0{,}5145 / 0{,}49 = 526 \text{ (kW)} \triangleq 716 \text{ (HP)}$$

which means a saving of 40% for the Hysucat.

The hull propulsive power comparison of the 20m and 30m Hysucat designs tested under (3) follows in a similar way to :

20 m Craft:	Δ	V_s knot	$F_{n\nabla}$	ε	P.C.	P_B kW	P_B HP
HYSUCAT	65	40	3,28	0,126	0,46	3595	4889
Catamaran	65	40	3,28	0,225	0,46	6419	8730
Monohull (18)	65	40	3,28	0,142	0,46	4051	5510

30 m Low Speed Craft	Δ	V_s knot	$F_{n\nabla}$	ε	P.C.	P_B kW	P_B HP
HYSUCAT	190	32	2,2	0,093	0,5	5708	7762
Catamaran	190	32	2,2	0,146	0,5	8899	12103
Monohull (18)	190	32	2,2	0,110	0,5	6751	9182

The Hysucat improves strongest in the range of high Froude numbers as pointed out before. It is expected that by systematical design optimization the Hysucat resistance can still be improved considerably –which does not apply to the fully developed planing hull.

4.2Fuel Consumption

For the safe operation of ships the amount of fuel necessary to cover the planned range has to be known. The fuel consumption of the ship depends on the applied power over the running time and varies with speed. To enable the operator to estimate the fuel storage for an envisaged voyage the craft's specific consumption depending on speed must be known.

The specific consumption ratio of the craft C* is given as the litres of fuel consumed per kilometer traveled at steady speed divided by the ship's mass:

$$C^* = \frac{F_{fuel}}{km \cdot \Delta} \quad \left(\frac{\text{litre of fuel}}{km \cdot t} \right) \qquad 4.5$$

The method in pracitical use is often still the older system's miles/gallons, wherein USA-gallons and landmiles are used. The metric system equivalent is better used in reversed form. The specific fuel consumption of the engine itself is given as

$$C_{mot} = \frac{\text{kilogramme fuel}}{\text{kW shaft power and hour}} = \frac{M_{fuel}}{P_B \cdot t} \quad \left(\frac{kg}{kW \cdot h} \right)$$

The steady speed distance traveled by the ship is

$$S_t = V_s(m/s) \cdot t(s) \quad \text{in meters} \qquad 4.6$$

The fuel consumption per kilometer of the engines during ship operation follows to:

$$C = C_{mot} \cdot P_B \cdot t/S_t \qquad \ldots\ldots\ldots 4.7$$

and with (4.7) follows to:

$$C = \frac{C_{mot} \cdot P_B \cdot t/S_t}{V_s \cdot t} = \frac{C_{mot} \cdot P_B}{V_s} \qquad \ldots\ldots\ldots 4.8$$

The brake shaft power P_B needed to propel the craft is after Equation (4.4)

$$P_B = 9,81 \cdot 1000 \cdot c \cdot \Delta \cdot V_s / P.C. \quad \text{(with } \Delta \text{ in (t))}$$

which gives for the consumption ratio of the craft C in Equation (4,8)

$$C = 9,81 \cdot 1000 \cdot \varepsilon \cdot \Delta \cdot C_{mot} / P.C.$$

The dimensions of the craft's consumption ratio C follow to:

$$C = 9,81 \cdot 1000 \cdot C_{mot} \cdot \varepsilon \cdot \Delta(t) / P.C. \quad (\text{kg fuel/km}) \quad ..... \quad 4.9$$

The specific craft consumption ratio C^1 is the craft's fuel consumption ratio per ton displacement and follows to :

$$C^1 = \frac{C}{\Delta(t)} = 2,725 \cdot \varepsilon \cdot C_{mot} \ (\text{kg fuel/kW·h}) / P.C. \ (\text{kg fuel/km}) \quad ..... \quad 4.10$$

As petrol is usually sold in litres the craft's specific consumption ratio can be transferred to have the dimensions litre of fuel per kilometer traveled of a ton displacement:

$$C^* = C^1/0,75 = 3,633 \cdot \varepsilon \cdot C_{mot} (\text{kg fuel/kW·h}) / P.C. \ (\text{litre/km·t}) \quad ..... \quad 4.11$$

With the fuel's specific density being s = 0,75.

In the older literature the motor-power is measured in horse power (1.36 HP equals 1kW) and then the craft's specific consumption ratio follows to:

The development of the craft's specific consumption ratio shows that it is only dependent on the specific consumption of the engine C_{mot}, the resistance coefficient e and the overall propulsive coefficient P.C., the later two are dimensionless.

It shows that the craft's specific consumption curve (over speed) must be of similar shape as the resistance curve e in the range of constant propulsive coefficients and engine efficiencies.

The craft's specific consumption coefficient C^1 can be used to evaluate any ship performance by simply measuring the consumed fuel over a given distance for various steady speed runs. Hardly any measuring equipment is necessary and reasonable accurate results are achieved once the traveled distance is determined accurately. For outboard engine driven boats the consumed fuel can easily be measured with a spring balance on the fuel tank. Faster results are achieved by use of the commercially available VDO-fuel flow meters and VDO-Sumlog III which gives speed and distance.

The measurement of the craft's specific consumption coefficient allows the determination of the propulsive coefficient P.C. once the engine brake test has given the engine efficiency C_{mot} and the resistance test the resistance coefficient e.

5. BMI-HYSUCAT Sea Model

5.1 General

In view of the promising Hysucat model test results with various hulls the Bureau for Mechanical Engineering at the University of Stellenbosch (BMI) sponsored the design and construction of a first real proto type, a sea-going pleasure or sport-fishing boat. The design request was for four persons and 300 kg of payload and after a pre-project study the decision was taken to design a 5,6m craft driven by twin outboard engines. The first prototype was intended to be used as a sea-going model and for safe storage of instrumentation a small cabin was requested. Much effort was put into the development of the hull lines to achieve a practical and pleasant looking prototype comparable to commercially available Ski-boats, in order, to allow for later mass-production. After a preliminary cost study of the modern boat building materials, the performed Kevlar-PVC-Sandwich structure was abandoned because of extremely high material costs and the more conventional GRP structure with some PVC- and Balsa Core Sandwich structures selected.

The primary goal of the BMI Hysucat Prototype was to prove that a sea-worthy and pleasant boat could be designed on the Hysucat principle and economically be built, which can be handled as easy as any conventional boat. The launching from usual road-trailers and the possibility of landing on sandy beaches were important additional features.

5.2 Design and Construction

The BMI designed Hysucat is based on the principle of the auto-trim-tandem-hydrofoil-system as explained in Chapter 2, corresponding to the ideas developed in (3). Fully asymmetrical demi-hulls with deep-V-planing craft characteristics were selected, which results in a tunnel between the demi-hulls with parallel vertical sidewalls. Such craft have proven best sea-going abilities and also provide minimum inflow variations to the hydrofoils in rough water. The tunnel ceiling, connecting the two demi-hulls and forming the wet-deck structure was placed sufficiently high above the keels to keep it out of water-contact at any speed. The intention was to operate the craft in it's whole speed range and even in the low speed buoyant mode as a pure catamaran. In the design, this allowed the construction of a horizontally straight and flat tunnel ceiling. A wave-spoiler was added to the forward part of the tunnel ceiling in order to prevent the flat tunnel ceiling area hitting the water abruptly in steep choppy waves at low speeds when the craft is still deeply submerged, which is the case for line-fish-trawling in S.A. sea conditions.

A relatively large forward cabin was added in order to provide a safe and dry storage place for equipment and instrumentation. The cabin with it's windscreen also provides shelter against wing and sea-spray. The longitudinal center of gravity of planing catamarans has to be positioned in the design relatively far astern (30% to 35% L_p forward of transom) to achieve optimum performance always free of porpoising.

By placing the cabin the remaining deck space is foreseen to allow 4 persons to move around without off-setting the required LCG position too much (a persons weight being a considerably part of the total weight for a small craft!).
The center part of the foredeck was raised to prevent under-cutting solid water in steep wave encounters at low speed. In such conditions the lower forward demi-hull deck sections allow water to stream off sideways once the tunnel has filled up completely in a heavy low-speed wave encounter, (however, it is hoped that this would happen rather seldom). The raised center deck, which resulted in an unconventionally looking foreship design reduces the "shipping of green water" effectively and increases the near-range visibility for the helmsman. It became a typical feature of a series of Hysucat designs.
The S.A. sports fisherman prefers to stand upright behind the steering wheel to have sufficient view when navigating difficult areas with sea weed beds and shallow reefs in always present waves. The arrangement of seats also restricts the space needed for line fishing action.

In the view of later production as Sport fishing boat, this first Hysucat was, therefore, not equipped with usual motorboat seats but passenger seating was foreseen on the fish or equipment box in the center of the wet-deck area. Hysucat designs for other operational areas can well be equipped with high-seated pilot chairs behind the bulkhead and windscreen.

The relatively high cabin with windscreen additionally to the wet-deck arrangement results in a craft with a relatively high vertical center of gravity (VCG) and large frontal area with resulting high air resistance. The stability reserves of the Hysucat are sufficient to allow for high VCG positions. The high air resistance which can be amplified if the craft runs into strong headwind was accepted in return for the comfort of the wind and weather protection of the high bulkhead and windscreen.

The demi-hulls are foreseen with two strong keel beams (40mm x 40mm) stretching all over the length and forming a strong "backbone" for additional strength in the case of ground contact, float contact, beaching or trailering.

The strong keel beams from solid GRP laminations are also used for the attachment (by stainless steel bolts) of the mainfoil without penetrating the hulls which could lead to leakages. The strong localized lift-forces of the hydrofoil are well distributed by the keel beams before entering the demi-hulls. The tunnel width was chosen to allow about 40 to 50% of the boat weight to be taken up by the hydrofoils. The hydrofoils were designed with a sweep angle of 25° and a small dihedral angle of 3°, in order to allow for undisturbed periodical penetration of the water-level when running in choppy waves. This is a very important feature to achieve soft and smooth running in rough water. The mainfoil was attached to achieve 25mm keel clearance. The tandem foil corresponding to (3) shown in Fig.3 and 4, was designed as a pair of strut foils with an area of 25% of the mainfoil. Strut foils in comparison to a mono-foil stretching the full tunnel width can be built much "stiffer" with less deflection under excessive load in this special case with such a small foil area.

The arrangement of the strut foils follows after Equation 11. The attack angle of the strut foils were compensated for an average downwash velocity of the mainfoil. In this case of boats with considerably increased weights the strut foil attack angle needs a slight increase of 1° to 1,5° to compensate for the higher downwash velocities behind the mainfoil or eventually a foil system re-design.

A bow rail and a stern rail (overoll bar) from stainless steel tubing were added for safer handling.

The Main Dimensions of the BMI Hysucat are:

L_{oa}	=	5,65 m
L_c	=	5,51 m
B_{max}	=	2,35 m
B_T	=	0,96 m
$B_{c\ demihull}$	=	0,561 m (including spray strip)
$D_{m\ ot\ tip}$	=	0,580 m afloat to keel at stern
$?_{design}$	=	0,95 t for Kevlar-Design, 1,25 t for GRP -design.
$?_{mean}$	=	22°
V_{design}	=	29 knot
P_{engine}	=	22 to 30 (kW) (30 to 40 HP)

Foil Arrangement:

L_c	=	0,200 m
Sweep angle	=	25°
$L_{c\ tandem\ foil}$	=	0,150 m
$B_{tandem\ foil}$	=	0,200 m
$a_{mainfoil}$	=	-2,5°
$a_{trimfoil}$	=	-1°
$LCP_{mainfoil}$	=	43% forward heel of transom
$LCP_{trimfoil}$	=	6% forward heel of transom

The photograph in Fig. 29 and 30 show the completed BMI Hysucat during weight tests from beneath, revealing the auto -trim tandem foil arrangement.

Figure 29

Figure 30

The hull is built in standard GRP with the larger flat surfaces containing a PVC sandwich structure, the wet-deck a Balsa Core-GRP structure and the cabin panels are stiffened by Core-mat-GRP structure. The hydrofoils are cast to size in Aluminium-Bronze (usual high performance propeller material) and then polished off for smooth and even (fairing) surface finish.

The plug was built by "Ton Cup Yachts" in Cape Town with an extremely high surface finish as well as the mould and the first cast, the 5,65m BMI Hysucat. The final equipment of the craft including the motors, control and steering systems were finished by BMI. Two 35 Johnson Outboard Engines (28,5 HP on shaft) mounted for the initial trial runs. For later tests two 40 Suzuki Outboard Engines, donated for the tests by the Suzuki main distributor in Cape Town, Mr. Jack Rivers, were mainly used because of better spares back-up (Propeller variation).

5.3 Model tests on BMI Hysucat

The BMI Hysucat design is based upon data received from the model tests on the Hysucat 5 and 6, chapter 3. The hull lines were altered to achieve best sea-keeping, especially running into rough head-seas, which resulted in sharper bow lines with forward sections of increased deadrise angles. For the design approval model tests on the final demi-hulls were required. A check-out on the principle idea concerning the auto-trim tandem hydrofoil arrangement after (3) was necessary to assure a practical and successful design.

A model of the BMI Hysucat in a scale of 1 in 12,25 for tests in the small high speed water-circulating tunnel (Fig. 7) and a larger model in a scale of 1:5 for towing tank tests were built. The small model consisted mainly of the underwater part including the wet deck structure, but no cabin. The larger model was built complete with cabin and windscreen for inclusion of model wind resistance in the towing tank tests. Later wind tunnel tests are foreseen.

Water-circulating Tank Tests

The small BMI Hysucat model without cabin was used in the water-circulating tank tests. The model hydrofoils were built with a 30% increased area to partly compensate for the lift-force reduction at small Reynolds numbers and the foil incidence angles were increased by 2° for further compensation. Otherwise the tandem foil arrangement as calculated for the prototype was reconstructed on the model.
Various displacements were tested but for the final tests the corresponding prototype displacements of 900 kg and 1220 kg were used.

For every test series the resistance and trim angles were measured in the full speed range corresponding to Froude-displacement numbers of $F_{n\nabla}$ = 2 to 4,5. The longitudinal center of gravity positions were systematically varied in the range of 28% to 38% of L_c from the stern-heel. The LCG variation test, Fig. 32, indicate the degree of sensitivity of the Hysucat to load shifts inside the boat, which is claimed to be much lower than for usual deep-V-planing craft.

The tandem foil arrangement was also systematically varied and six different arrangements tested with the mainfoil at different longitudinal positions and the trim foils with various heights over the keel. The results from these tests indicate that the calculated tandem foil arrangement gives the best overall result.

If the foils are placed further away from each other length-wise the Hysucat becomes less sensitive to LCG shifts but the mainfoil's pressure point near the LCG position delivers the resistance minimum. On small craft considerable LCG shifts are encountered in practical service and therefore the mainfoil's pressure point LCP at 43% L_c from stern heel was maintained as the resistance changed minimally in the LCG position range of 28 to 38%. The resistance change with LCG shifts is dependent on the speed with lower sensitivity at high speeds. The model's resistance increase was 12% from it's best value at LCG = 32% to LCG = 38% at full speed. LCG shifts towards the stern (up to LCG = 28%) resulted in very small resistance increases of about 2,4% at full speed. Near the hump resistance at $F_n\nabla = 2$ the resistance increase was 23% forward (LCG = 38%) and 25% sternwards (LCG = 28%).
This indicates that for low hump resistance the boat should be operated with the optimum center of gravity position which for this design is between 32% and 36%. The higher LCG shift sensitivity of the Hysucat at lower speeds is due to the lower carrying capacity of the foils at low speed. The sensitivity is then determined by the demi-hull characteristics. A comparable mono-hull after (13) is much more sensitive to LCG shifts which can be as much as 35% resistance increase for a LCG shift of only 4% near the hump resistance. For higher speeds the sensitivity also becomes less.

The Hysucat prototype will be less sensitive to forward LCG shifts than it's model as the increase is mainly frictional resistance which for the larger craft is smaller in proportion to the residual resistance than for their models. The Hysucat claim for low LCG shift sensitivity is, therefore, fully justified. During tests it was found that the scale effects on the geometrically similar mainfoil with sweep were considerably higher and the tests were continued with a straight mainfoil with equal area. The trim angles, however, were determined with the model equipped with the swept foil as this is believed to influence the trim motions.

The model resistance test results in the final deign condition with the straight foil and LCG variation are shown in Fig. 31 for a corresponding displacement of 1220 kg. The trim angles ? for similar mainfoil (with sweep) are given in Fig. 31. Fig. 34 shows the small model in the water-circulating tank simulating the BMI Hysucat with 900 kg at 25 knots. The photograph shows clearly the wake formation behind the craft.

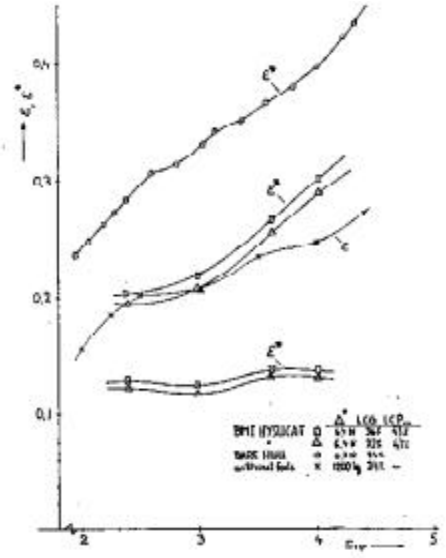

Figure 31: BMI Hysucat with and without Hydrofoils, Model and Prototype

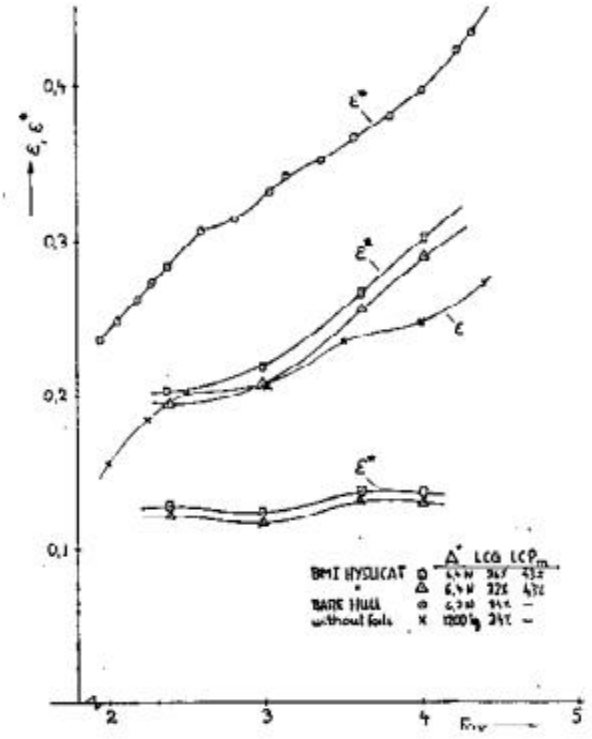

Figure 32: BMI Hysucat, Model test results, ? = 12,25

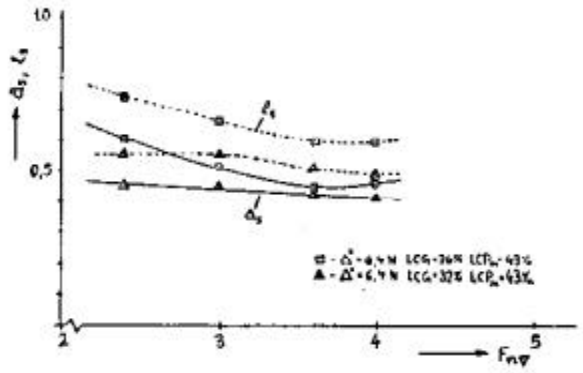

Figure 33: BMI Hysucat, wetted lengths l_s and areas a_s

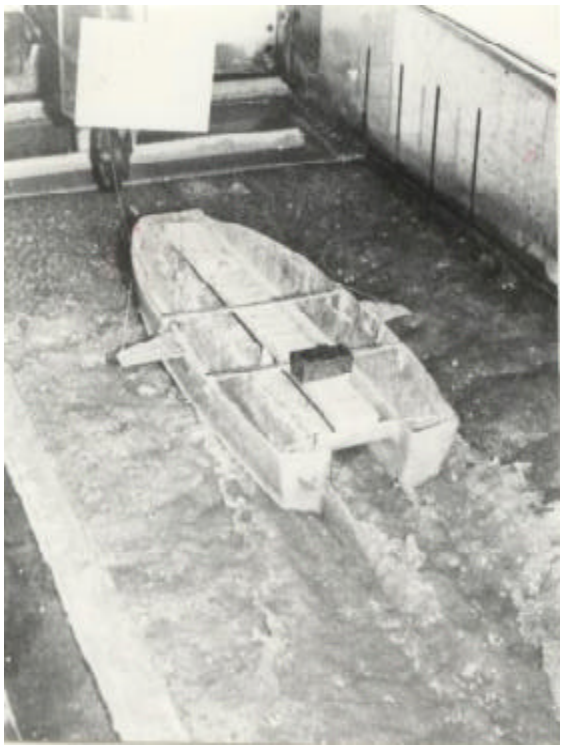

Figure 34: BMI-Hysucat Small Model in Water-circulating tank
? = 904 kg, v = 25 knot

The prediction of the BMI-Hysucat resistance results in slightly higher values than for the Hysucat 5 hull and is between e = 0,12 to e = 0,14 in the planing speed range. The increased resistance was expected and is mainly due to the fact that the BMI-Hysucat has a smaller absolute size (higher viscous friction influence), strong keel beams which increase the wetted area by 8% to 12% and the sharper bow lines required for smoother wave going.

The considerable resistance improvement due to the supporting hydrofoils becomes visible in Fig. 31 where also the bare-hull resistances are shown. The trim behaviour of the BMI-Hysucat is completely different compared to the models of the Hysucat 5 and 6 equipped with mono-hydrofoils. Where the later maintain the nearly constant trim angles at all planing speeds the BMI-Hysucat runs with an increased trim angle (?*) at lower speed, the maximum near the hump resistance with trim angle reduction with speed increase for all LCG positions. In this way the BMI Hysucat reacts like a usual Deep-V-Planing craft.

This effect was intended in the design and is desired in sea-going craft. When the speed has to be reduced in rough weather the BMI Hysucat lifts the bows up and assures dry running in choppy waves even when the hulls sink deeper into the water when the craft operates in the buoyant mode.
The higher trim angle at lower speeds also results in higher lift forces created due to increased foil incidence angles allows the craft to reach the planing stage at lower speeds.

Altogether, the small model tests indicate that the BMI Hysucat functions well in the whole speed range and for the planned loads. No porpoising or course instabilities were observed. The design proposal was accepted.

The required propulsion power for the design speed of V_s = 27 knots and a main displacement of ? = 1250 kg follows after Equation 4.4 to :

$$P_B = \frac{0,12 \cdot 1,250 \cdot 9,81 \cdot 27 \cdot 0,5145}{0,48}$$

$$= 42,59 \text{ (kW)} \triangleq 57,9 \text{ (HP)}$$

Or with e = 0,14 (P_B = 67,57 (HP))

The P.C. = 0,48 of outboard engines is relatively low in spite of high propeller efficiencies of 65% to 70%. The main reason is the high underwater transmission part drag. Resistance additions for the craft have still to be made for air-resistance, wind resistance and wave resistance or one has to except the corresponding speed reductions. The nearest outboard engine choice was for two 30 HP and two 40 HP Outboard Engines. Sea operated craft require after law two independent propulsion plants in S.A.

Towing Tank Tests

A series of towing tank tests on the larger BMI Hysucat model (ℓ = 5) were conducted by Steunenberg (26) in the towing tank at the University of Stellenbosch (92 m x 4,64 m x 2,65 m). The model included the fully built-up cabin and windscreen to simulate also the air drag of the craft which is a considerable resistance component at top speed (~30%). It was envisaged to correlate the air drag together with the residuary resistance component. The influence of the Reynolds number on the air drag is assumed to be negligible as the craft has sharp edges for distinct flow-break-off and the air drag is mainly pressure resistance. The results shall allow a direct comparison with the planned sea tests on the 5,65 m BMI Hysucat.

In the towing tank two displacements and six various LCG positions were tested systematically (26). The bare hull without the foil system was tested first and, then, under the same conditions the hull with the tandem-hydrofoil-system as designed for the 5,65m Hysucat. Other test series comprised variations of the hydrofoil attack angles, from which it was found that the design attack angles gave the best results.

Unfortunately the demi-hulls were not equipped with the spray strakes along the chine for early water break-off. It was later found that the spray strake (as designed) has a strong influence on the proper functioning of the Hysucat especially for the lower planing speeds.

The swept main-hydrofoil was replaced by a straight model foil for reduction of scale effects. No compensation for reduced lift at low Reynolds numbers was made. The initial idea was to compensate with increased hydrofoil incidence angle.
However, no improvements could be reached this way and the early stalling (due to ventilation) of the model hydrofoil sets a tight limit to this compensation method.

The model and prototype resistance coefficients for the design load of 1200 kg and LCG positions of 34% and 36% are shown in Fig. 35. To compare with the water-circulating tank test the air drag on the model was calculated assuming a drag coefficient of C_D = 0,9 (as for open sports cars) and the isolated hull resistance correlated additionally.

The predicted bare-hull resistance including air drag is slightly higher than the prediction from the water-circulating tunnel (which contains no air drag) see Fig. 35. However, would the air drag be deducted the predicted bare-hull resistance of the towing tank tests would be slightly lower in the top speed range ($F_{n\nabla}$ = 3,5).
The predicted BMI Hysucat resistance coefficient without air drag compares well in the top speed range. For the lower speeds and especially near the hump resistance-speed the towing tank tests predict a slightly higher value which indicates that the model hydrofoil lift creation is not sufficient. The omitted spray strakes along the chine also can have an influence on the higher hump resistance.

In principle, the tendencies of both test series indicate an average hull resistance coefficient at planing speeds of e = 0,12 to e = 0,15 (for hump resistance) which was the basis for the design.

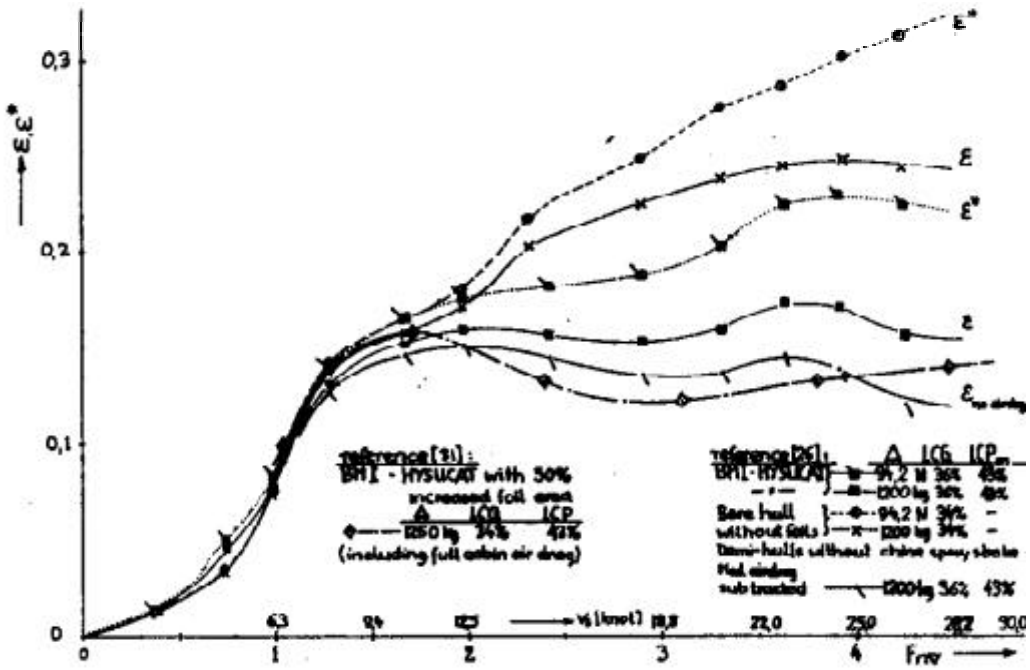

Figure 35: Outboard Engine Tests

5.4 Outboard Engine Tests

During the Sea Tests on the 5,65m Hysucat one of the outboard engines was tested in the laboratorium to establish the Power, Torque and specific consumption curves over the full speed range of the engine in the same running stage for which it was used in the sea trials. The laboratorium test covered a wide range of torque loads by use of several different torque-propellers to enable the determination of the power during sea testing by use of the fuel flow and engine speeds measurements. This way, the propulsive coefficient P.C. can be determined. The outboard engine was tested by Van Dyk and Martin (28) in the stability Basin of the Mechanical Engineering Department at the University of Stellenbosch which has the dimensions of 5 m x 10 m with a water-depth of 0,8 m.

A motor test stand was built and placed in the basin with the propeller submerged and the torque reaction of the engine mounted on a friction free shaft was measured with an electrical loadcell-amplifier and recorder system.

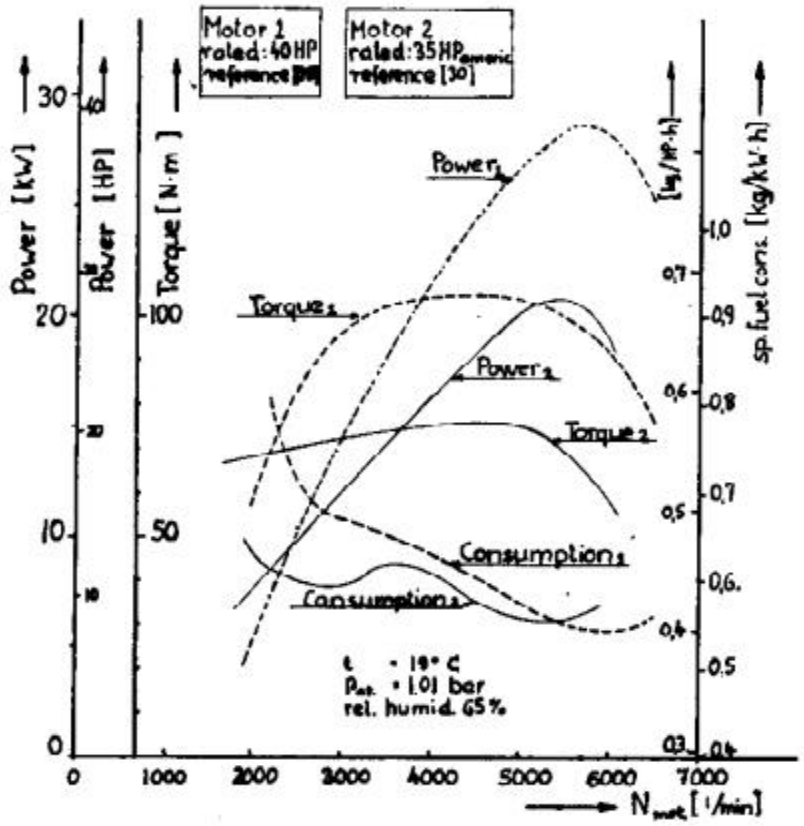

Figure 36: Outboard Engine Characteristics

and the VDO-fuel flow meters, which were calibrated prior to testing. The test equipment is visible on the photograph in Fig. 38 with the Hysucat in the background. The measured data were computed and 3rd power polynomial functions developed which allow safer inter- and extrapolations.

The engine characteristics for maximum operating conditions are shown in Fig. 36. The two stroke engine's specific fuel consumption is relatively high when compared to four stroke engines, especially in the range of lower engine speeds.

Fig. 37 shows the compound diagram of the engine test results which allows the determination of torque and power in the sea test by measuring fuel flow rate and engine speed for several constant speed test runs.

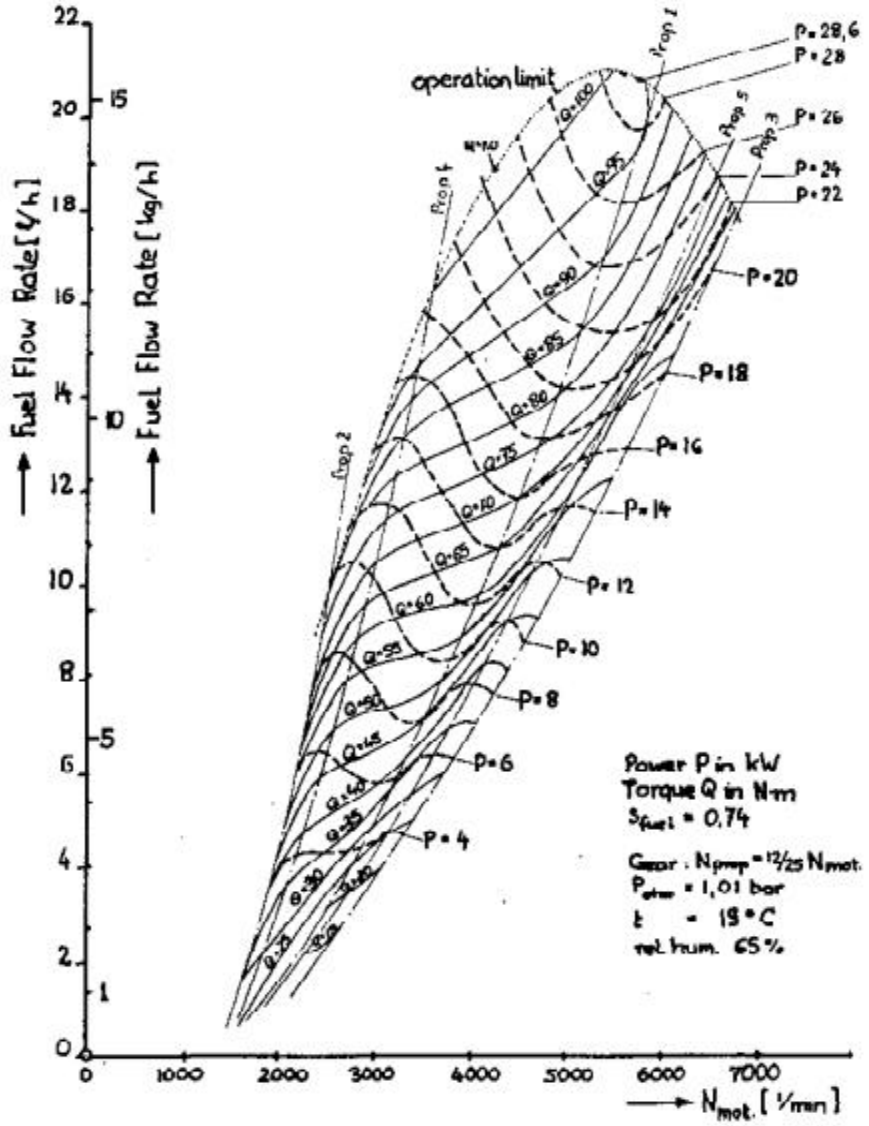

Figure 37: Engine speed – Fuel Consumption – Power – Torque Curves

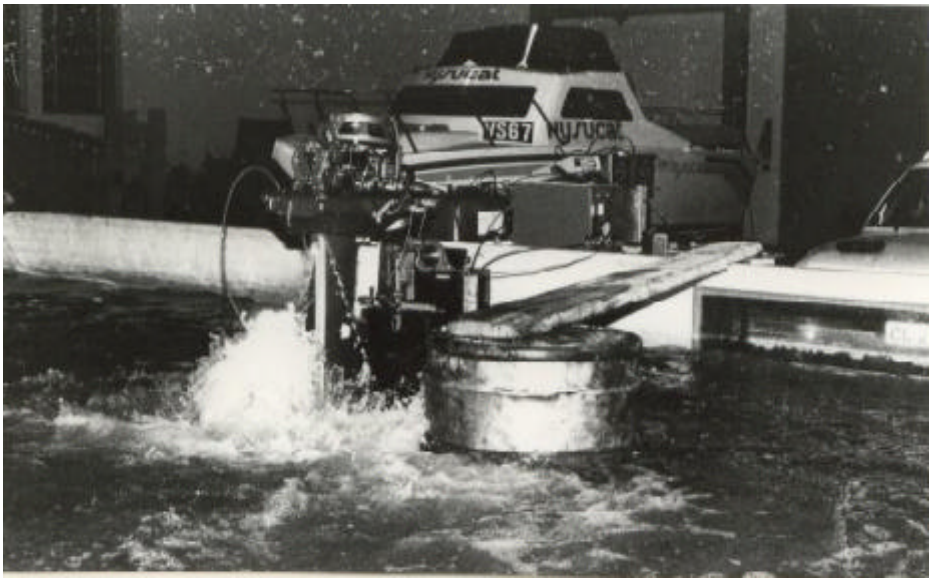

Figure 38: Outboard Engine Laboratory Test

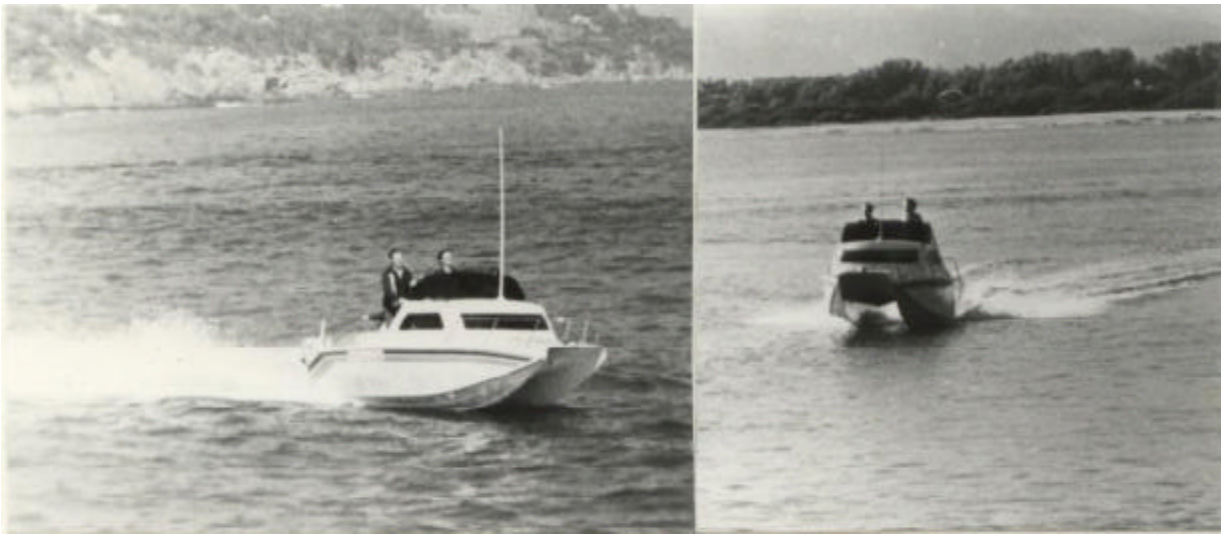

Figure 39

5.5 Hysucat Sea Tests

The Sea trials with the BMI Hysucat were conducted in the Atlantic Ocean, mainly in False Bay off Gordonsbay, off Hout Bay and also on the sea off Knysna. Flat water tests performed on the artificial lakes Zeekoevlei and Theewaterkloofdam, where runs of several kilometer lengths with 6 m to 10 m waterdepths are possible.

General Sea-keeping and Handling

In the first ten days of the sea-trials the BMI Hysucat was run under various sea state conditions to investigate it's sea-keeping and handling under calm and adverse weather conditions. No problems what-so-ever were encountered and with the helmsman's growing confidence in this new type of craft, extremely severe sea conditions with sometimes very strong winds of up to 40 knot and heavy swell were tried. These tests were conducted with the initially installed Johnsons 35's. Surprisingly, even in 40 knot headwinds the BMI Hysu cat could maintain it's 25 knot top speed. The runs in short choppy waves were unbelievable smooth and comfortable and even when "jumping' the crest of the large swell wave the boat entered relatively smoothly in the following crest. In large swell waves it was tried to broach the Hysucat without success. Sharp turns could be performed even in strong waves with approaching crests. The boat runs very dry and even at low speeds no "green water was shipped". The sea-keeping and handling tests gave fully satisfying results and some of the conditions were so severe that similar tests on conventional mono-hulls are unthinkable. Fig. 39 shows the typical running attitude of the Hysucat in calm seas, at 25 knots riding high above the waves.

Fuel Consumption

In these initial tests only the speeds and the fuel consumptions over measured distances at various constant speed runs were recorded. The results are given in the diagram in Fig. 45 in the form of the specific fuel consumption ratio for 1000 kg displacement (C*) which is relatively constant with C* = 0,58 for all planing speeds and shows a little "hump" (up to 0,68) for speeds for which the hump resistance appears (8 to 10 knot).

Systematcial Sea Trials

A series of systematical sea trials were conducted by Loubser and Nieder-Heitman (27). For these tests the BMI-Hysucat was equipped with a VDO Sumlog III to record more accurately the speeds and traveled distances. The Sumlog III was carefully calibrated. The fuel consumption was measured with a sensitive Bourdon Gage to establish data about the suction load of the through-hub-exhaust system of the outboard engines. The suction load was found to be small at all speeds. The exhaust gas pressure at outlet was nearly and about equal to barometric pressure. In the later trials these tests were abandoned.

Thrust

A thrust measuring device was designed to determine the thrust force transmitted on to the hull by both outboard engines. This thrust force does not include the drag of the outboard underwater parts (in short called let-drag). The outboard trimming-pins were removed and the outboard engine's forces and torque on the shaft were measured and calibrated against the propeller shaft thrust force. Initially the torque was measured by a lever-system acting on a spring balance which was later replaced by an electrical load-cell with amplifier and recorder system.

The results of two test runs with a total displacement of 1270 kg are given in Fig. 40 in the form of the thrust over weight ratio e_T over Fn ∇. The diagram also contains the model test predictions to allow a comparison.

The thrust-weight ratio e_T shows higher values than the model test prediction. The over-read increases with speed. A direct comparison between e_T and e is not possible as the thrust influence on the craft's resistance and trim is not exactly known. The over-read is due to the fact that the resultant leg-drag is not in line with the thrust force (but above it due to the cavitation plates and strong upper leg part) which means that the moment acting on the outboard engine and which is calibrated against the thrust force contains a disturbing compoment which increases with V_s^2.

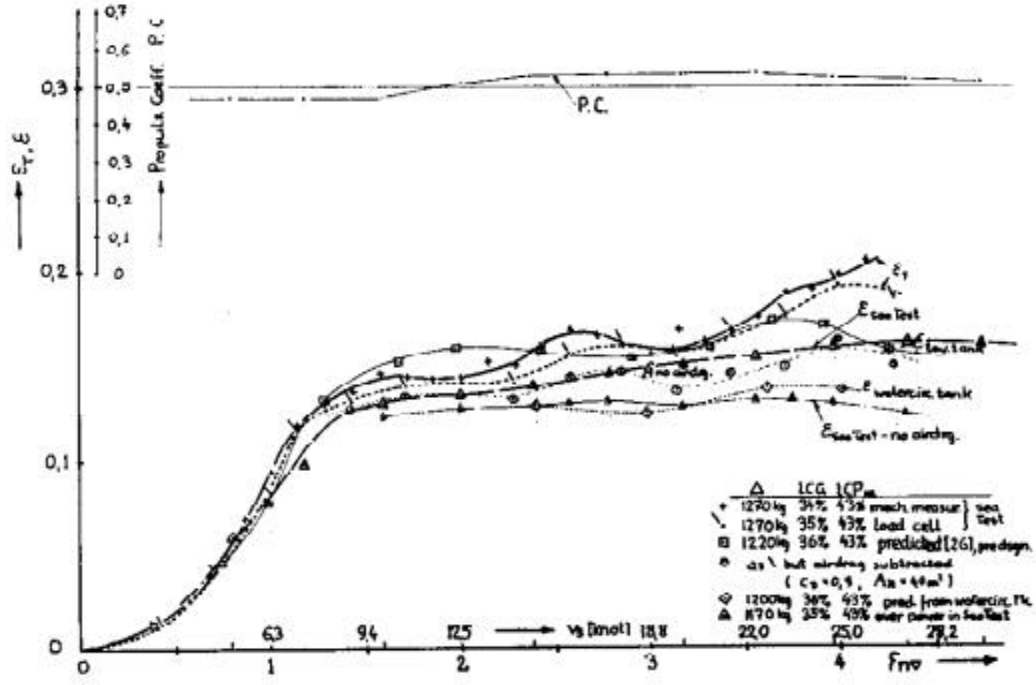

Figure 40: BMI-Hysucat (5.65), Resistance in Sea Test

The vertical pressure forces on the outboard leg additionally introduce a disturbing moment. The method of compensation for the thrust influence as used in (27) therefore, is not sufficiently accurate. This thrust force measurement is only an approximation to the resistance and useful to show general tendencies.

Trim

The trim at speed of the BMI Hysucat was measured photographically and with aid of a water-balance-trim-device which functions accurately only at steady speed and was useful in the lake test series (27). The trim test results are shown in Fig. 41 and are compared to the model test predictions. The trim of the craft at speed is strongly influenced by the trim-settings of the outboard engines, which are actually used to balance the craft optimally at speed. The sea test results show good agreement in the middle speed range, but, show lower values at top speed. This is believed to be due to the strongly rising forces with speed on the outboard engine's cavitation plates which create a stern up force, which is not present in the model tests.

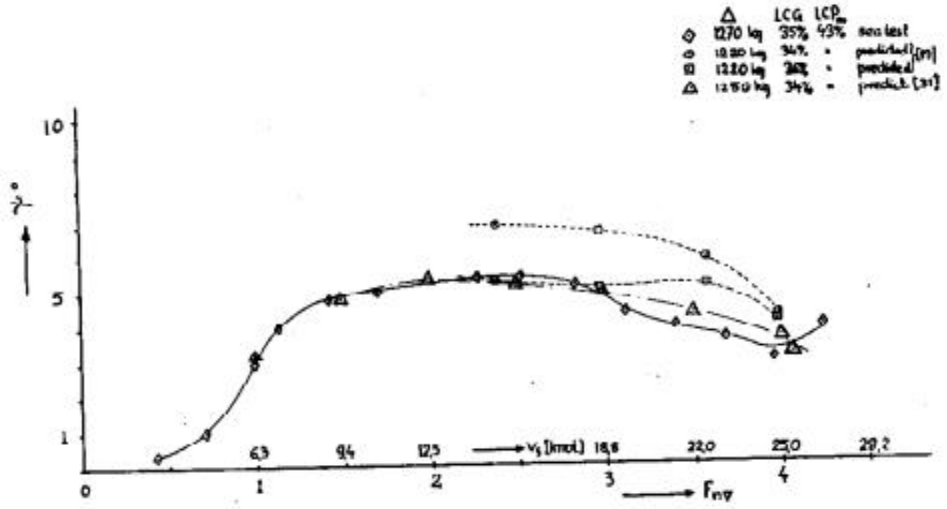

Figure 41: BMI Hysucat (5.65m), Trim in Sea Test

However, the measured trim angles at speed are not deviating strongly from the design values which formed the basis of the tandem hydrofoil arrangement.

Outboard Leg Resistance

The resistance of the outboard engine Leg (all parts which are submerged at speed) which is not included in the above thrust measurement, was measured on one engine. The outboard engine was kept in exactly the same position as used in the sea tests, but with the propeller removed.

To reach hull planing speeds with the craft, a third engine was mounted in the center plane at the transom over the tunnel. The forces on the outboard engine leg were recorded by the thrust measuring device as used for the thrust tests, the load-cell being able to measure forces in the opposite direction after calibration. The results of these trials are shown in the diagram in Fig. 41 in the form of the resistance D_{leg} for one engine alone.

The drag coefficient $C_{D\,leg}$, based on the cross-sectional area in the flow at a speed of 24 knot, including the component of the cavitation plates having an angle to the flow which corresponds to the trim angle at this speed, is plotted on the same graph.

The dimensionless resistance coefficient of both engine legs for the hull under test conditions

$$\varepsilon_{legs} = 2 \cdot D_{leg} / \Delta$$

is also incorporated in the diagram in Fig. 42.

The outboard engine legs create a strong resistance which is especially steeply rising around the “hump-speed” of the craft.

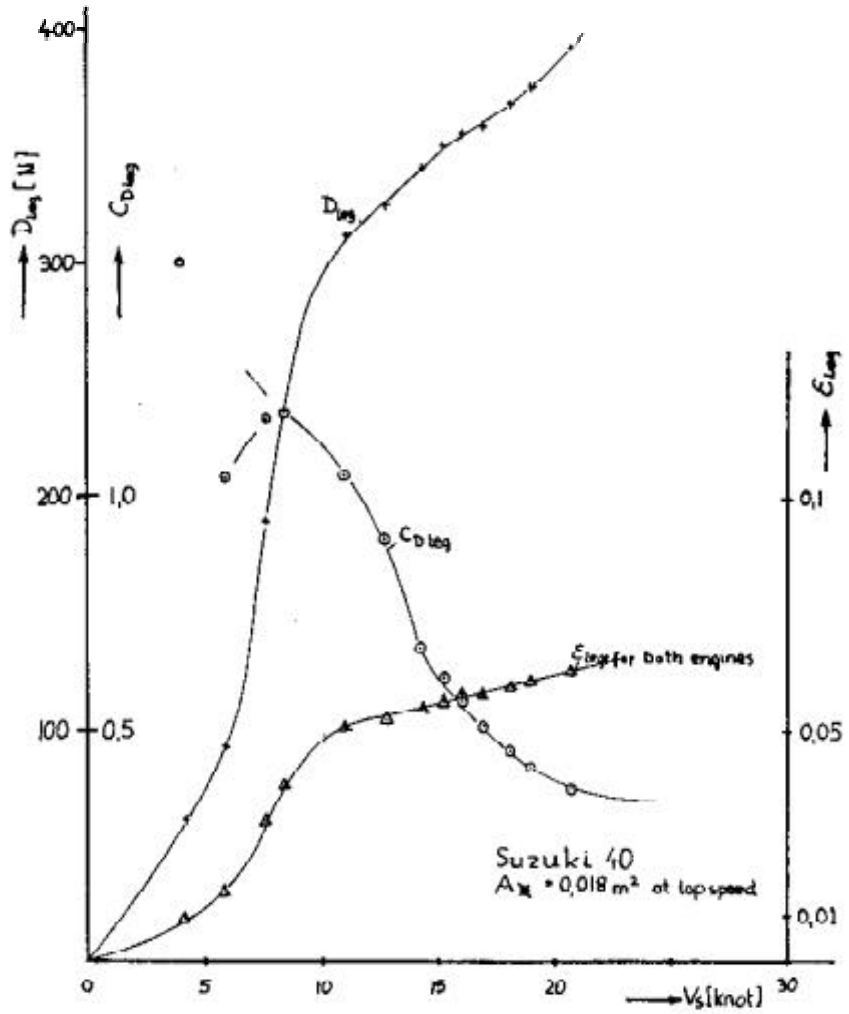

Figure 42: Outboard Engine Leg Resistance

The drag coefficient is about 0,40 in the mean planing speed area. The comparison of the resistance coefficient e_{egs} constitutes nearly 30% of the hull resistance. This means, 30% of the fuel burnt is used to "only" hold the propellers at their positions.

The drag coefficient $C_{D\,leg}$ in Fig. 42 indicates that at lower speeds near the "hull hump resistance" (7 to 10 knots) the leg resistance increases un-proportionally. This is due to the fact that much larger leg cross-sectional areas come underwater at these speeds – even though they are in the "wake field" of the transoms. This aggravates the hump resistance problem further for which special engine power reserves are necessary to get the craft into the planing stage.

Fuel Consumption

The fuel consumption of one engine at the time was measured with the VDO fuel flow meter for constant speed runs at pre-determined engine speeds. This way the boat speed and the engine speed could be correlated for this specific hull condition. The results are shown in the diagram in Fig. 43. The measuring points of the fuel flow plotted over engine speed, vary around an average curve because only one fuel flow meter was available and one engine was connected at the time. In a repeat test, in which it was tried to keep both engines again at the same position and revs, the second engine's fuel flow was then recorded. In the varying sea conditions this leads to small fluctuations in the final result. For the processing of the data the average between the star board and port engine results are used. The fuel consumption increases roughly proportionally to the engine speed, but around "hump-speed resistance" (2800 r.p.m to 3400 r.p.m.) a stronger fuel flow was measured – as expected.

Propulsion Power and Specific Consumption

The above fuel flow and engine speed measurements allow the determination of the propulsion shaft power P_B which the propeller absorb by aid of the engine characteristic, shown in Fig. 37, which was established in the laboratorium test. The result is given in the diagram in Fig. 44 where the absorbed shaft power P_B and specific consumption of the craft during the sea trials are plotted over the boat speed.

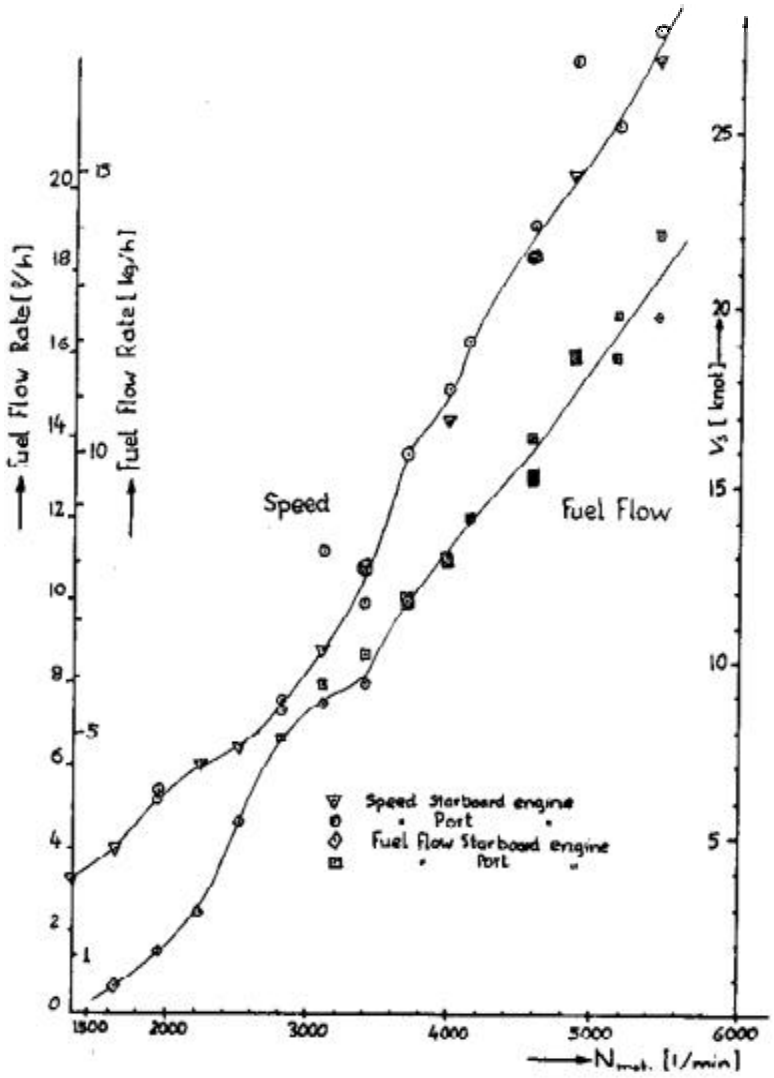

Figure 43: BMI Hysucat Sea Test Result

The power P_B is roughly proportional to the boat speed and the maximum power which is limited by the pitch of the used propellers is about 72 HP. The available motor-power is about 78 HP which shows that there is a nearly 10% power reserve. A similar power reserve exists at "hump speed" . The engine rating is sufficient. The specific consumption during sea trials, which means the Outboard Engines in combination with the BMI Hysucat, has it's best value at full speed with about 380 (gr / HP *h) . For lower speeds the specific consumption rises and has the worst value at lowest measured speed (or lowes r.p.m.) with about 570 (gr / HP * h), see Fig. 44.

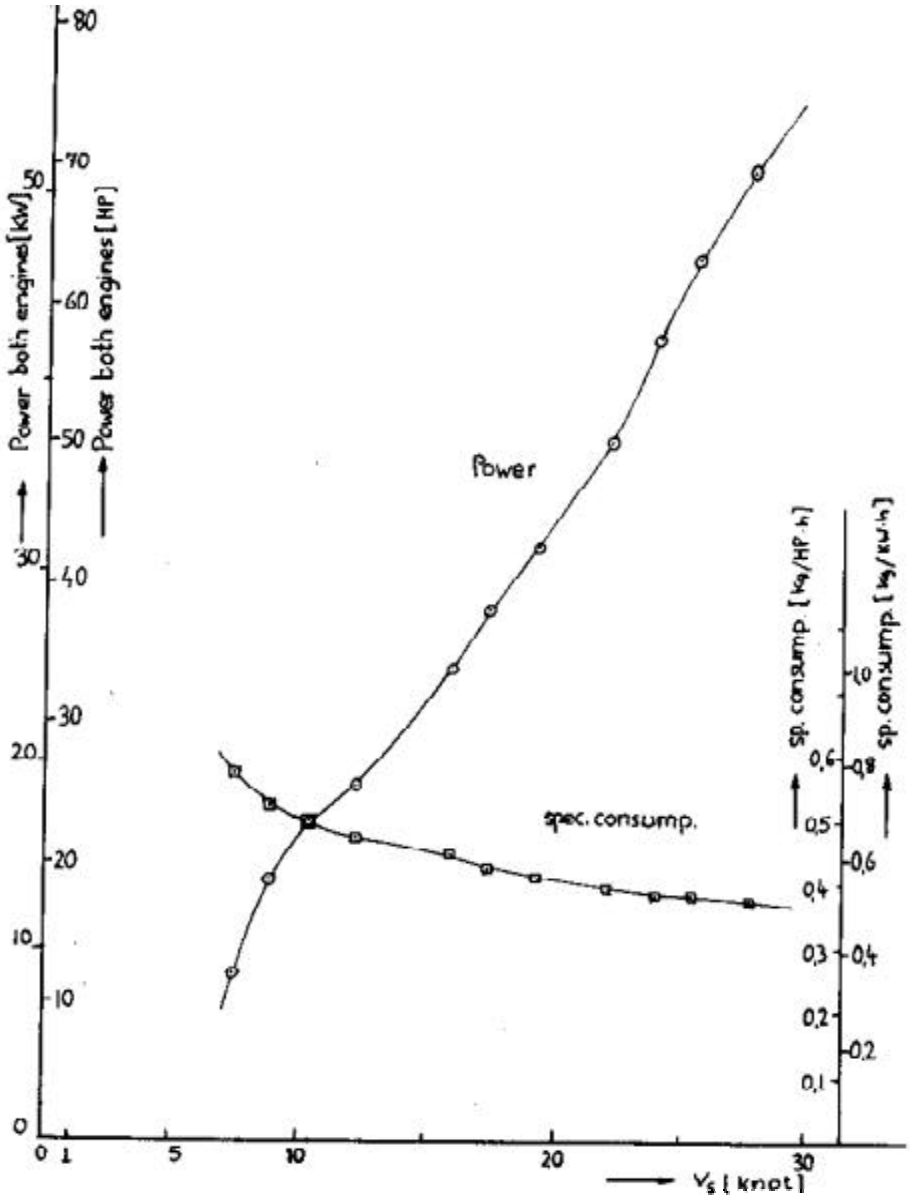

Figure 44: BMI Hysucat, Consumption and Power

Outboard engines are mostly built on the two-stroke-cycle and designed for simplicity, reliability and low weight. Against the more sophisticated four-stroke engine, they have the disadvantage of higher fuel consumption. A comparable inboard four-stroke engine, as for example the BMW B130 has a specific consumption at top speed of about 225 (gr / HP * h) which means a 68% lower value. At half speed the difference is even stronger with 430 (gr / HP * h) for the two-stroke engine, a ratio of 2,05. This fact is the main reason that inboard propulsion systems are so much more fuel efficient (however, on the cost of increased space, weight and capital costs.)

Fig. 45 shows the specific fuel consumption of the craft C*, which is given in litre of fuel per kilometer traveled for 1 ton craft-weight, which was achieved from the sea trial results.

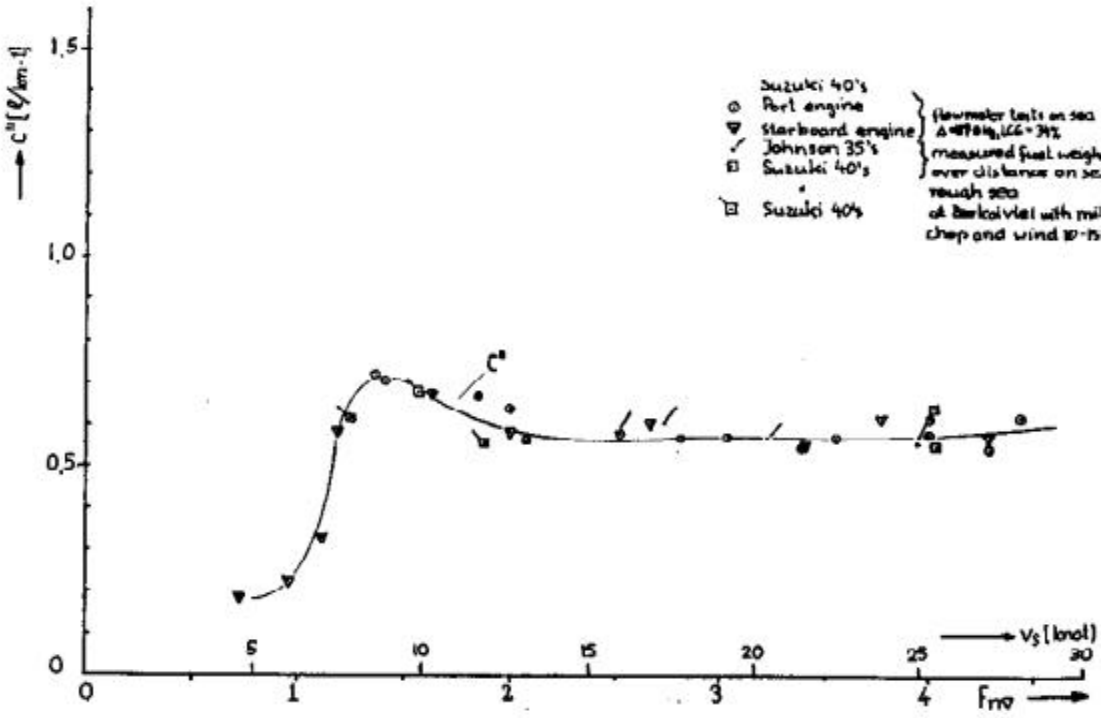

Figure 45: BMI Hysucat (5,65m), Fuel Consumption in Sea Test

The craft's specific consumption C* (in Fig. 45 : C"!) is nearly constant over the planing speed range with an average value of about 0,58. At "hump resistance speed" it increases slightly to a maximum of 0,70. The propulsive overall coefficient P.C., based on propeller-shaft-power (as measured in the laboratorium test) instead on the usual crankshaft power was worked out from the sea trial results and is shown in Fig. 40. The P.C. has a best value of P.C. = 0,53, slightly above P.C. = 0,5, which is usually taken in the preliminary design. The propulsive coefficient P.C. contains the outboard leg resistance. Otherwise, the propeller free running efficiency is much higher and around 70%.

The P.C. is relatively constant over the planing speed range but drops to P.C. = 0,47 at "hump resistance speed".

Resistance Determination through Power Measurement

Once the power was known through the fuel consumption and engine speed measurements in the sea trials, the resistance coefficient $e_{sea\ test}$ was determined by aid of Equations 4.4. The propulsive coefficient P.C. is assumed to be near to the propeller free running efficiency $?_P$ in planing craft, if the power to overcome the appendage resistance (outboard engine leg drag) is subtracted from the total measured power. The propeller efficiency $?_P$ was approximately determined by aid of empirical data from systematical Propeller Series Test (Gawn-Standard-Series), so that $e_{sea\ test}$ follows to:

$$e_{sea\ test} = \frac{(P_B - P_{leg}) \cdot 1000 \cdot \eta_p}{\Delta \cdot V_s} \qquad \ldots\ldots \quad 5.1$$

The BMI Hysucat resistance coefficient $e_{sea\ test}$ is shown in Fig. 40 in the full speed range. It still contains the air-resistance of the craft , which can be approximated by

$$R_{air} = \rho_{air} \cdot V_s^2 \cdot A \cdot C_D/2 \qquad \ldots\ldots \quad 5.2$$

with A = cross-sectional area in air and
C_D = air drag coefficient.

The cross-sectional area including the tunnel and windscreen is about A = $4m^2$ and the drag coefficient C_D = 0,9, as used for open sports-cars.

The BMI Hysucat resistance coefficient without the airdrag, which was calculated with Equation 5,2, is also shown in Fig. 40 and compares well with the prediction from the model test in the water-circulating tank. The towing tank tests indicate higher resistances in the pre-design condition (no sp ray strakes on demi-hulls and without compensation for hydrofoil scale effects!) . The resistance coefficient $e_{sea\ test}$ is therefore, the more reliable one.

5.6 Discussion of Results

The results of the sea trials confirm in principle the Hsyucat design data and model test predictions. Figure 46 shows the Hysucat resistance coefficient as measured for the mean load condition ? = 1270 kg, the air resistance substracted, in comparison to conventional craft. It can be seen that the Hysucat resistance coefficient e is nearly constant in the planing speed range, only rising slightly for the high Froude numbers. The resistance coefficient is around e = 0,12 and a maximum of e ~ 0,16 at top speed. As can also be seen, the BMI Hysucat has a slightly higher resistance coefficient as measured on the mono-foil models Hysucat 5 and Hysucat 6. Partly the resistance increase is due to the higher viscous skin friction component of the relatively small prototype and the strong keel beams which account for about 8% of the total resistance at top speed but which are necessary to carry the hydrofoils without bolts penetrating the hull and which form a strong back-bone to allow for beaching and ground contact. Other reasons for the resistance increase have to be found in the general design compromise. In this first Hysucat design a careful approach to the hydrofoil loading was made, resulting in a relatively small foil area with a low load

capability. This way, the remaining hull load guarantees sufficient transverse stability at all speeds.

Model tests in the towing tank (20) indicate that the original maximum foil load in relation to the much lighter Kevlar-Sandwich-Structure-Design resulted in a much lower resistance coefficient of e = 0,11 as mean value. Financial restraints prohibited the building of this craft.

It can be deducted that larger foils on the existing BMI Hysucat can improve the resistance coefficient considerably, especially the hump-resistance at about $Fn_{\nabla} = 1,5$ and the medium planing speed resisance at $Fr_{\nabla} \sim 3,0$.

In view of the very good sea-keeping and handling characteristics of the BMI Hysucat with always sufficient transverse stability reserves at all speeds, larger hydrofoils could well be attached.

For the heavier production boats in Transvaal which are mainly used on the east-coast with beach-landing requirement a larger mainfoil with 25% increased area was designed and built. The boats equipped with these larger foils operate well, however, no sea trial results are available to date.

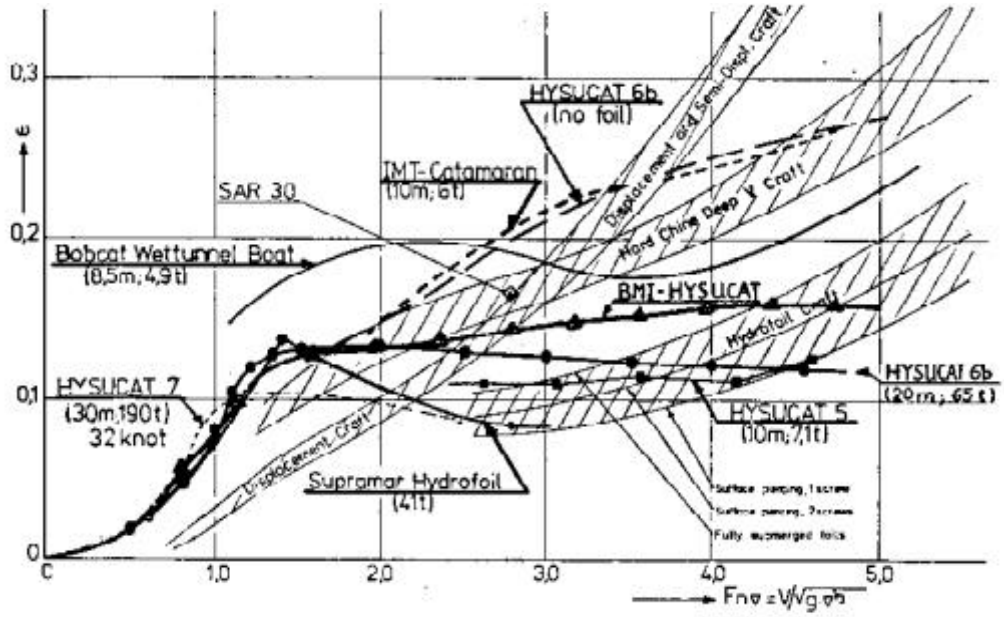

Figure 46: Resistance-Displacement Ratios e of Sea Craft

For important sea-keeping, especially running into the waves, the BMI Hysucat demi-hulls were designed extremely slender in the fore-ship with increased deadrise-sections, which tend to increase the high-speed resistance. In view of the good wave-going characteristics of the BMI Hysucat, a shape which favors low resistance on the cost of some sea-keeping quality could be adopted in new designs.

The design of a hydrofoil system which would penetrate deeper than the hull's lateral area could improve the resistance of the Hysucat considerably but was ruled out for the design of the smaller craft which are transported on trailers and which are sometimes beached. For larger craft, which float permanently in the sea such deep penetrating hydrofoil systems are attractive as aside of further resistance improvement the sea-keeping in waves will be improved.

It is the authors belief that still considerable improvements in the Hysucat design are possible by systematical optimization. This has to include the experience gained in sea tests, as sea-keeping and handling can not easily be determined in model tests. For the evaluation of the hydrodynamic parameters of the BMI Hysucat the propulsion system characteristics where needed. As no published data about the outboard motors used could be traced, one of the motors was tested in the laboratorium and at sea. The torque tests indicate relatively high specific consumption ratios. The outboard motor appendage resistance was also determined in the sea drag test and found to be relatively high, accounting for 23% of the crafts total propulsion power.

The craft's specific consumption ratio C* defined by Equation 4.11 as measured in the sea tests compare well with outboard engine driven deep -V-planing craft, which have considerably higher consumptions. However, due to the outboard engines high specific consumption (0,380 kg / HP h) and the parasitic leg drag, the craft's specific consumption ratios C* are relatively high when compared with planing craft equipped with 4-stroke inboard petrol engines (0,225 kg HP * h) and z-drives (Volvo, BMW). The application of inboard engines could reduce the Hysucat consumption ratio C* by 40% at top speed and over 50% at medium speed (by application of Equation 4,12). To achieve more fuel efficient Ski-boat or pleasure craft designs outboard engines with specific consumption ratios similar to the modern car engines are needed with hydrodynamicaly efficient propulsion systems, which is technically possible. The resultant gain will be much larger than what is possible by further planing hull optimization. In the large Hysucat designs (over about 8m) petrol inboard or Diesel engine propulsion systems will be foreseen and considerable improvements in fuel economy will be possible.

Altogether, the first prototype of a Hysucat, the BMI Hysucat, has proved a seaworthy craft with unparallel sea-keeping, reduced power and consumption. The logical background to the Hysucat design was approved in the sea trials and allows the immediate building of larger craft. The Hysucat principle has fulfilled it's promise.

Outlook

The 5,65m BMI Hysucat formed the base on which the Hysucat production boats are built with varied deck layout for deep-sea fishing, and another version as ski-boat with reduced keel beams for beach landing. Two builders in RSA produce the Hysucat under license to BMI. Nearly forty boats have been completed, which shows the popularity of the new craft (in-spite of a strong recession). Fig. 47 shows a short-cabin Hysucat built by HYSUCO-Skicraft during it's maiden voyage.

Figure 47: HYSUCO-Skicraft built production Hysucat in Sea Trials

After extensive testing of the BMI Hysucat by the S.A. Bureau of Standards the BMI and the designer Dr. K.G. Hoppe received the Shell Design Award 1983 in the Category of Consumer Products as an example of good product design.

The original BMI Hysucat raised considerable interest on the Hannover Trade Show in West-Germany , April 1984. The Hysucat is also manufactured under BMI-license in Canada and Australia. A 5,6m Hysucat was shown on the Toronto Boat Show early 1984.

To complete the ski-boat range, BMI had designed a 4,8 m Hysucat as the smallest sea-going craft, shown in Fig. 48, and a 6,5 m Hysucat as work, fishing or rescue craft in Fig. 49.

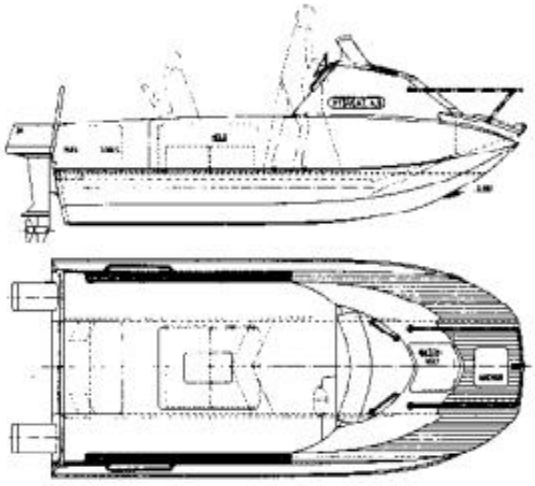

Figure 48: The 4,8 m Ski-boat design

Both designs are marketed and shall be produced in 1984/85.

Many enquiries are received from all over the world concerning the existing designs and larger craft. The principle hull concept, used in the existing Hysucat designs, allows favorable Hysucat craft to lengths of up to about 30 m / 190 t with speeds of 30 to 50 knots. For larger craft the semi-displacement type of demi-hull has to be used. Further research work is necessary to establish the design parameters and to find the range of favorable applications of the large Hysucat designs.

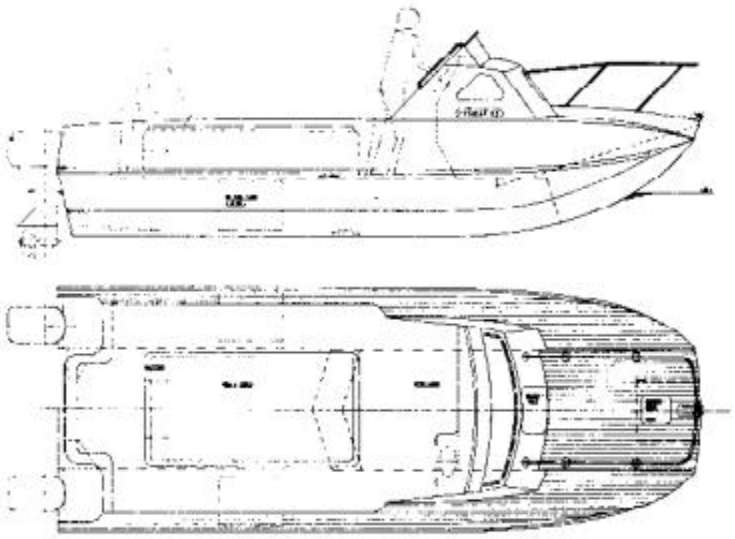

Figure 49: The 6,5m Workboat Design

Acknowledgement

I would like to express my gratitude to Professor Hattingh, Director of BMI, and Mr. Gerdsen, Hysucat Engineering, for early recognition of the potential behind the Hysucat principle and continuous support in the development, to the University of Stellenbosch for establishing the ground on which the research work was possible, to the staff of BMI and SMD at the University who all contributed to the development of the Hysucat, to the ski-boat enthusiasts Mr. James of "HYSUCO" and Mr. van der Ryst of "Motor and Skiluv" who pioneered the Hysucat building and all the students mentioned in the references who contributed valuable research results in their thesis work concerning the testing of Hysucat models and prototype.

8. Literature

(1)	DuCane,	:	"High Speed Small Craft".
(2)	Hoppe, K.G.	:	"Catamaran with Hydrofoils", S.A. Patent No. 80/5400 entered by BMI and overseas applications.
(3)	Hoppe, K.G.	:	"Catamaran with Hydrofoils", S.A. Patent No. 83/3503 entered by BMI and overseas applications.
(4)	Cantiere Navaltecnica Brit	:	Patent Specification 1524938 1977 "Improvements Relating to Catamarans".
(5)	Wai Po Loo	:	United States Patent Specification 3,179,077 – 1965 - "Hydro Wing Ship".
(6)	Hanns Schertel von Burtenbach	:	Swiss Patent Specification 605244 – 1977 "Tragflügel – Katamaranboot". (Supramar AG, Stansstad)
(7)	Nanditt, Horst	:	German Patent Specification 1531592 1970 "Motorboot".
(8)	International Aquavion S.A.	:	Swedish Patent Spesification 752,639 - 1954 "Hydrofoil Craft".
(9)	Valdant, M.P.	:	French Patent Specification 1.523.480 "Engin nautique perfectionné a sustentation hydrodynamique".
(10)	Water Craft	:	United States Patent Specification 3,236,202 – 1966.
(11)	Hoppe, K.G.	:	"Comparative Planing Hull Model Tests in a Water-circulating Tank, Memorandum, No.1 Department of Mechanical Engineering, University of Stellenbosch, 1977.
(12)	Hoppe, K.G.	:	"Model Tests on IMT Catamaran Dolomede" Bureau for Mechanical Engineering, University of Stellenbosch, 1979.
(13)	Clement, E.P. and Blount, D.L.	:	"Resistance Tests of a Systematic Series of Planing Hull Forms", SNAME, Nov. 1963.
(14)	Comstock, E.P.	:	"Princip les of Naval Architecture", SNAME, 1967.
(15)	Gouws, J.D.	:	"Bou van Eksperimentele Watersirkuleer-kanaal", Skripsie Department Meganiese Ingenieurswese, Universiteit van Stellenbosch, 1975.

(16) Baron Hanns von Schertel, : "The Deign and Application of Hydrofoils and their Future Prospects", IME, London, 1973.

(17) Müller, B. : "Widerstandsversuche für ein 41 t Tragflügelboot", Bericht Nr. 247/63 Versuchsanstalt für Wasserbau und Schiffbau, Berlin, 1963.

(18) Bosch v. Denn, J.J. : "Comparative Tests on Four Fast Motor Boat Models etc", TNO, Report N1965, Delft, 1974.

(19) Hoppe, K.G. : "The Hydrofoil Support Catamaran – Evaluation and Model test", Progress Report 1980, Mechanical Engineering Department, University of Stellenbosch.

(20) Bart, D.P. : "Ship Model Testing:, 1970.

(21) Wadlin, K.L., Shuford, C.L., and Mcgrehee, J.R. : "A Theoretical and Experimental Investigation of the Lift and Drag Characteristics of Hydro-foils at Subcritical and Supercritical Speeds", N.A.C.A. Report 1232, 1955.

(22) Smit, C.S. : "Model Tests on a Catamaran Type Boat", Research Project for BSc-Thesis at the Mechanical Engineering Department of the University of Stellenbosch, 1980.

(23) Smit, C.S. : "Design and testing of a Towing Mechanism for the Model Towing Tank", Design Project for BSc-Thesis at the Mechanical Engineering Department of the University of Stellenbosch, 1980.

(24) Fourie, S.A. : "Hydrofoil Support Catamaran having an increased Slenderness Ratio (Hysucat 7), Research Project for BSc-Thesis at the Mechanical Engineering Department of the University of Stellenbosch, 1981.

(25) Pietersen, J.C.L. : "Optimisation of the Foil Arrangement on a 20m-Hysucat", Research Project for BSc-Thesis at the Mechanical Engineering Department , University of Stellenbosch, 1981.

(26) Steunenberg, F. : "The Optimisation of the Hydrofoil Arrangment of the BMI-Hysucat by Model Tests", BSc-Thesis at the Mechanical Engineering Depart-Ment, University of Stellenbosch, 1982.

(27) Loubser, L.B. Nieder-Heitman,C. : "Weerstandstoetse op die Hysucat en Skaal-model", BSc-Thesis at the Mechanical Engineering Department of Stellenbosch, 1983.

(28) Martin, P.L., Van Dyk, E.A.N. : "Design and Testing of an Experimental Method to determine Outboard Engine Characteristics", BSc-Thesis at the Mechanical Engineering Department of the University of Stellenbosch, 1983.

(29) Visser, J.G. : "Development of a FORTRAN Computer Program for Planing Mono Hull and Catamaran Calculations", BSc-Thesis at the Mechanical Engineering Department of the University of Stellenbosch, 1983.

(30) Smit, F.J.J., Stemmet, E.O. : "Design and Testing of a Torque Propeller to determine Outboard Engine Characteristics", BSc-Thesis at the Mechanical Engineering Department of the University of Stellenbosch, 1984.

(31) Claussen, N., Du Plessis, J. : "The BMI-Hysucat Model Systematic Tests on Different Hydrofoil Arrangements", BSc-Thesis at the Mechanical Engineering Department of the University of Stellenbosch, 1984